

WINNER- 1990-91 AIAA/GD AIRCRAFT DESIGN CONTEST

AOE FILE COPY

The Griffen

Close Air Support Fighter Design

SAMPLE REPORT
AOE DESIGN LAB

COPY (2)

DO NOT REMOVE

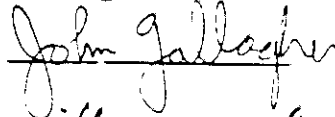
Group II

Virginia Polytechnic Institute & State University

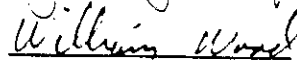
Robert Narducci
Design Leader



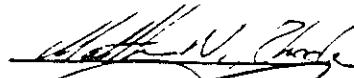
John Gallagher
Configuration



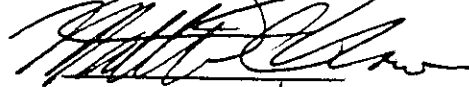
William Wood
Weights and Balance



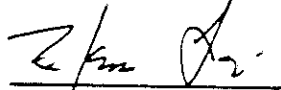
Matthew Rhode
Aerodynamics



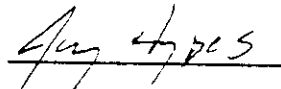
Matthew Nowinski
Propulsion



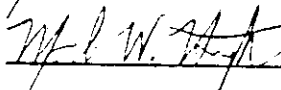
R. James Lanzi
Stability and Control



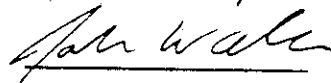
Jay Hypes
Mission Performance



Mark Herrington
Systems and Avionics

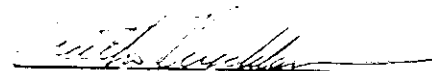


John Walker
Structures



Advisors


W.H. Mason


Nathan Kirschbaum

April 24, 1991

Group II

John Gallagher.....Application Filed
Mark Herrington300635125
Jay HypesApplication Filed
R. James Lanzi300211380
Robert Narducci.....300211364
Matthew Nowinski.....300326055
Matthew Rhode.....300635281
John Walker.....300635927
William Wood.....300326881

ADVISORS.....W.H. Mason
.....Nathan Kirschbaum

Executive Summary

The Virginia Tech aircraft design group 2 is pleased to present the Griffen in response to the AIAA/General Dynamics Corporation Design Competition request for proposal¹. The Griffen is a 48,100 lb, twin engine, close air support aircraft heavily armed with 20 Mk-82 500 lb bombs, 2 AIM-9L Sidewinder missiles and 1350 rounds of ammunition for the GAU-8 30mm cannon. The Griffen incorporates an active gust control system to increase pilot comfort during on-the-deck flight. Additionally, 2-D thrust vectoring nozzles and the low drag conformal weapons carriage enhance the performance of the aircraft. At a cost of \$21.8 million per aircraft, the Griffen exceeds all the requirements specified in the RFP.

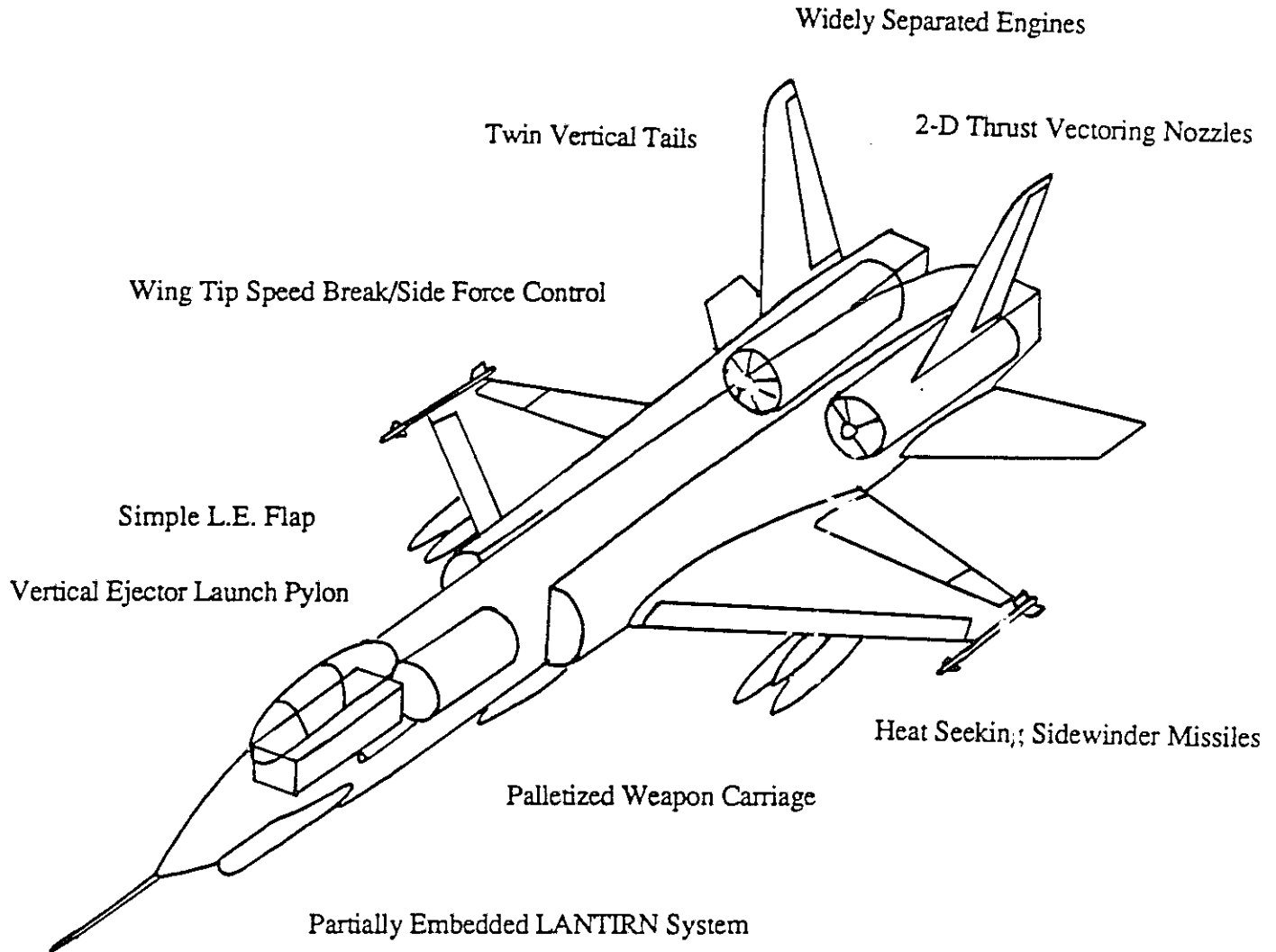


Table of Contents

List of Figures	iv
List of Tables	vi
List of Symbols and Abbreviations	vii
1 Introduction	1-1
2 Mission Description	2-1
3 Concept Selection	3-1
3.1 Relationship of Mission to General Design Configuration	3-1
3.2 Baseline Design Configuration	3-2
3.3 Common Configuration Characteristics	3-3
3.4 Configuration Comparison	3-3
3.5 Performance Comparison	3-4
3.6 The Final Baseline Concept Selection	3-5
4 Configuration	4-1
4.1 Basic Configuration	4-1
4.2 Survivability and Vulnerability	4-4
4.3 Weapons.....	4-6
5 Weights and Balance	5-1
5.1 Weights	5-1
5.2 Balance	5-3
6 Aerodynamics	6-1
6.1 Wing Geometry	6-1
6.2 Airfoil Selection	6-1
6.3 Design and Prediction of Lift	6-2
6.4 Prediction of Drag	6-5
6.5 Aerodynamic Performance	6-7

7	Propulsion	7-1
7.1	General Configuration	7-1
7.2	Air Intake System	7-1
7.3	Exhaust Nozzle Configuration	7-3
7.4	Installation Losses	7-3
7.5	Summary	7-6
8	Stability and Control	8-1
8.1	Method of Analysis	8-1
8.2	Wing Longitudinal Placement & Longitudinal Stability Determination	8-1
8.3	Control Surface Concept Selection & Sizing	8-2
8.4	Open Loop Dynamic Characteristics	8-4
8.5	Open Loop Ride Quality Characteristics	8-5
8.6	Stability Augmentation & Active Ride Quality Control	8-5
9	Performance	9-1
9.1	Methods	9-1
9.2	Mission Performance	9-1
9.3	Point Performance	9-1
9.4	Flight Conditions and Sensitivities	9-5
10	Avionics	10-1
10.1	Hydraulics	10-1
10.2	Electrical	10-2
10.3	Back-up	10-2
10.4	Environmental Control System (ECS)	10-2
10.5	Canopy	10-2
10.6	Flight Controls	10-2
10.7	Fuel System	10-3
10.8	Landing Gear	10-3
10.9	Miscellaneous Systems.....	10-4

10.10 LANTIRN	10-5
10.11 Radar	10-5
10.12 Inertial Navigation System (INS)	10-6
10.13 Electronic Counter Measures (ECM)	10-6
10.14 Radar Warning Receivers	10-7
10.15 Identify Friend or Foe (IFF)	10-7
10.16 TACAN	10-7
10.16 Miscellaneous Avionics.....	10-7
11 Crew Station	11-1
11.1 Cockpit	11-1
11.2 Control Stick	11-2
11.3 Ejection Seat	11-2
12 Structures	12-1
12.1 V-n Diagram	12-1
12.2 Structural Arrangement	12-2
12.3 Material Selection	12-4
12.4 Weight Savings	12-9
13 Manufacturing	13-1
13.1 Management	13-1
13.2 Manufacturing	13-3
14 Cost Estimation	14-1
15 Future Expansion	15-1
16 Conclusion	16-1
References	R-1
Appendix A: Stability Derivatives	A-1
Appendix B: Description of SSAPP	B-1
Appendix C: Weight Reduction Calculations	C-1

List of Figures

2-1	Mission profiles	2-2
3-1	Baseline design concept	3-2
3-2	Variable geometry carpet plot	3-5
3-3	Canard carpet plot	3-5
3-4	Griffen carpet plot	3-6
4-1	Three view of the Griffen	4-2
4-2	Inboard profile of the Griffen	4-3
4-3	F-4 with conformal weapons carriage	4-7
5-1	Side cg profile	5-4
5-2	cg travel during flight	5-4
6-1	SC(2)-0010 supercritical airfoil	6-2
6-2	Pressure distribution on SC(2)-0010 airfoil at cruise	6-3
6-3	Lift prediction	6-4
6-4	Breakdown of maximum lift	6-5
6-5	Zero lift drag	6-6
6-6	Drag breakdown at cruise	6-7
6-7	Drag polar at various flight conditions	6-7
6-8	L/D at various flight conditions	6-8
7-1	Griffen inlet configuration	7-2
7-2	Griffen nozzle configuration	7-4
8-1	Wing placemant chart	8-1
8-2	Trim drag increment	8-2
8-3	Schematic of the Griffen stability augmentation / ARQCS	8-5
8-4	Cockpit g-level vs gust length	8-9
9-1	Field performance	9-4
9-2	Operating envelope	9-5

9-3	Sensitivity	9-6
10-1	Hydraulic systems layout	10-1
10-2	Fuel system	10-3
10-3	Landing gear	10-4
10-4	Selected systems and avionics	10-5
10-5	LANTIRN navigation and targeting pods	10-6
11-1	Cockpit layout	11-1
11-2	McDonnell-Douglas ACES II zero-zero rocket ejector	11-3
12-1	V-n diagram of the Griffen	12-1
12-2	Structural configuration	12-3
12-3	Protective armor and firewalls	12-6
12-4	Materials selection	12-6
12-5	Fatigue crack growth	12-7
13-1	Corporate structure	13-1
13-2	Manufacturing facility	13-2
13-3	Proposed production rate	13-3
13-4	Proposed aircraft schedule	13-3

List of Tables

3-1	RFP mission specifications and related configuration responses	3-1
3-2	Common design features	3-2
3-3	Configuration comparison	3-4
3-4	Concept selection considerations	3-7
4-1	Survivability and vulnerability issues	4-5
5-1	Weight, moment, and balance data	5-1
5-2	Summary weights and balance sheet	5-2
6-1	Wing dimensions and parameters	6-1
6-2	Summary of L/D information	6-8
7-1	Installation thrust losses	7-5
8-1	Open loop response characteristics & associated specifications	8-4
8-2	Closed loop longitudinal response characteristics & gain schedule	8-6
8-3	Lateral/directional closed loop response characteristics & gain schedule	8-7
8-4	Long. closed loop response characteristics during RD flight conditions	8-8
9-1	Design mission summary	9-2
9-2	Secondary mission summary	9-3
9-3	Requirement summary	9-3
12-1	Weight savings	12-10
14-1	Comparative price list	14-1
14-2	Aircraft cost breakdown	14-1
14-3	Operation cost breakdown	14-2
C-1	Wing component failure modes	C-1
C-2	Strength to weight ratios	C-2
C-3	Adjusted weight calculation	C-3

List of Acronyms and Abbreviations

A/B	- After-burner
A/C	- Aircraft
AC	- Alternating Current
ACSYNT	- Aircraft Synthesis
AIM	- U.S. designation for Air Intercept Missile
AMAD	- Airframe Mounted Accessory Drive
AP	- Approach
ARQCS	- Active Ride Quality Control System
CAD	- Computer Aided Design
CF	- Construction Factor
cg	- Center of Gravity
CR	- High Altitude Cruise
CRT	- Cathode Ray Tube
DATCOM	- Airforce Stability Derivative Program
DOF	- Degree of Freedom
ECM	- Electronic Countermeasures
ECS	- Environmental Control System
ESF	- Engine Scale Factor
FOD	- Foreign Object Damage
FS	- Fuselage Station
GA	- Ground Attack
HOTAS	- Hands-on-Throttle-and-Stick
HUD	- Head Up Display
IFF	- Identify Friend or Foe
ILS	- Instrument Landing System
INS	- Inertial Navigation System
kts	- Knots
KVa	- Kilovolt-Amperes
LANTIRN	- Low-Altitude Navigation and Targeting Infrared System for Night
LIDRAG	- Lift Induced DRAG
LE	- Leading Edge
L-Q-R	- Linear-Quadratic-Regulator
MAC	- Mean Aerodynamic Chord
MER	- Multiple Ejection Rack
MFD	- Multi-function Display
Mk	- Mark
NASA	- National Aeronautics and Space Administration
nm	- Nautical Mile
psi	- Pounds per Square Inch
RAT	- Ram Air Turbine
RD	- Return Dash
RDTE	- Research Development Test and Evaluation
RFP	- Request for Proposal
SL	- Sea Level
SM	- Static Margin
SPF/DB	- SuperPlastic Forming/Diffusion Bonding
SSAAP	- State Space Analysis of an Airplane Computer Program
TACAN	- Tactical Air Navigation
TE	- Trailing Edge
TOGW	- Takeoff Gross Weight
TQM	- Total Quality Management
T/O	- Takeoff
T/W	- Thrust to Weight Ratio

UHF	- Ultra-High Frequency
V	- Volt
VG	- Variable Geometry
VHF	- Very-High Frequency
VLM	- Vortex Lattice Method
VSD	- Vertical Situation Display
W/S	- Wing Loading
2-D	- Two- Dimensional

List of Symbols and Subscripts

Abar	- Cockpit g-Level / fps Gust Input
Al	- Aluminum
Al-Li	- Aluminum-Lithium Alloy
a_N	- Cockpit Normal Acceleration
b	- Span
c	- Chord
c_r	- Root Chord
c	- MAC
C_D	- Drag Coefficient
C_{D_0}	- Drag at Zero Lift
C_L	- Lift Coefficient
C_l	- Section Lift Coefficient
C_M	- Moment Coefficient
D	- Drag
I_{xx}	- Rolling Moment of Inertia
I_{yy}	- Pitching Moment of Inertia
I_{zz}	- Yawing Moment of Inertia
k	- Weight Adjustment factor
K_{ij}	- Feedback Control Gain for control-j on state-i
L	- Lift
L/D	- Lift to Drag Ratio
M	- Mach Number
M_{DD}	- Drag-diverget Mach Number
Ni-Cad	- Nickel-Cadmium Alloy
n_{max}	- Maximum g-level
n_{min}	- Minimum g- level
[Q]	- State Weighting Matrix
[R]	- Control Weighting Matrix
[S]	- Cross Weighting Matrix
S	- Wing Area
T	- Time Constant
T_2	- Time to Double Amplitude
u	- Aircraft Control Vector
x	- Aircraft state vector
x_{np}	- Neutral Point Station
x_{cg}	- cg Station
x_{wing}	- Station of Theoretical Wing Apex
u	- Body x-component of wind speed
v	- Body y-component of wind speed
V_D	- Dive Speed
w	- Body z-component of wind speed

p	- Body x-component of angular velocity
P_s	- Excess Energy
q	- Body y-component of angular velocity
q	- Dynamic Pressure
r	- Body z-component of angular velocity

Greek Symbols

α	- Angle of Attack
$\alpha_{CL\ max}$	- Angle of Attack at max C_L
δ_a	- Aileron Deflection
δ_r	- Rudder Deflection
$\delta_{s.b.}$	- Speed Brake Deflection
δ_t	- Tail deflection
ΔC_{Dtrim}	- Drag increment due to trimming the aircraft
μ	- Coefficient of Friction
λ	- Taper Ratio
Λ	- Wing Sweep
ω	- Natural Mode Frequency
ζ	- Damping Ratio
θ	- Pitch attitude
ϕ	- Bank angle

Longitudinal Stability Derivatives:

$C_{L\alpha}$	- $\partial C_L / \partial \alpha$
$C_{D\alpha}$	- $\partial C_D / \partial \alpha$
$C_{m\alpha}$	- $\partial C_m / \partial (\alpha c / 2u_0)$
C_{Lq}	- $\partial C_L / \partial (qc / 2u_0)$
C_{mq}	- $\partial C_m / \partial (qc / 2u_0)$
C_{LM}	- $\partial C_L / \partial M$
C_{DM}	- $\partial C_D / \partial M$
C_{mM}	- $\partial C_m / \partial M$
$C_{L\delta_t}$	- $\partial C_L / \partial \delta_t$
$C_{m\delta_t}$	- $\partial C_m / \partial \delta_t$
$C_{L\delta_a}$	- $\partial C_L / \partial \delta_a$
$C_{m\delta_a}$	- $\partial C_m / \partial \delta_a$

Lateral/Directional Stability Derivatives:

$C_{Y\beta}$	- $\partial C_Y / \partial \beta$
$C_{l\beta}$	- $\partial C_l / \partial \beta$
$C_{n\beta}$	- $\partial C_n / \partial \beta$
C_{lp}	- $\partial C_l / \partial (pb / 2u_0)$
C_{np}	- $\partial C_n / \partial (pb / 2u_0)$
C_{lr}	- $\partial C_l / \partial (rb / 2u_0)$
C_{nr}	- $\partial C_n / \partial (rb / 2u_0)$
$C_{l\delta_a}$	- $\partial C_l / \partial \delta_a$
$C_{n\delta_a}$	- $\partial C_n / \partial \delta_a$
$C_{l\delta_r}$	- $\partial C_l / \partial \delta_r$
$C_{n\delta_r}$	- $\partial C_n / \partial \delta_r$
$C_{l\delta_t}$	- $\partial C_l / \partial \delta_t$
$C_{n\delta_{sb}}$	- $\partial C_n / \partial \delta_{sb}$

Stability and Control Subscripts:

P	- Phugoid
S.P.	- Short period
D.R.	- Dutch Roll
R	- Roll Mode
S	- Spiral Mode
α	- Angle of Attack
$\dot{\alpha}$	- $\partial\alpha/\partial t$
β	- Side Slip Angle
L	- Lift Force
l	- Roll Moment
m	- Pitching Moment
n	- Yawing Moment
p	- Roll Rate
q	- Pitch rate
r	- Yaw rate
Y	- Side Force

1. Introduction

In ancient mythology, the Griffen†, a savage creature with the body of a lion and the head and wings of an eagle, had speed, agility, and power. Today's Griffen is designed to accomplish the close air support role as detailed in the AIAA/General Dynamics Corporation request for proposal¹. The 48,100 lb Griffen is heavily armored with 20 Mk-82 500 lb bombs, 2 AIM-9L heat-seeking Sidewinder missiles, and 1350 rounds of high explosive, armor piercing ammunition for the tank busting General Electric GAU-8 30mm cannon. To survive in the lethal environment over today's battlefield, the Griffen is extensively protected with a combination of titanium and Kevlar armor. Twin engines, twin vertical tails, and redundant systems allow the Griffen to take damage and still return the pilot to safety.

From short and rough fields, the Griffen maneuvers to its targets at transonic speed, on-the-deck with the aid of an active gust relief system, improving pilot comfort and weapons delivery. Day or night, in any weather, the LANTIRN system, the eyes of the Griffen, enables the aircraft to seek and destroy its targets. Upon landing, a low drag conformal bomb pallet system reduces turn-around time, allowing the Griffen to return to the battle field. Flexibility for expanded systems and weapon loads is built into the design so the Griffen can meet future threats and changing mission requirements. At \$21.8 million the Griffen is both affordable yet advanced.

† Griffen, some times spelled Griffin or Griffon

2. Mission Description

The Griffen fulfills two close air support combat missions as specified in the RFP¹. The primary mission is a high speed, sea level dash to the combat site. The secondary mission is a high-low profile, including a loiter, to the combat site. For both missions the weapons payload consist of the GAU-8 30mm cannon with 1350 rounds of ammunition, 2 AIM-9L infrared Sidewinder missiles, and 20 Mk-82 500 lb bombs. During the combat phase, the aircraft makes two passes each consisting of a 360° sustained turn, a 4000 ft energy increase, and a bomb drop of half its air-to-ground weapons. The aircraft is also designed for a ferry mission.

The low level primary mission is divided into 5 legs as described in the Request for Proposal (RFP)¹:

- Warm-up, taxi, takeoff, and accelerate to cruise speed.
- Dash at sea level at 500 knots or maximum speed at military power for 250nm.
- Combat phase.
- Dash at sea level at 500 knots or maximum speed at military power to return to base.
- Land with fuel for a 20 minute loiter at sea level.

The high-low-low-high, or secondary mission legs are:

- Warm-up, taxi, takeoff, and accelerate to cruise speed.
- Climb on course at intermediate power to best cruise altitude and speed.
- Cruise outbound at best altitude and speed to a total accumulated range of 150nm.
- Descend to sea level.
- Loiter at sea level at best speed for maximum endurance.
- Dash 100 nm at sea level.
- Combat phase.
- Dash 100 nm at sea level.
- Climb on return course to best cruise altitude and speed.
- Cruise back to base at best altitude and speed.
- Descend to sea level.
- Land with fuel for a 20 minute loiter at sea level.

The ferry mission consists of:

- Warm-up, taxi, takeoff, and accelerate to cruise speed.
- Climb on course at intermediate power to best cruise altitude and speed.
- Cruise outbound at best altitude and speed for at least 1500nm.
- Descend to sea level.
- Land with fuel for a 20 minute loiter at sea level.

The ferry mission is performed with all 20 Mk-82 bombs replaced with fuel. Air-to-air refueling is not used during this mission; however, a provision is made for in-flight refueling during other flights. Mission profiles are graphically represented in Figure 2-1.

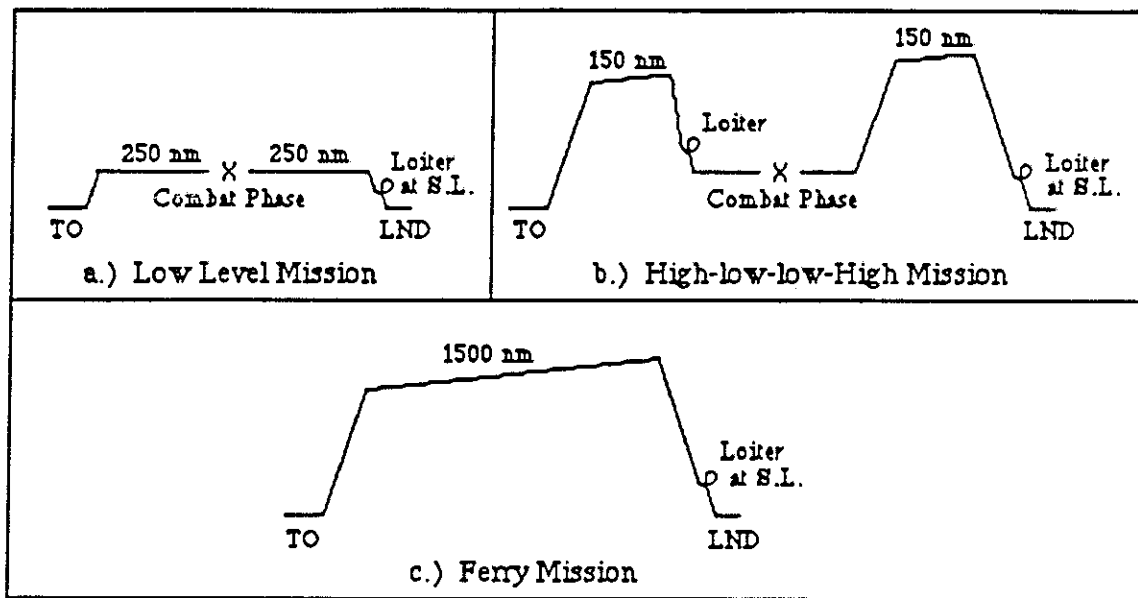


Figure 2-1: Mission profiles

As well as MIL SPEC handling quality standards, the aircraft meets or exceeds the following RFP defined point performance requirements:

- acceleration from 0.3 to 0.5 Mach at sea level in less than 20 seconds,
- sustain a 4.5 g turn (6.0 instantaneous g loading),
- reattack time of less than 25 seconds,
- takeoff and land within 2000 feet on a hard dry surface.

3. Concept Selection

3.1 Relationship of Mission to General Design Configuration

The RFP¹ requirements for the CAS aircraft dictate a number of key configuration responses, as presented in Table 3-1.

Mission Specifications	Configuration Response
M = 0.76, SL Dash (Transonic)	<ul style="list-style-type: none"> • Wing sweep/thickness ratio, clean shape, optimized bomb placement
High Gust Environment	<ul style="list-style-type: none"> • Active gust relief system • Fatigue resistant structure with high moments of inertia • High W/S • Low $C_{L\alpha}$
High Threat Combat Zone Survivability Rapid Target Acquisition GAU-8 Cannon Operation Reattack Time	<ul style="list-style-type: none"> • Widely separated engines • Redundant systems, surfaces, power • Armor, flare, and chaff • LANTIRN pods • Wide field of view from cockpit • Side-force control • Six D.O.F. flight control system • High, side-mounted inlets to avoid gun gas ingestion • Muzzle flash suppression • Thrust vectoring • High T/W
Short Field Performance	<ul style="list-style-type: none"> • Blown flaps • L.E. flaps • Drooped ailerons • Variable sweep wings
Low Operation Cost	<ul style="list-style-type: none"> • Proven Technologies • Low fuel weight • Low maintenance
Payload of 20 MK 82 Bombs	<ul style="list-style-type: none"> • Low drag weapon arrangement

Table 3-1: RFP mission specifications and related configuration responses

Some of the more stringent requirements include: (1) the sea level dash, (2) the twenty-five second reattack time, and (3) the large weapons load. The low-level buffeting associated with the 500 knot, sea level dash can cause significant pilot discomfort. The twenty-five second reattack time requires tradeoffs between W/S, T/W, and aspect ratio. Weapons placement on the aircraft severely restricts other configuration choices, such as inlet and wing placement.

3.2 Baseline Design Concepts

Three distinct wing/control surface concepts were investigated for the CAS mission, as presented in Figure 3-1:

- Canard
- Variable-Geometry Wing with Aft Tail
- Conventional Wing/Tail

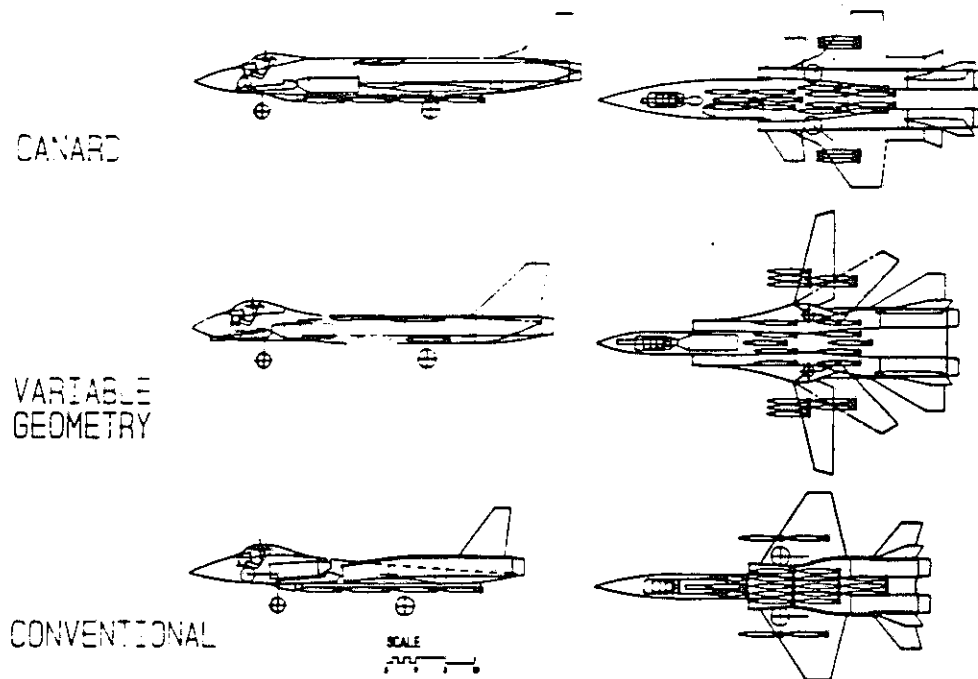


Figure 3-1: Baseline design concepts

These baseline concepts were derived from nine designs created by individual efforts. Each of the three concepts was sized independently in order to evaluate its unique capabilities afforded to the CAS mission.

3.3 Common Configuration Characteristics

In order to make a fair comparison of the three baseline concepts, certain features were incorporated into each design. These common features are specified in Table 3-2.

Concept Element	Reason
Moderate LE sweep Thin airfoil	Reduce transonic drag
Dual tail	Redundant control surface for survivability
20° cant on vertical tail	Avoidance of airflow blockage from body at high angles of attack
High, side-mounted engine inlets	Avoidance of gun gas, foreign object damage, and pilot egress difficulties
Wing shape	High taper to reduce structural fatigue Trapezoidal shape to best simulate elliptical lift distribution
Horizontal tail	Sized to meet T/O requirement Low mounted
Engine separation	Redundant system for survivability
Gun placement	Avoidance of pilot temporary blindness from muzzle flash Centered in aircraft to avoid force moments during use

Table 3-2: Common design features

3.4 Configuration Comparison

The baseline concepts weights were calculated using an in-house sizing routine. In the configuration comparison presented in Table 3-3, takeoff gross weight (TOGW) is used as a figure of merit closely related to aircraft cost.

	Conventional	Canard	Variable Geometry	A-10	Tomado
TOGW (lb)	48,100	53,200	55,500	50,000	60,000
T/W	0.94	0.69	0.66	0.40	0.53
Fuel (lb)	10,100	11,600	11,950	10,500	10,800
W/S ($\frac{\text{lb}}{\text{ft}^2}$)	153	166	202	99	190
T/O Distance (ft)	2000	2106	2191.7	4000	2950
Aspect Ratio	2.7	2.62	7.43/3.09	6.54	-

Table 3-3: Configuration comparison

As shown above, the conventional concept has the lowest TOGW. Also, the conventional aircraft has a relatively low W/S, however active gust alleviation is expected to relieve the associated cockpit g's. The canard aircraft's forward control surface provides positive lift during takeoff and is readily amenable to an active gust relief system. However, ammunition can access, underside bomb placement, and inlet system integration restrict canard placement such that the moment arm from the canard to the center-of-gravity is too small. The variable-geometry aircraft's high wing loading and low $C_{L\alpha}$ ($C_{L\alpha}=0.0524/\text{r}$, $\Lambda=70^\circ$) provide for passive buffet suppression, but the added structural weight and complexity of the wing configuration result in increased cost.

3.5 Performance Comparison

The carpet plots presented in Figures 3-2, 3-3, and 3-4 demonstrate the relationship between weights/sizing and point performance for each of the three baseline concepts. T/W and W/S are the variable parameters in these carpet plots. T/W is varied by using the Engine Scaling Factor (ESF) in the NASA-Ames developed ACSYNT (Aircraft Synthesis) code⁵. The three original configurations were designed based upon the takeoff, 4.5 g turn, and acceleration constraints specified in the RFP¹. In a later stage of the analysis, the twenty-five second reattack time requirement and ride quality considerations were determined to be the true driving constraints, as reflected in Figure 3-4. The takeoff, 4.5 g turn, and acceleration constraints shown in Figures 3-2 and 3-3 are satisfied by the conventional aircraft and fall below the range of the sizing carpet shown in Figure 3-4.

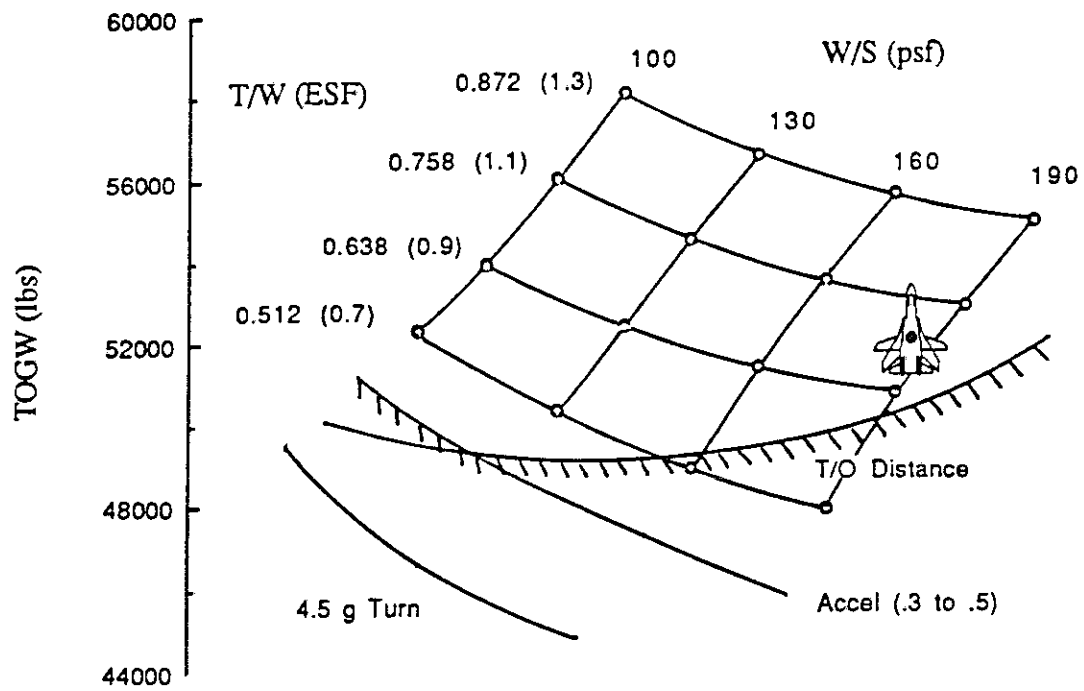


Figure 3-2: Variable Geometry Carpet Plot

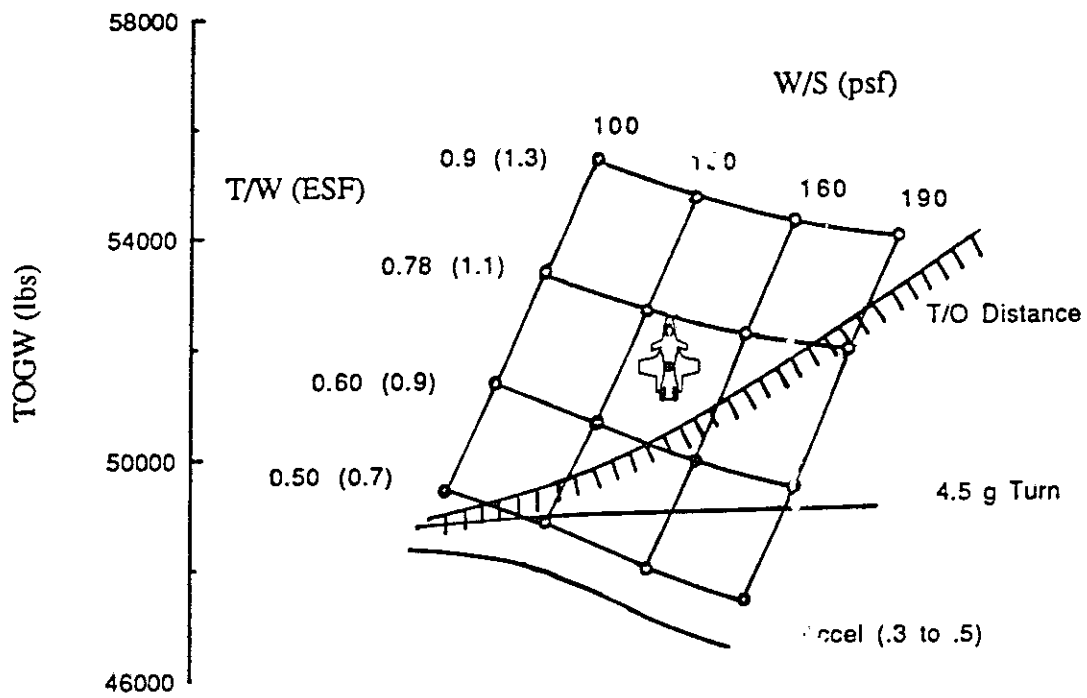


Figure 3-3: Canard Carpet Plot

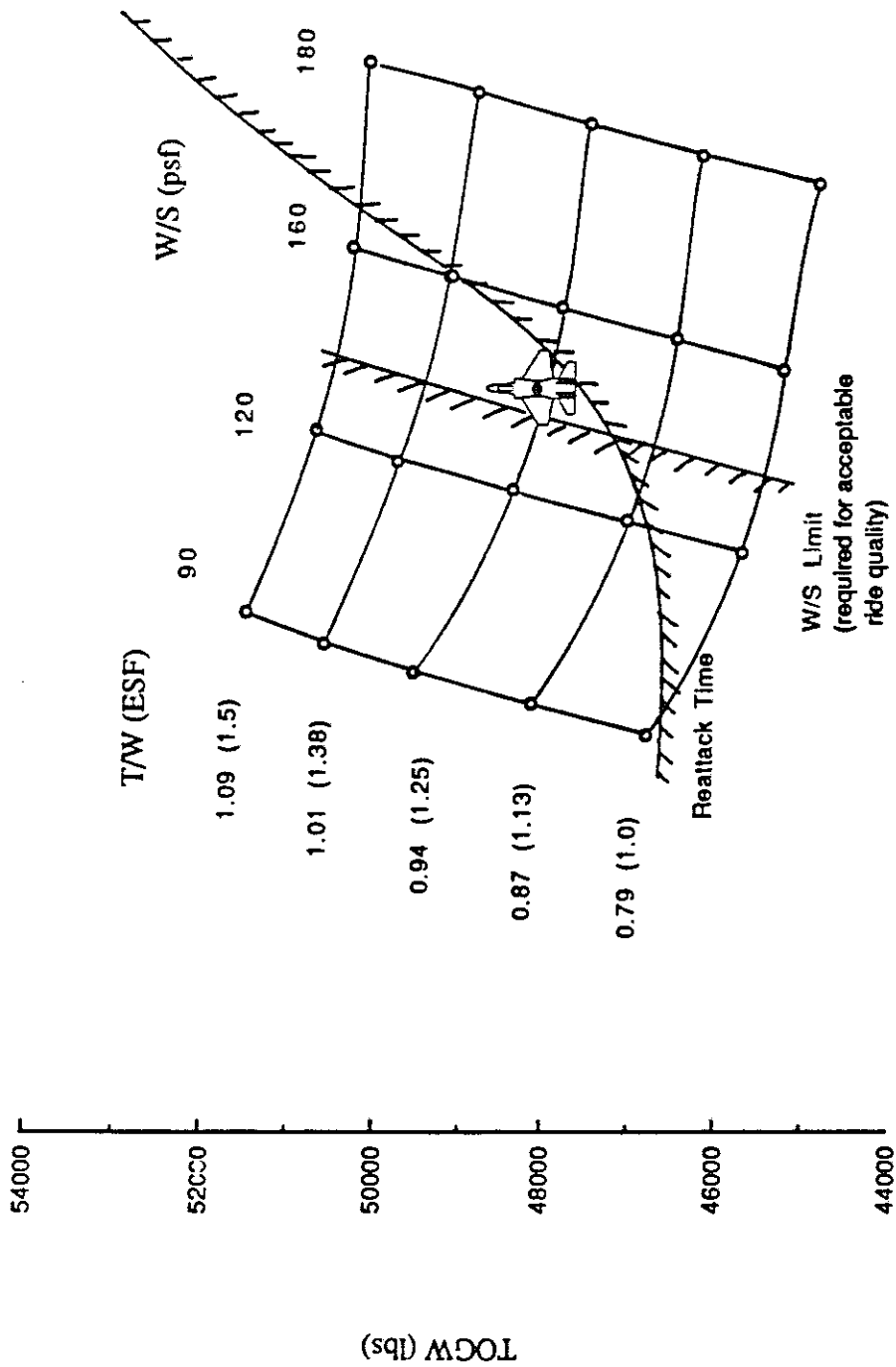


Figure 3-4: Griffen Carpet Plot

3.5 The Final Baseline Concept Selection

Table 3-4 lists the advantages and disadvantages of the three baseline concepts.

Configuration	Advantage	Disadvantage
Conventional	<ul style="list-style-type: none"> ▪ Low TOGW ▪ Short field performance ▪ Low cost ▪ Good reattack time ▪ Fast acceleration 	<ul style="list-style-type: none"> ▪ Less adaptable to alternate missions ▪ Less adaptable to a gust relief system
Canard	<ul style="list-style-type: none"> ▪ Positive canard lift for T/O ▪ Easily adaptability to an active gust relief system 	<ul style="list-style-type: none"> ▪ High installation thrust loss ▪ High weapons drag ▪ Poor ordnance integration
V.G.	<ul style="list-style-type: none"> ▪ Small weapons drag ▪ Adjustable wing sweep for optimal performance ▪ High wing loading ▪ More adaptable to alternate missions 	<ul style="list-style-type: none"> ▪ High TOGW ▪ Sluggish roll performance ▪ Structurally complex wing spar

Table 3-4: Concept selection considerations

The conventional concept, dubbed the Griffen CAS aircraft, was chosen for development for the reasons listed below:

- 5,000 - 7,000 lb lower TOGW; translating into lower aircraft acquisition cost
- Ability to meet and exceed the RFP¹ point performance requirements
- 15% lower fuel weight; translating into lower aircraft operating cost

4. Configuration

4.1 Basic Configuration

The Griffen is a twin-engine, single seat CAS aircraft with a low wing, dual vertical tails and an all-flying horizontal tail, providing pitch and roll control. The three view and inboard profile of the Griffen are shown in Figures 4-1 and 4-2 (Numbers in parentheses refer to items in Figure 4-2).

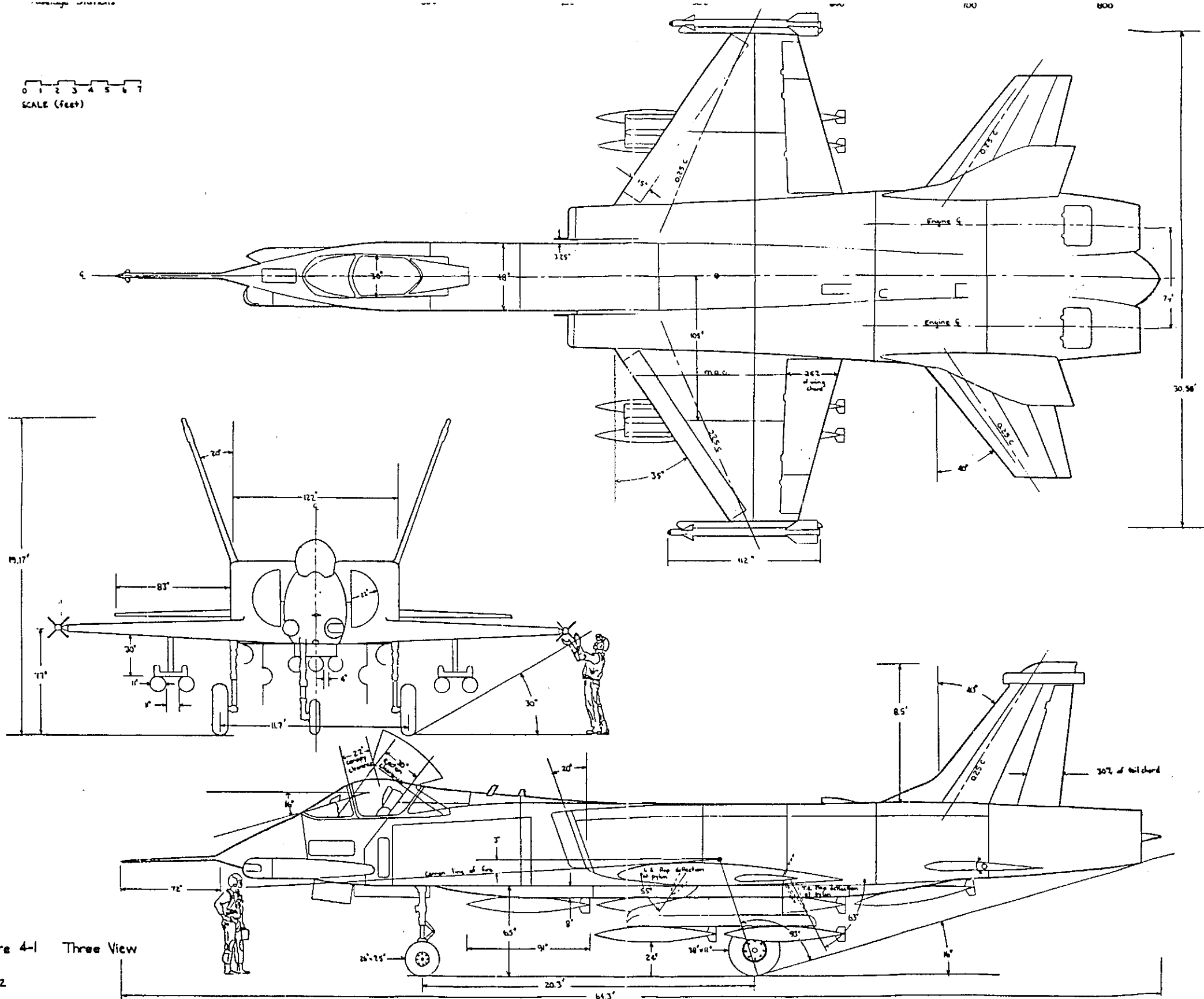
The two engines, mounted in the aft fuselage section, are separated by 74 inches to reduce the likelihood of one engine damaging the other in the event of failure. The engines are equipped with thrust vectoring and reversing exhaust nozzles (79) and are supported by four rear bulkheads. The airframe mounted accessory drives (AMAD)(63) with two independent 4000 psi hydraulic systems and two independent electrical generators, are mounted to the bulkhead at station 615. Access to the AMAD is easily achieved from under the fuselage by removing the rearmost bomb rack pallet when the Griffen is in the combat configuration. During normal peacetime operations the Griffen is flown without pallets to reduce operational costs making access to the AMAD routine.

The engine ducts (28) are side-mounted and run above the wing spar. The inlets are spaced three inches from the fuselage surface and equipped with a splitter plate (27) to prevent boundary layer ingestion. The inlet face is initially semicircular, gradually becoming near rectangular before transitioning to a circular shape to match the engine face. The duct cross section shape is optimized throughout its length for a smooth area transition and maximum use of space inside the aircraft.

The wings are mounted low to allow the landing gear (45) to be stowed in and beneath the wing and to allow all fuel to be placed in the fuselage where it is less vulnerable to ground fire. The control surfaces on the wing include a blown flap (25% chord)(54), a full-span, fixed-width leading edge flap (44), and an outboard aileron (55) that can split for braking or be used in conjunction with rudder deflection for side-force generation.

The nose landing gear (19), has a 26 x 8 inch tire and is offset to avoid the gun barrel (20) which is located on the aircraft's centerline. The nose gear is stowed under the pilot and swings down and rearward into position. The main gear, each with a 38 x 11 inch tire for soft field operation, also swings down and rearward but the wheel requires a 90° rotation to store flat inside

0 1 2 3 4 5 6 7
SCALE (feet)



GEOMETRIC DATA

Spans, Aspect Ratios, Chords and Lengths	
Fuselage length	56.25 ft
Canopy length	11.25 ft
Duct length	17.08 ft
Wing span	30.58 ft
Horizontal tail span (exposed)	14.33 ft
Vertical tail height (exposed)	8.50 ft
Root chord	18.66 ft
Tip chord	3.60 ft
Wing M.A.C.	12.83 ft
Horizontal tail M.A.C. (exposed)	5.58 ft
Vertical tail M.A.C. (exposed)	6.34 ft
Wing AR	2.67
Horizontal tail AR	2.57
Vertical tail AR	1.47
T.E. flap span	14.08 ft
Droop aileron span	4.58 ft
L.E. flap span	19.17 ft

Areas	
Wing	350.0 ft ²
Horizontal tail (exposed)	80.0 ft ²
Vertical tail (exposed)	98.0 ft ²
T.E. flaps	42.0 ft ²
Droop ailerons	6.6 ft ²
L.E. flaps	35.4 ft ²
Rudder	30.6 ft ²

Wetted Areas	
Fuselage	920 ft ²
Canopy	65 ft ²
Wing	405 ft ²
Horizontal tail	160 ft ²
Vertical tail	196 ft ²

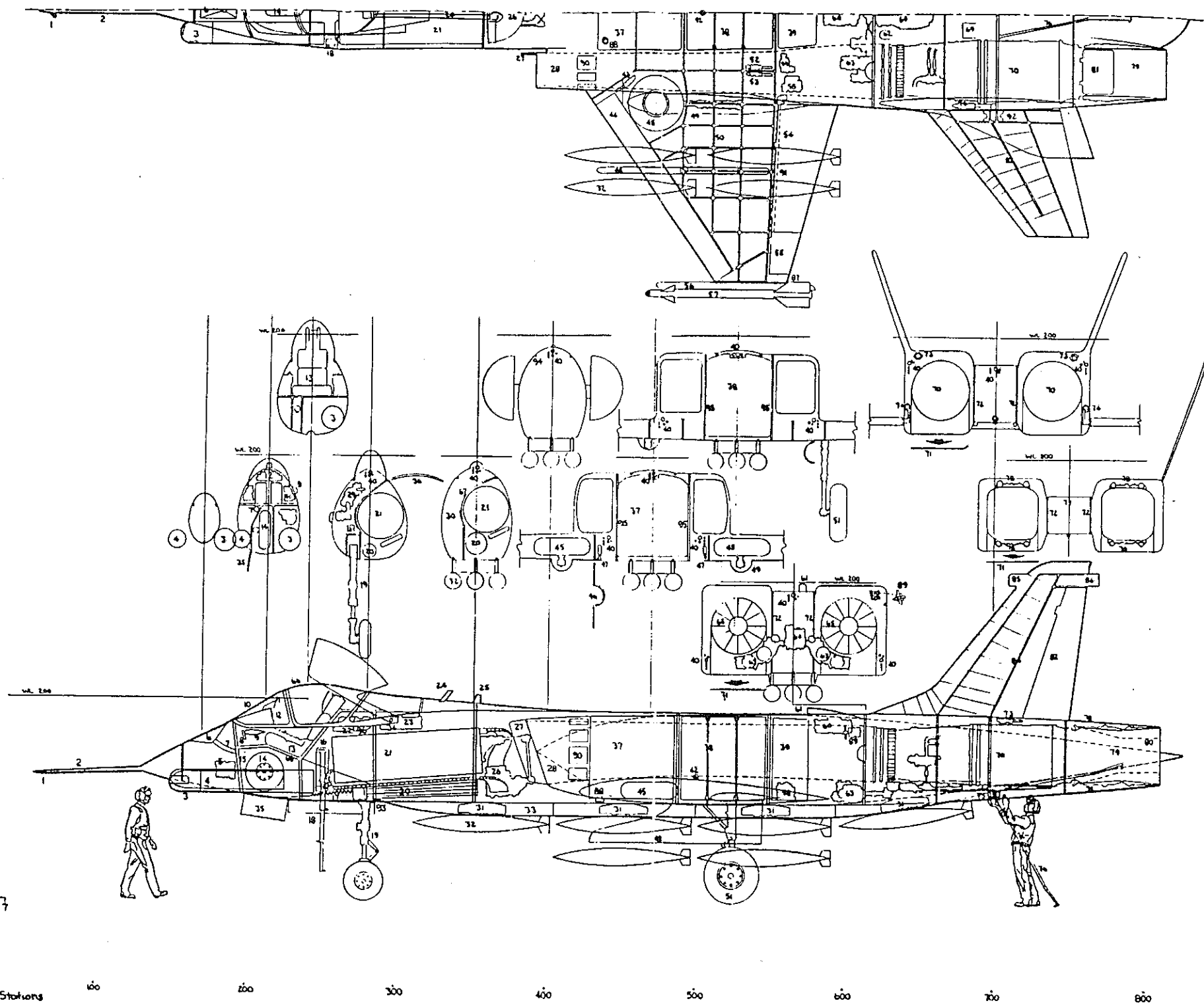
Angles	
Wing L.E.	35°
Wing quarter-chord	26°
Wing T.E.	-13°
Horizontal tail L.E.	40°
Horizontal tail quarter-chord	35°
Horizontal tail T.E.	15°
Vertical tail L.E.	40°
Vertical tail quarter-chord	35°
Vertical tail T.E.	15°
Wing dihedral	3°
Horizontal tail dihedral	0°
Vertical tail outboard cant	20°
Wing incidence Angle	1°

Taper Ratios, Thickness to Chord Ratios	
Wing taper ratio	0.193
Horizontal tail taper ratio	0.452
Vertical tail taper ratio	0.334
Wing t/c	0.10
Horizontal tail t/c	0.08
Vertical tail t/c	0.06

Engines (uninstalled at S.L.)	
Thrust (A/B)	40,380 lbs
Thrust (non A/B)	22,517 lbs
Bypass ratio	1.8
Overall pressure ratio	27

Deflections	
Ailerons	± 25°
L.E. flaps	+ 30°
T.E. flaps	- 50°
Rudder	± 30°
Horizontal tail	± 35°

Figure 4-1 Three View



Inboard Profile Components

- | | |
|---|---|
| 1.) AOA and sideslip sensor | 49.) blister for main strut |
| 2.) sensor boom | 50.) wing spars |
| 3.) LANTIRN targeting pod | 51.) main gear (extended) |
| 4.) LANTIRN navigation pod | 52.) trailing edge flap hydraulic actuator |
| 5.) gust relief computer | 53.) aileron/airbreak hydraulic actuator |
| 6.) inflight refueling receptacle | 54.) trailing edge flap |
| 7.) refueling fuel line | 55.) aileron/speedbreak |
| 8.) rudder pedal | 56.) missile launch rail |
| 9.) forward radar warning antenna | 57.) AIM-9L sidewinder |
| 10.) plexiglass windscreen | 58.) hydraulic reservoir |
| 11.) HUD | 59.) fuel pump |
| 12.) cockpit instrument panel | 60.) heat exchanger |
| 13.) ejection seat | 61.) heat exchanger intake port |
| 14.) nose wheel (retracted) | 62.) heat exchanger exhaust port |
| 15.) forward pressure bulkhead | 63.) AMAD |
| 16.) rear pressure bulkhead | 64.) jet fuel starter |
| 17.) gun gas deflector | 65.) engine compressor face |
| 18.) telescoping entry ladder | 66.) canopy |
| 19.) nose gear (extended) | 67.) ammunition canister armor |
| 20.) GAU-8 cannon | 68.) cockpit armor |
| 21.) ammunition canister | 69.) jet fuel starter exhaust port |
| 22.) flight control computer | 70.) engine |
| 23.) canopy hydraulic actuator | 71.) engine maintenance access panel |
| 24.) VHF/AM antenna | 72.) engine firewall |
| 25.) IFF antenna | 73.) rudder hydraulic actuator |
| 26.) ammo feed mechanism | 74.) horizontal tail hydraulic actuator |
| 27.) splitter plate | 75.) horizontal tail pivot |
| 28.) engine inlet duct | 76.) emergency arrestor hook |
| 29.) environmental control system | 77.) flare/chaff dispenser |
| 30.) avionics bay | 78.) thrust vector actuator |
| 31.) bomb ejector | 79.) thrust vectoring nozzle (augmented position) |
| 32.) Mk-82 | 80.) non-augmented nozzle position |
| 33.) conformal carriage pallet | 81.) thrust reversal exhaust vent |
| 34.) battery | 82.) rudder |
| 35.) nose gear bay door | 83.) horizontal tail spars |
| 36.) ammunition can access door | 84.) vertical tail spars |
| 37.) fuel tank #1 | 85.) VOR antenna |
| 38.) fuel tank #2 | 86.) rear warning radar antenna |
| 39.) fuel tank #3 | 87.) fuel jettison port |
| 40.) electrical and hydraulic lines | 88.) single point refueling port |
| 41.) radio | 89.) ram air turbine |
| 42.) takeoff cg location | 90.) auxiliary air intake doors |
| 43.) leading edge flap hydraulic actuator | 91.) trailing edge flap blowing duct |
| 44.) leading edge flap | 92.) horizontal tail pivot spigot |
| 45.) main gear (retracted) | 93.) jack points |
| 46.) main gear bay door | 94.) longerons |
| 47.) main gear door hydraulic actuator | 95.) keel |
| 48.) wing pylon | 96.) onboard oxygen generation |

0 1 2 3 4 5 6 7
SCALE (feet)

Fuelage Stations 100 200 300 400 500 600 700 800

Figure 4-2 Inboard Profile

the wing on retraction. To retain the structural integrity of the wing box, the main gear struts are not stored in the wing, but are covered by a fairing underneath the wing box. In an emergency situation both the nose and main gear extend by gravity and lock-down by dynamic pressure.

A key consideration in designing an aircraft for a CAS mission is pilot comfort and work load. A high wing loading and an active gust relief system are incorporated to lower cockpit g-levels. An angle of attack sensor (1) is installed in a six foot boom attached to the nose of the aircraft as part of this system. Information management systems are used to reduce the work load required to fly the aircraft so that the pilot may concentrate on the attack procedures.

High sortie rates are achieved by using a palletized bomb system (33). Two sets of bombs pallets are used so that, while the aircraft is flying its mission with one set of pallets, the other set is back at its base being preloaded with bombs. When the aircraft returns from its mission its empty pallets are removed and the loaded ones quickly raised into place. The second set of pallets can be attached to the first allowing the aircraft to transport all of its own equipment wherever needed. To facilitate rapid repairs and maintenance, major aircraft systems are accessible to mechanics on the ground. No routine maintenance work requires platforms or other special equipment. For removal, the engines are slid rearward on a supporting rail and onto an engine trolley.

4.2 Survivability and Vulnerability

The Gr.7en's configuration along with lightweight armor protection enhances the survivability of critical flight systems and surfaces. The design process was carried out with survivability and vulnerability issues in mind, evidenced in the redundant vertical tails, separated engine layout, wing spar structure, and the Low-Altitude Navigation and Targeting Infrared System for Night (LANTIRN)(3,4) system placement. A summary of key survivability issues is presented in Table 4-1.

One of the most vulnerable components of the aircraft is the pilot. Due to the nature of the CAS mission, the cockpit will be subjected to intense ground fire mainly from 7.62, 14.3, and 23mm cannon fire². The fore and aft sections of the cockpit are protected by titanium armored bulkheads while ventral and side shielding is provided by Kevlar 29 with an outer lining of ceramic material to defeat armor piercing projectiles. Kevlar is chosen over titanium because of its lighter

Vertical Tail	<ul style="list-style-type: none"> ▪ Sized to fly with one fin only ▪ Separation reduces likelihood of single hit destroying both fins
Engines	<ul style="list-style-type: none"> ▪ Aircraft can fly with one engine out ▪ Separation reduces likelihood of single hit destroying both engines
Wing Spars	<ul style="list-style-type: none"> ▪ Titanium wing spars and supporting bulkheads allow operation with any one spar completely severed
LANTIRN	<ul style="list-style-type: none"> ▪ Placed in nose to reduce exposure to ground fire

Table 4-1: Survivability and vulnerability issues

weight, lower material and construction cost, and greater energy absorption capability.

The ammunition can (21) is also protected to avoid detonation of the shells. Drum shielding is provided through a layered system. The drum is placed away from the aircraft skin and is surrounded on the lower and starboard sides by Ceramic/Kevlar 29 and on the port side by the titanium access door. The fuselage around the drum is not armored in the normal sense, but is fitted with spoil (trigger) plates to detonate an incoming round before it reaches the drum.

The engine area is also susceptible to ground fire and is protected by titanium armor because of limited space requirements and higher temperature considerations. Protection in this region consists of ventral shielding, firewalls (72) between and in front of the engines, and empennage surface actuator coverings.

In order to maintain system operation there will be a quadruple redundant flight control system along with three independent hydraulic lines (40) for redundancy. The fluid in the hydraulic lines is non-flammable so, in the event of a ruptured line, it will not start or spread a fire. Further, the vertical tail is sized for single control capability. The large moment arm from the center of pressure of the vertical tail to the cg (18 ft), keeps the tail area, and in particular the height, smaller than the F-15 Eagle. Thus the Griffen is guaranteed to fit in Air Force bunkers suitable for the F-15.

The fuselage fuel tanks (37, 38, 39), are self-sealing bladder tanks, interconnected to equalize fuel levels and maintain the cg location. The three cells are also independently connected to the engines so each tank can supply fuel. There is also armor shielding (ceramic/Kevlar 29) underneath

the mid fuel tank to assure enough fuel for a return-home flight. Empty space between the aft fuel cell and the engine is available for future mission fuel considerations.

In the event of an emergency landing, a yoke type arresting hook (76) is available to assist in stopping the aircraft. The hook is located at station 697 with the yoke attached to the low two inner longerons.

4.3 Weapons

The Griffen carries 20 Mk-82 500 pound bombs (32), 2 AIM-9L Sidewinder missiles (57) and is armed with a GAU-8 30mm cannon (20). The cannon is located below and behind the cockpit and is equipped with a gun gas deflector (17) so that muzzle-flash does not blind the pilot. The gun's barrels are angled down at 3° to direct the recoil force through the aircraft's center of gravity. The ammunition can carries 1350 rounds and is located above the cannon. This arrangement shortens the cannon system and allows access to the cannon and the ammunition drum through a single door. The can is removed by rotating it about a pivot point.

Bombs are loaded on the aircraft in the following arrangement:

- 4 rows of 3 bombs placed under the fuselage, each row on a preloadable pallet.
- 4 bombs carried on each wing on dual tandem vertical ejection racks.

The bombs under the fuselage use the conformal weapons carriage system tested on the F-4 Phantom II³. In this arrangement, the racks are hidden from the airstream by a low-drag fairing. A picture of the arrangement on an F-4 is shown in Figure 4-3. Bombs are attached to removable pallets which bolt directly to longerons. Bombs not stored under the fuselage are carried on wing pylons (48) 115 inches from the aircraft centerline. These pylons are sufficiently deep to accommodate auxiliary fuel tanks or large-finned guided weapons. The entire bomb load is centered about the takeoff cg location.

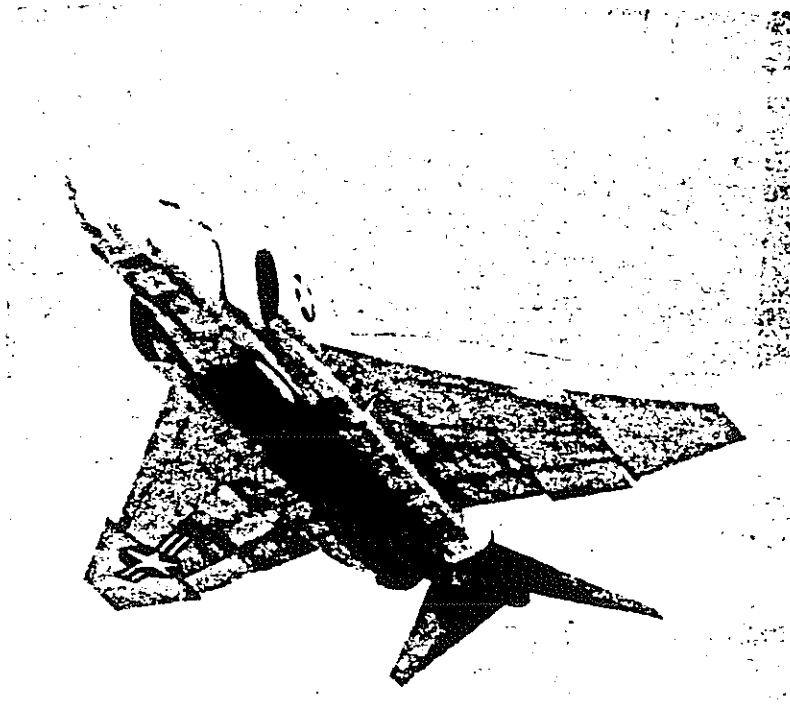


Figure 4-3: F-4 with conformal weapons carriage³

The conformal weapons carriage provides several benefits:

- improves aircraft performance due to reduced external stores drag and reduced drag of the empty weapons carriage system
- improved stores separation
- improved aircraft handling qualities
- versatility for carrying future weapon shapes

The ejector loads are directly transferred to a keel beam (95) thereby imparting full ejector velocity to the bomb. This improves the reproducibility and accuracy of the bomb drops. Finally, the low weapons drag allows for the possibility of supersonic speeds in future Griffen designs.

For the ferry mission six 300 gallon auxiliary fuel tanks can be carried on the weapon stations with one tank on each wing pylon and four under the fuselage, mounted in a dual tandem configuration on the pallet's outer racks.

5. Weights and Balance

5.1 Weights

The Griffen in the primary mission takeoff configuration has a gross weight of 48,145 lbs. with a wing loading of 137 psf and a wet thrust to weight ratio of 0.857. 12,345 lbs. of expendable ordnance is carried along with 10,118 lbs. of fuel. Pitching, rolling, and yawing moments of inertia about the aircraft center of gravity (cg) and aligned with the principle axes in sl-ft² are 197,153, 26,413, and 212,843, respectively. Table 5-1 presents the aircraft gross weight, three principle moments of inertia, and cg location as percentage of total aircraft length for the takeoff, start of return dash, and approach to landing points in the mission.

	Takeoff	Begin Return Dash	Approach to Landing
Gross Weight (lbs)	48,145	32,878	28,728
I _{yy} (sl-ft ²)	197,153	171,838	168,898
I _{xx} (sl-ft ²)	26,413	14,504	14,020
I _{zz} (sl-ft ²)	212,843	180,296	177,416
cg (% fuselage len.)	55.4	55.6	55.4

Table 5-1: Weight, moment, and balance data

A summary weights statement is presented in Table 5-2 containing a breakdown of component weights and cg locations, referenced to the fuselage stations in Figure 4.1 (in-board profile). The Griffen incorporates a mix of armor, using low weight Kevlar to protect the cockpit, ammunition canister, and return dash fuel tank while titanium shields the airframe mounted auxiliary drive and engine cores where space is at a minimum and Kevlar would be too bulky. The Kevlar achieved a 25% net weight reduction over equivalent titanium protection. Composite materials are also used in the wings, vertical tails, horizontal tail, and fuselage, providing respective 20.0%, 31.7%, 31.3%, and 8.0% weight savings over comparable conventional structures. The details of

Configuration	Weight		X	Y	WX	WY
Griffen						
Wing (incl. surfaces)	1433		506	135	725098	193455
Vertical tail (incl. surfaces)	538		714	224	384132	120512
Body	2862		455	160	1302210	457920
Alighting gear	1266	up / down	463 / 487	135 / 107	586158/616542	170910/135462
Arresting gear	85		712	138	60520	11730
Engine section	73		660	161	48180	11753
Air induction	840		517	163	434280	136920
Horizontal tail	215		715	138	153725	29670
Structure subtotals -lbs	7311	gear up	505	155	3694303	1132870
Structure/TOGW	0.1506	gear down	509	150	3724687	1097422
Structure/wt.empty	0.3329					
Propulsion						
Engine installation	5853		680	166	3980040	971598
Accessory gearbox	295		603	141	177885	41595
Exhaust system	42		762	165	32004	6930
Thrust vectoring system	600		760	165	456000	99000
Engine controls	54		603	141	32562	7614
Starting system	50		603	141	30150	7050
Lube system	77		680	166	52360	12782
Fuel system	1094		499	162	545906	177228
Inflight refuel system	50		180	170	9000	8500
Flt. controls (incl. autopilot)	781		590	139	460790	108559
Instruments	151		212	175	32012	26425
Hydraulic and pneumatic	172		590	139	101480	23908
Electrical	766		455	150	348530	114900
Avionics	2425		252	158	611100	383150
Armor	1520		478	152	726560	231040
Furnishings & equipment	218		247	170	53846	37060
Air conditioning & anti-ice	348		452	158	157296	54984
Load and handling group	15		455	150	6825	2250
Weight empty - lbs	21821	gear down	529	156	11539033	3411995
Crew	225		240	178	54000	40050
Fuel - unusable	573		499	162	285927	92826
Fuel - usable	9546		499	162	4763454	1546452
Ammunition (1350 rds)	1485		311	159	461835	236115
Flare and chaff	370		685	144	253450	53280
Stores						
Sidewinders (2)	390		532	135	207480	52650
Mk 82 (20)	10100		499	117	5039900	1181700
Rail launchers	174		532	135	92568	23490
Pylons & racks	1000		499	130	499000	130000
Cannon	2461		345	136	849045	334696
Useful load	26323		475	140	12506659	3691259
Zero fuel & stores gross wt.	26254		507	153	13319573	4017601
Zero fuel gross weight	38599		499	144	19282238	5556802
Takeoff gross weight	48145		499	147	24045692	7103254

Table 5-2: Summary weight and balance sheet

the composite weight savings are presented in the Materials Selection section. 370 lbs. of flares and chaff have been added to the expendable stores for enhanced survivability. The two LANTIRN pods, weighing nearly 1000 lbs uninstalled, contribute to the relatively heavy 2,425 pounds of installed avionics. Their location in the nose adds 13,500 sl-ft² to the pitching moment of inertia, nearly two-thirds the moment of one engine. Both the cannon and the ammunition canister generate similarly large moments, all of which leads to a total pitching moment of inertia roughly 50% larger than is common for planes of comparable wing planform area and gross weight. This large I_{yy} serves to damp gust induced pitching. The two-dimensional thrust vectoring system increased the weight of each engine by 300 lbs. over the standard referee engine.

The Griffen was sized using two independent methods, both of which yield the results of Table 5-2. Raymer⁴ chapters 3, 6, 15, and 19 formed the basis of an in-group sizing program to check the performance of ACSYNT⁵, a commercially available sizing program developed by NASA-Ames and available through The ACSYNT Institute located at Virginia Tech. The weights shown earlier in the carpet plot of Figure 3-2 were generated by ACSYNT for the various thrust to weight and wing loading permutations.

5.2 Balance

A side profile of the individual component cg locations L_c provided in Figure 5-1. The Griffen is balanced for a -4.5% takeoff static margin, with placing the cg at only 55.4% of the total fuselage length, as opposed to 58-65% in most aircraft, the moment arm L_c to the pilot, and hence the gust induced cockpit g-level, is minimized. Symmetric Mk-82 bomb installation around the cg coupled with an even fuel weight distribution about the same point confines the cg travel during flight to only 3 in. for all three missions. Figure 5-2 contrasts the static margin shift through the flight regime for the primary mission with a maximum cg excursion represented by expending all ordnance over the battlefield. Three self-sealing bladder tanks between bulkheads in the fuselage contain the 10,118 lbs. of trapped and usable fuel. Tank #1, measuring 74x50x57 in³, contains 4245 lbs. of fuel with a cg at X = 457. Tank #2, 54x49x58 in³, holds 4248 lbs. at X = 517 and 1625 lbs. at X = 562 are in the 34.20 ft³ tank #3. Placing no fuel in the wings provides ample

room for high-lift blowing ducts while eliminating the risk of fire or explosion when the wings are pierced by gunfire or shrapnel, increasing survivability. It also allows high sortie rates even with crudely patched, battle damaged wings. Tank #2 is the "go-home" fuel tank. It is protected by forward and aft bulkheads, residual fuel in the tanks fore and aft, the skin and duct structures on the side, and Kevlar armor below. Tank scheduling to maintain the -3.9% to -5.8% static margin shown in Figure 5-2 proceeds as follows: burn 3,000 lbs in tank #1, switch to tank #3 until empty, burn another 600 lbs. from tank #1 over the battlefield, burn 2,500 lbs. from tank #2 for the return dash, empty tank #1, and switch to Tank #2 for loiter and landing.

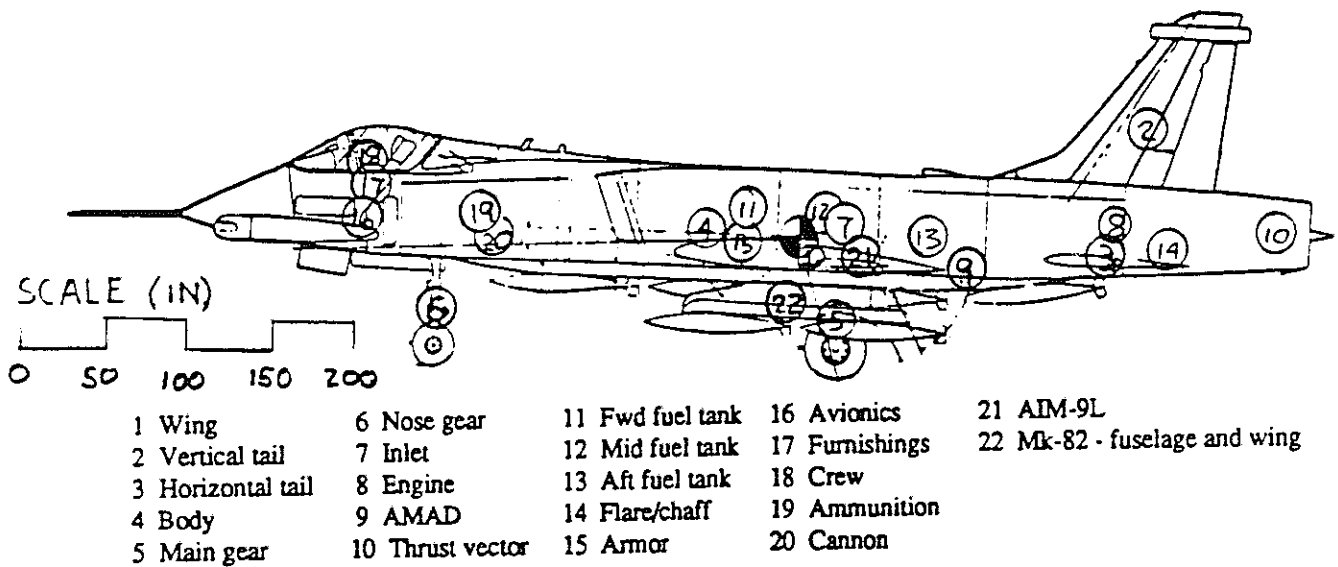


Figure 5-1: Side cg profile

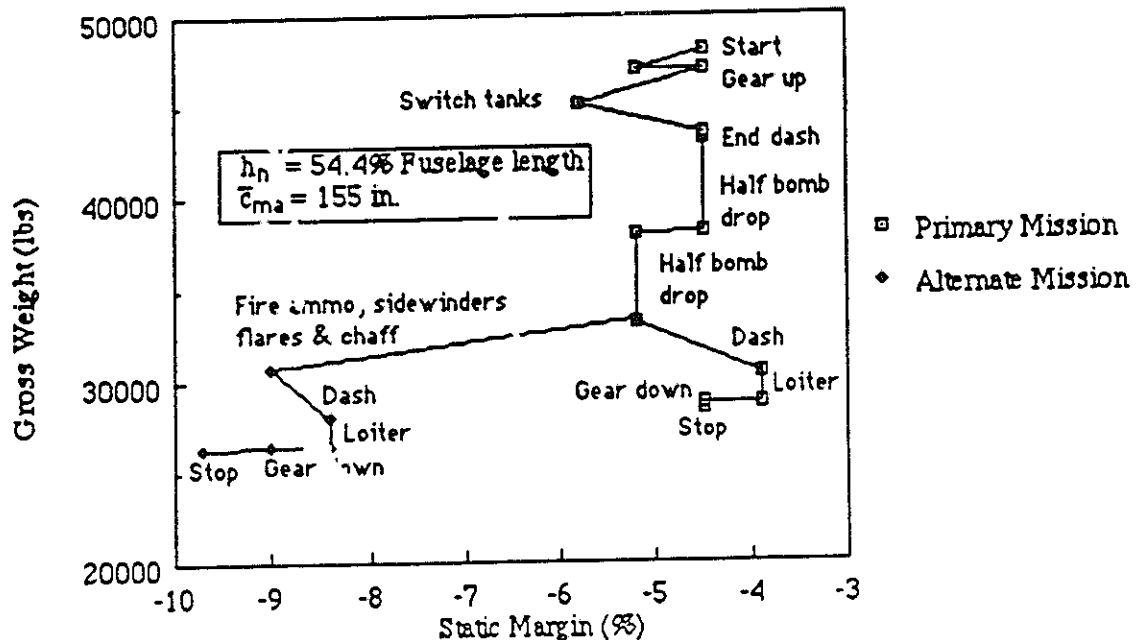


Figure 5-2: cg travel during flight

6. Aerodynamics

Mission requirements impose certain aerodynamic considerations on the design of the aircraft. Low drag is desirable to reduce the weight and becomes particularly important at low altitude where the dynamic pressure is highest. Transonic wave drag at cruise affects the selection of airfoils and the wing planform as does the takeoff/landing requirement.

6.1 Wing Geometry

The Griffen features a trapezoidal wing planform of high taper and moderate sweep. A taper ratio of 0.19 was chosen as a compromise between reduced wing structural weight and a near-elliptical span loading for minimized induced drag. The moderate sweep angle allows an elliptical span loading to be achieved with little wing twist, reducing the trim drag penalty at off-design flight conditions. Wing dimensions and parameters are presented in Table 6-1.

b	30.6 ft
S	350 ft ²
AR	2.67
λ	.193
c_r	18.66 ft
\bar{c}	12.83 ft
Δ_{LE}	35°
Δ_{TE}	-13°
$\Delta_{c/4}$	26°

Table 6-1: Wing dimensions and parameters

6.2 Airfoil Selection

The airfoil section for the Griffen was chosen for high lift capability and a moderate thickness for reduced wing structural weight. Because of the low sweep of the maximum thickness line

(15.9° at 41% chord), supercritical airfoil technology ⁶ was employed to delay transonic drag rise. The following airfoils were selected for use on the Griffen:

- Wing: SC(2)-0010
- Horizontal Tail: NACA 64A-008
- Vertical Tail: NACA 64A-006

An uncambered airfoil was selected due to the low C_L required during the cruise segments. The wing is set nominally at 1° incidence to the fuselage to reduce the fuselage angle of attack during flight. When higher lift is required, camber can be simulated through flap deflection. An illustration of the wing supercritical airfoil is shown in Figure 6-1.

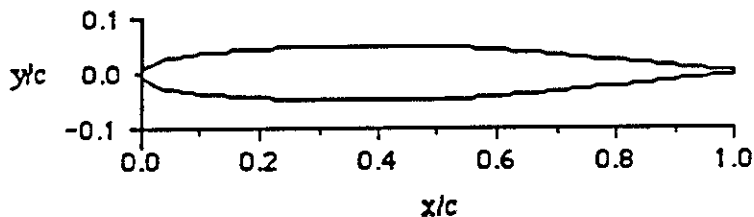


Figure 6-1: SC(2)-0010 supercritical airfoil

6.3 Design and Prediction of Lift

Section lift and pitching moment coefficient data as well as pressure distribution data were calculated for the supercritical airfoil using PANEL ⁷, a two-dimensional incompressible potential flow code. The stall limits for the airfoil were estimated from data in Abbott and von Doenhoff ⁸ for a NACA 64A-010 airfoil, which has a shape similar to the supercritical airfoil. Data for the empennage airfoil sections were also obtained from Reference 8.

The airfoil pressure distribution is particularly important at transonic speeds to ensure minimum local supersonic flow for minimum wave drag. To analyze the transonic flow over the supercritical airfoil, FLO36 ⁹ was used. FLO36 is an inviscid, two-dimensional potential flow code which uses conformal mapping to satisfy the boundary conditions exactly. An illustration of the pressure distribution at the design C_L for cruise is shown in Figure 6-2.

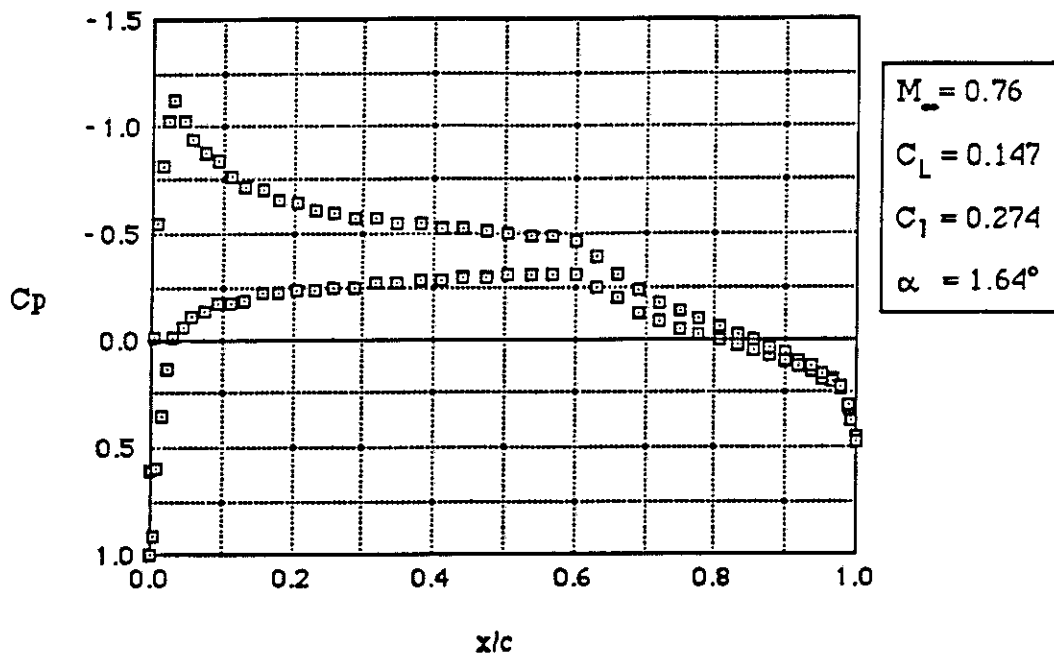


Figure 6-2: Pressure distribution on SC(2)-0010 airfoil at cruise

The pressure distribution does not show the aft loading typical of most supercritical airfoils. This helps to reduce the pitching moment during cruise. The flow expansion around the leading edge does not produce large negative pressures, reducing the possibility of flow separation and preventing local supersonic flow at the leading edge. Results from FLO36 show that no supersonic flow exists on the airfoil at cruise.

A vortex-lattice method code, VLM49^{7 10}, was used to obtain neutral point, lift-curve slope, and span load data for the Griffen over a range of Mach number and lift coefficient. The VLM geometries included proper dihedral and vertical separation between planforms, when appropriate, but no camber or twist. Because of the moderate wing sweep, no vortex lift augmentation was calculated.

The lifting ability of the Griffen is shown in Figure 6-3 for low-speed and cruise Mach numbers and for an approach condition. C_{Lmax} and α_{CLmax} were approximated from Raymer⁴. For an unflapped wing, stall occurs at $\alpha = 20^\circ$ at $C_L = 1.13$. Based on the weight at the start of the outbound cruise leg, the Griffen flies at $\alpha = 2.5^\circ$ for a $C_L = 0.15$.

In order to meet the takeoff/landing requirements specified in the RFP¹, the Griffen employs the following high-lift devices:

- 25%-chord, 75%-exposed span plain, blown flaps
- fixed-chord (9.74% mac), full-span leading edge flaps
- 25%-chord, 25%-exposed span droop ailerons

An illustration of the high-lift devices is found in Figure 4-2.

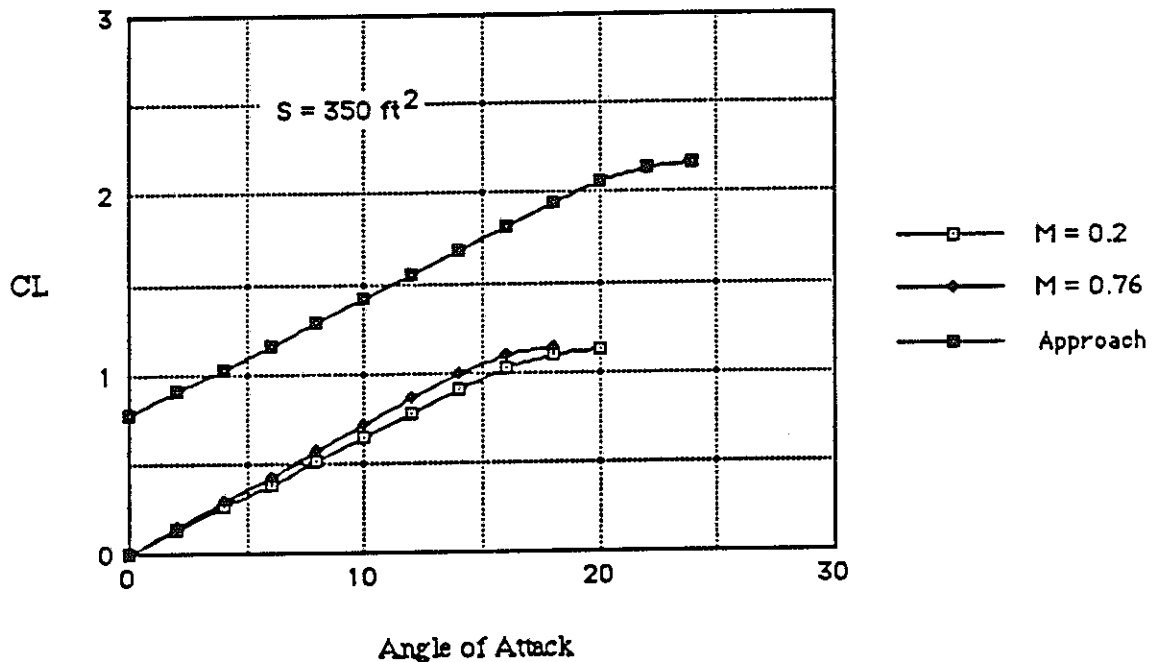


Figure 6-3: Lift prediction

Device effectiveness was estimated from Reference 4 and from experimental data in Lachmann¹¹ and Carr¹². A breakdown of the maximum lift contributions is shown in Figure 6-4. Note that the lift increment for blowing is virtually the same as for flap deflection, blowing thus doubling the effect of the deflected flap. The lifting ability of the aircraft with high-lift devices is shown in Figure 6-3. With the high-lift devices, stall occurs at $\alpha = 24^\circ$ at a $C_L = 2.16$. For an approach condition, the aircraft flies at an angle of attack, $\alpha = 10^\circ$.

The leading edge flaps are also used during combat to improve the lift on the wing and to prevent flow separation. An added advantage of the constant-chord leading edge flaps on the highly-tapered wing is that they effectively provide conical camber across the wing span when

$$C_{Lmax} = 2.16$$

$$S = 350 \text{ ft}^2$$

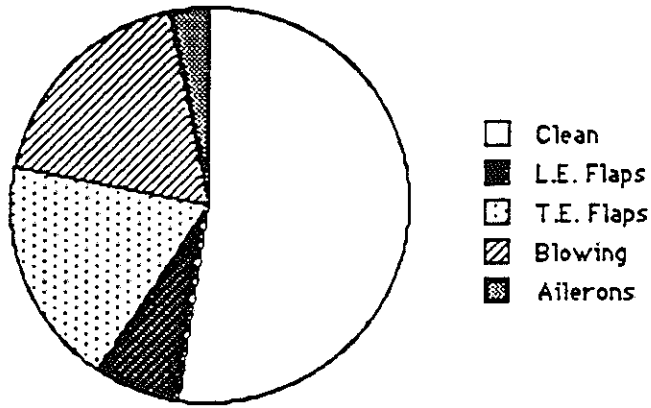


Figure 6-4: Breakdown of maximum lift

deployed. This has the same effect as washout and helps to improve the span efficiency of the wing, thus reducing the induced drag at off-design flight conditions. For the same reason, the leading edge flaps could be employed during a ferry mission where high L/D is desired for maximum range.

6.4 Prediction of Drag

The clean aircraft profile drag was estimated using FRICTION¹³, a program that calculates turbulent skin friction and form drag given component wetted areas and other geometric information. The wetted area of the fuselage was calculated by plotting the cross-sectional perimeter along the body axis and integrating the area under the curve. Zero-lift drags for landing gear, flaps, and speed brakes were estimated from Reference 10.

Stores drag, including the drag from the racks, pylons, and LANTIRN pods, was estimated from drag areas in the ACSYNT reference manual⁵. Mach number effects on the stores drag were also approximated from Reference 13. Interference effects were obtained from Bore¹⁴, Haines¹⁵, and Reference 4. Typical interference factors used were 1.4 for under-fuselage stores and 1.1 for wing-mounted stores, depending on the Mach number.

Two drag-saving features were incorporated into the design of the Griffen. A bomb pallet under the fuselage, similar to one tested on the F-4 Phantom as presented by Smith³, shields the bomb racks from the flow, resulting in a 37% reduction in stores drag. Moving the LANTIRN

Pods from underwing hardpoints to the nose added a further 26% reduction in stores drag, mostly due to the removal of racks and pylons. Overall, the two features result in a 39% reduction in total parasite drag.

The drag-divergent Mach number (M_{DD}) and transonic drag rise for the clean aircraft were estimated from Reference 10 and transonic drag rise for the stores was estimated from Reference 5. Using the Boeing definition, M_{DD} was calculated to be 0.80 with bombs and 0.82 without bombs. Without use of the supercritical wing, M_{DD} (with bombs) would have been at the cruise Mach number, and an additional 12 counts of drag would have resulted.

The Mach number effects on zero-lift drag are shown in Figure 6-5.

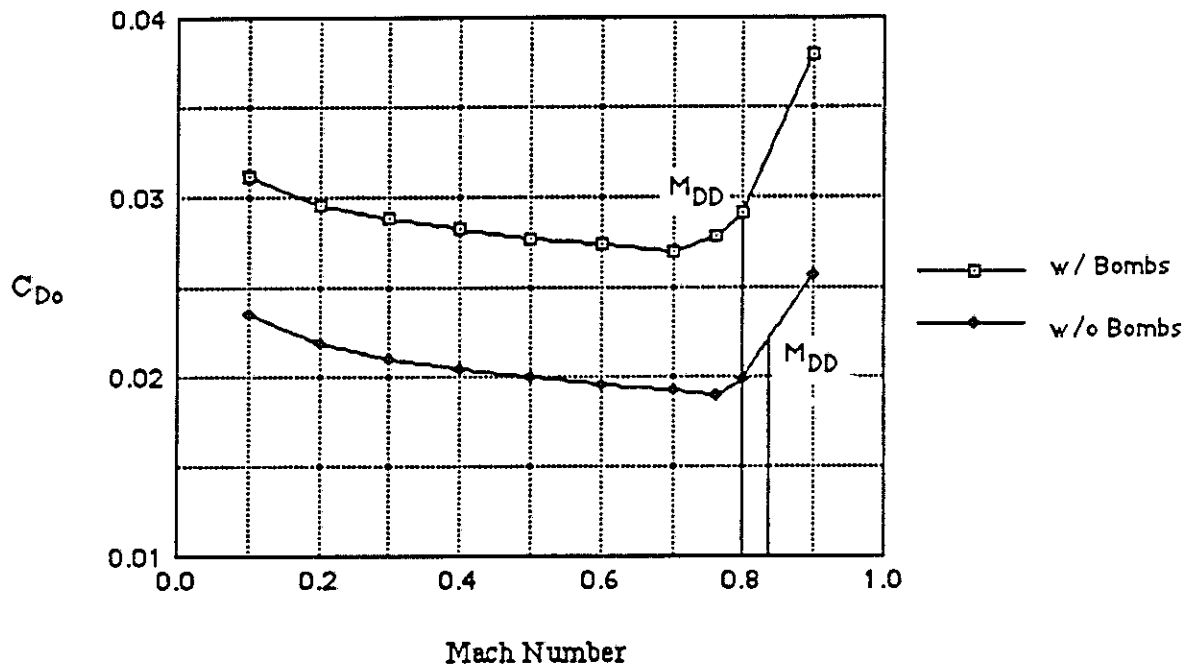


Figure 6-5: Zero lift drag

The induced drag was computed using a span efficiency, e , obtained from LIDRAG¹⁶. The span loading used as input in LIDRAG was provided from VLM4997. Trimmed for cruise, the Griffen has a span efficiency, $e = 0.95$. A breakdown of the total drag at cruise is shown in Figure 6-6.

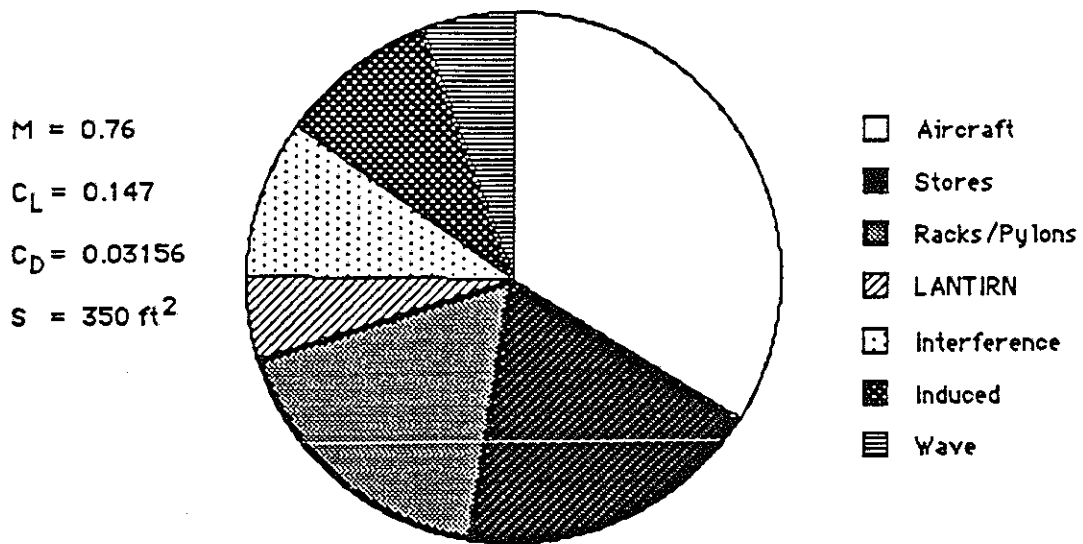


Figure 6-6: Drag breakdown at cruise

6.5 Aerodynamic Performance

Figure 6-7 shows the trimmed drag polars for the Griffen at low-speed and cruise Mach numbers and for an approach condition.

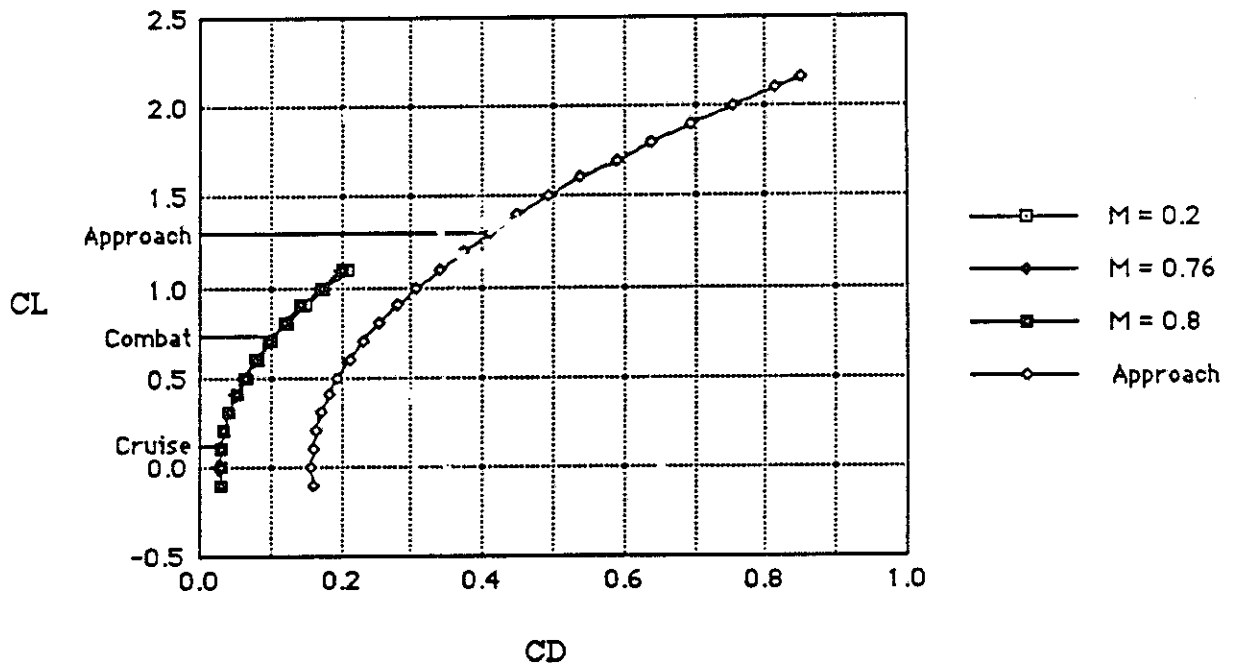


Figure 6-7: Drag polar at various flight conditions

Figure 6-8 shows the variation in lift-to-drag ratio (L/D) with C_L for the flight conditions mentioned above. The low L/D for the approach condition is caused by the high drag from extended flaps, landing gear, speed brakes, and from the induced drag. $(L/D)_{max}$ for the Griffen at the cruise Mach number is about 8.0. This is typical for current fighter aircraft. A summary of L/D information is given in Table 6-2.

For efficiency, it would be desirable for the aircraft to operate at L/D_{max} during cruise. However, since low altitude prevents cruise at C_L for L/D_{max} , the aircraft operates at $L/D = 3.3$, well below the maximum value. Hence, the low C_{D0} enables the aircraft to make the best use of its fuel at cruise.

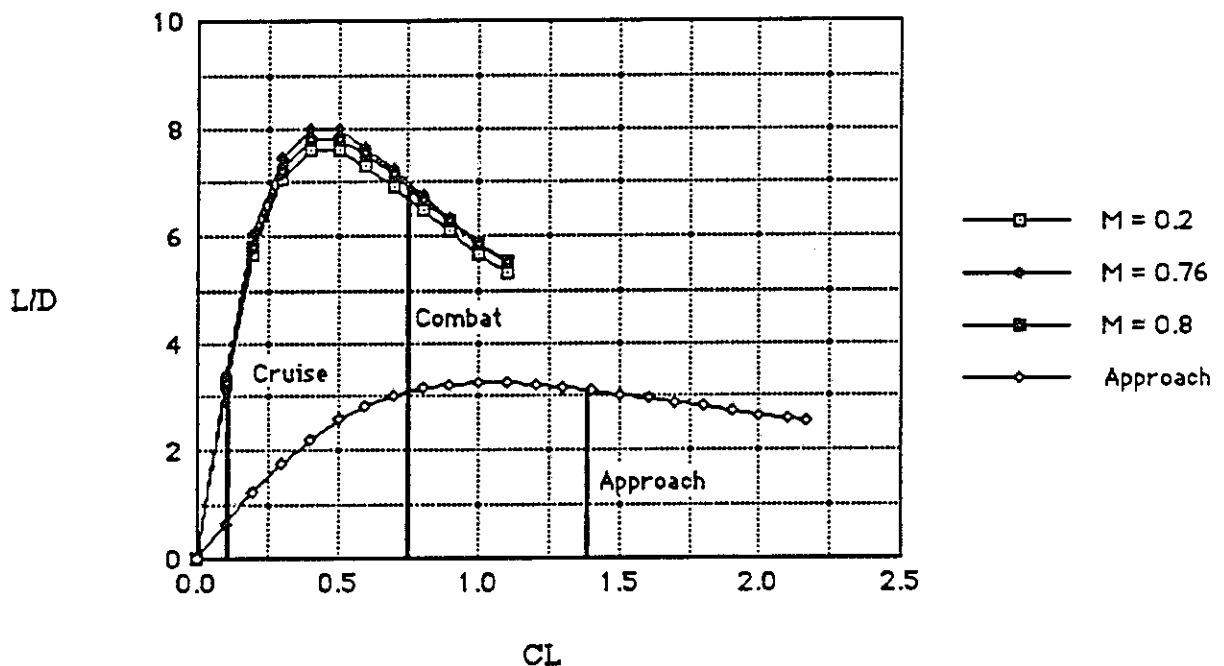


Figure 6-8: L/D at various flight conditions

Condition	M_{∞}	C_L	L/D	L/D_{max} @ M_{∞}
Approach	0.2	1.37	3.14	3.26
Cruise	0.76	0.47	3.3	8.01
Combat	0.8	0.75	6.9	7.82

Table 6-2: Summary of L/D information

7. Propulsion System

7.1 General Configuration

The Griffen is powered by two afterburning, low-bypass turbofan engines submerged in the aft section of its fuselage. The engine airflow inlet system is composed of dual, high side-mounted, subsonic inlets and straight-through air ducts. The inlets are equipped with auxiliary air intake doors and boundary layer diverters. The exhaust nozzle system is a two-dimensional, convergent/divergent, thrust vectoring configuration with thrust reversing capability.

Scaling of the referee engine (i.e. the baseline cycle data and geometric dimensions) was undertaken based on the Griffen's ability to meet the RFP¹ mission requirements as evaluated by the ACSYNT performance analysis. The twenty-five second reattack time requirement mandated that engine thrust be scaled by a factor of 1.25 per engine. Engine size and weight were scaled according to the specifications provided in Propulsion System Data for Close Air Support Aircraft¹.

7.2 Air Intake System

The primary intake throat area was sized based on the required engine airflow at the design condition, an assumed inlet throat Mach number of 0.75¹⁷, and duct pressure losses estimated using equations provided in Roskam¹⁸. The design flight condition selected for the purposes of this formulation was the sea level dash segment of the primary mission. A moderate inlet contraction ratio of 1.1 was chosen to reduce the potential for lip flow separation, while also incorporating drag reduction considerations directed at minimizing inlet frontal area. The required inlet capture area for the Griffen design was calculated to be 5.31 ft² per inlet. The approximately semi-circular inlet face shape and twenty degree entry stagger angle were selected to improve intake performance at a wide range of incidence.

Auxiliary air intakes are included in the Griffen's inlet design to reduce the extensive lip flow separation associated with static and low speed flight conditions, specifically take-off and climb (Figure 7.1). A preliminary estimate of the auxiliary intake area required during these conditions was made based on the difference between the free stream and inlet capture areas, assuming an average inlet flow ratio of 1.5. This area, approximately 2.65 ft², is divided into six separate intake

doors arranged along a line of perimeter surrounding the inlet, just aft of its face. These doors are spring-loaded and open inwardly to allow external flow to enter the intake. During low speed operation, the bleed doors are actuated by interior suction and reseal as airspeed (and intake interior pressure) increases.

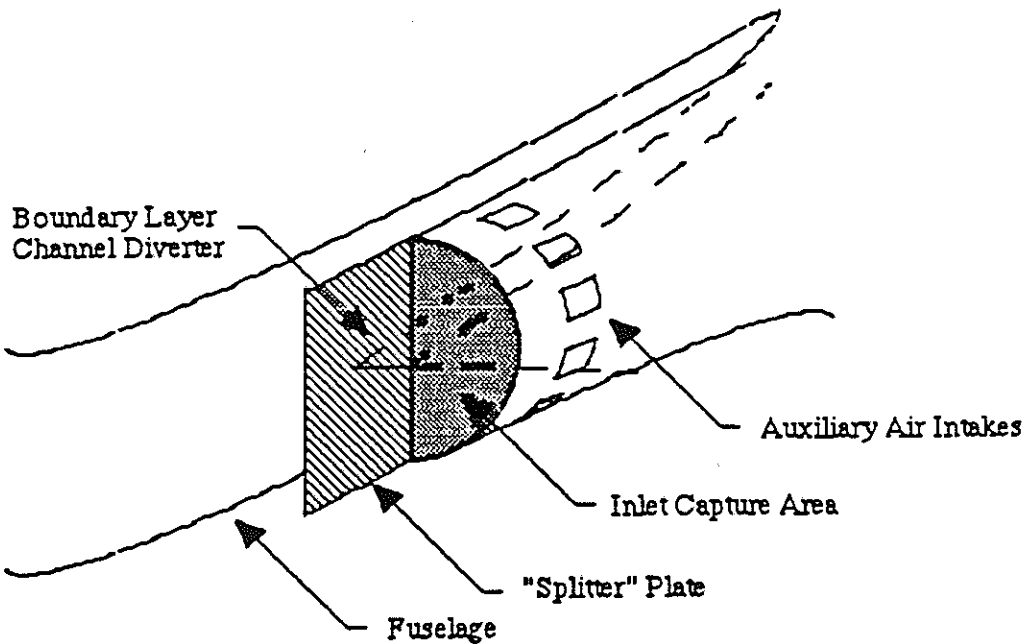


Figure 7.1: Griffen inlet configuration

To reduce the intake pressure losses associated with boundary layer ingestion, the Griffen's inlets are equipped with channel-type boundary layer diverters. In this design, the boundary layer portion of the inlet approach flow enters a channel bounded by the aircraft fuselage and a flat "splitter" plate. Within the channel, the boundary layer flow is diverted vertically into the external flow by triangular-shaped ramps. The included angle between the diverter ramps is sixty degrees, and the diverter thickness is 3.0 inches, corresponding to the boundary layer thickness as represented by one percent of the fuselage length in front of the inlet⁴.

7.3 Exhaust Nozzle Configuration

The selection of a two-dimensional thrust vectoring nozzle configuration was guided by the RFP reattack time requirement, and more specifically by the improvement in turning performance attained by the ability to direct thrust in the direction of the free stream. This system was chosen over a three-dimensional thrust vectoring configuration because of its proven performance. A very similar system has been installed and flight tested on the F-15 SMTD¹⁹.

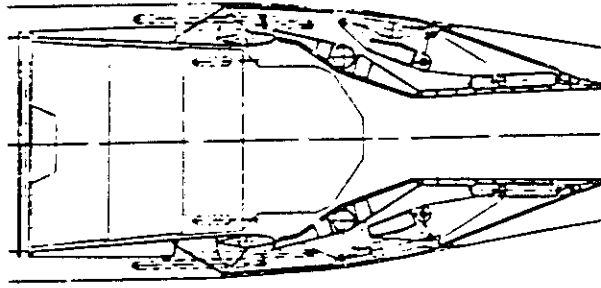
Figure 7.2²⁰ presents a schematic of the convergent/divergent, two-dimensional nozzle configuration in four different modes of operation. The nozzle flap system consists of upper and lower (1) primary flaps, (2) secondary flaps, and (3) slave flaps. The primary flaps form the nozzle throat area, and are invariably symmetrically actuated. The secondary flaps are hinged to the primary flaps and, during normal operation, form the nozzle divergence angle. In the vectoring mode, these flaps are responsible for deflecting the thrust. The maximum thrust deflection angle for this type of nozzle is (+/-) 30°. The primary role of the slave flaps is to vary the efflux area of the reverser ports during thrust-reversing operation.

The thrust reversing mode is characterized by a complete closing, full reverse mode, or partial closing, partial reverse mode, of the nozzle throat area and simultaneous opening of the reverser ports. During the partial reverse mode, the forward thrust can be deflected by the secondary flaps. The Griffen uses a combined deployment of thrust reversers and speed brakes for inflight and landing aerodynamic braking. The specific performance benefits of thrust reversing are detailed in Chapter 9.

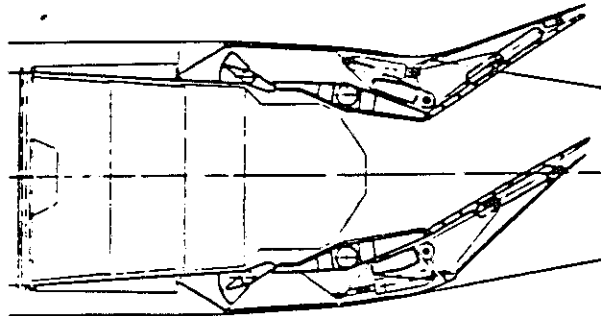
7.4 Installation Losses

The calculation of installation thrust losses for selected flight conditions was accomplished using equations provided in Roskan., Part VI¹⁹. The following components of installation loss were considered in the analysis:

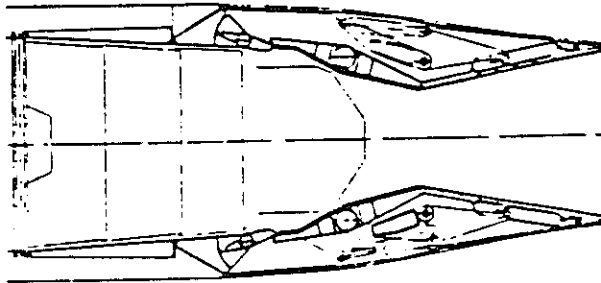
- Duct Stagnation Pressure Losses
- Power Extraction Requirements
- Boat Tail Drag



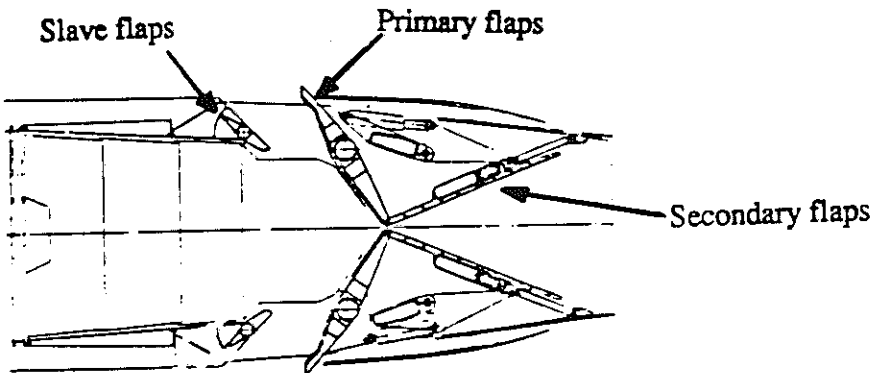
START



MAXIMUM DEFLECTION (START)



COMBAT



MAXIMUM THRUST REVERSAL

Figure 7.2: Griffen nozzle configuration²⁰

It was assumed that the effects of approach flow pressure losses were precluded as a result of the installation of boundary layer diverters. In addition, it was assumed that the inlet cowl lip design was such that, for the flight conditions considered, lip suction forces exactly negated additive drag forces.

The duct pressure losses were estimated based on a representative duct geometry and modified flat plate friction model¹⁸. Power extraction requirements included electrical and mechanical loads, approximately 100 shp each, as well as compressor bleed air, four percent of the compressor air flow, for various pneumatic aircraft systems. The boat tail drag term was estimated using a fixed $\Delta C_{D_{noz}}$ of 0.005 per nozzle (referenced to the maximum fuselage cross-sectional area), corresponding to a two-dimensional nozzle configuration⁴. The effect of the nozzle fairing on this drag term was approximated by treating the dual-nozzle/fairing combination as a single two-dimensional exhaust nozzle.

Table 7.1 presents the results of this installation loss analysis for four RFP¹ mission flight conditions. Required thrust and engine airflow values for each flight conditions were obtained from the ACSYNT performance analysis. These values were interpolated by that code from the uninstalled, up-scaled referee engine cycle data. A large fraction of the installation losses at the dash and ferry flight conditions corresponds to the boat tail drag term, resulting from the relatively low thrust settings characteristic of those mission segments.

The flight condition requiring the most careful consideration is takeoff. The power setting employed at this condition corresponds to the static, sea level maximum-afterburning thrust.

Mission Flight Condition	Percentage Thrust Loss
Sea Level Dash	6.84
Combat Accereation	3.14
Takeoff	11.05
Ferry Cruise	8.70

Table 7-1: Installation thrust losses

Hence, installation thrust losses at this condition corresponds directly to an increase in the required takeoff distance. The relatively large difference between uninstalled and available thrust at this condition is due to an additional five percent of engine airflow bleed from each compressor for use in flap-blowing. Specific takeoff performance characteristics are discussed in Chapter 9.

7.5 Summary

In general, the Griffen's propulsion configuration is modeled after similar subsonic attack aircraft systems. The inlet is of fixed geometry and characterized by rounded cowl lips to reduce flow separation. Auxiliary intake doors and boundary layer diverters have been installed to reduce inlet flow pressure losses. Combat and takeoff performance mission requirements mandated the installation of a thrust vectoring system. A two dimensional, convergent/divergent nozzle system was selected primarily because of its proven performance. A preliminary installation thrust loss analysis identified takeoff as a segment of the mission for which the performance was particularly sensitive to installation losses.

8. Stability and Control

8.1 Method of Analysis

The stability and control analysis on the Griffen was performed for four flight conditions deemed critical to the CAS mission: Approach (AP), Return Dash segment (RD), Ground Attack (GA), and high altitude Cruise (CR). All parameters defining these flight conditions can be found in Appendix A. Stability and control derivatives for each of the four flight conditions were calculated using the methods of Digital DATCOM supplemented by the methods presented in Etkin²¹ and Raymer⁴. The dynamic stability characteristics of the Griffen were computed from the uncoupled linearized equations of motion for each flight condition using the SSAAP program presented in Appendix B.

8.2 Wing Longitudinal Placement and Longitudinal Stability Determination

The RFP requires that the proposed CAS aircraft have a low operating cost. In keeping with the spirit of this specification, the trim drag of the Griffen was minimized for fuel efficiency during the dash segments of the mission. Neutral point and cg locations were computed with varying wing placements as shown in Figure 8-1. A static margin of -5% MAC was chosen.

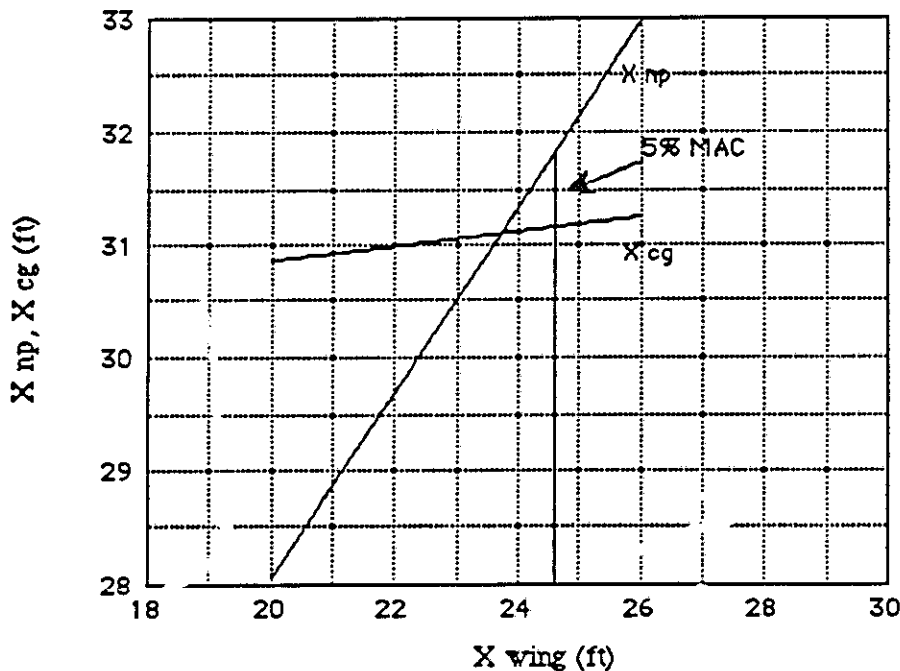


Figure 8-1: Wing placement chart

The resulting drag increment associated with trimming the aircraft is shown in Figure 8-2 plotted against the static margin of the aircraft in the dash flight condition. This plot was generated by computing the lift distribution between the wing and the tail as a function of c.g. location. Trim drag was then computed as:

$$\Delta C_{D \text{ trim}} = \left(\text{Induced drag on wing at trim} \right) + \left(\text{Induced drag on tail at trim} \right) - \left(\text{Induced drag on wing at dash } C_L \right)$$

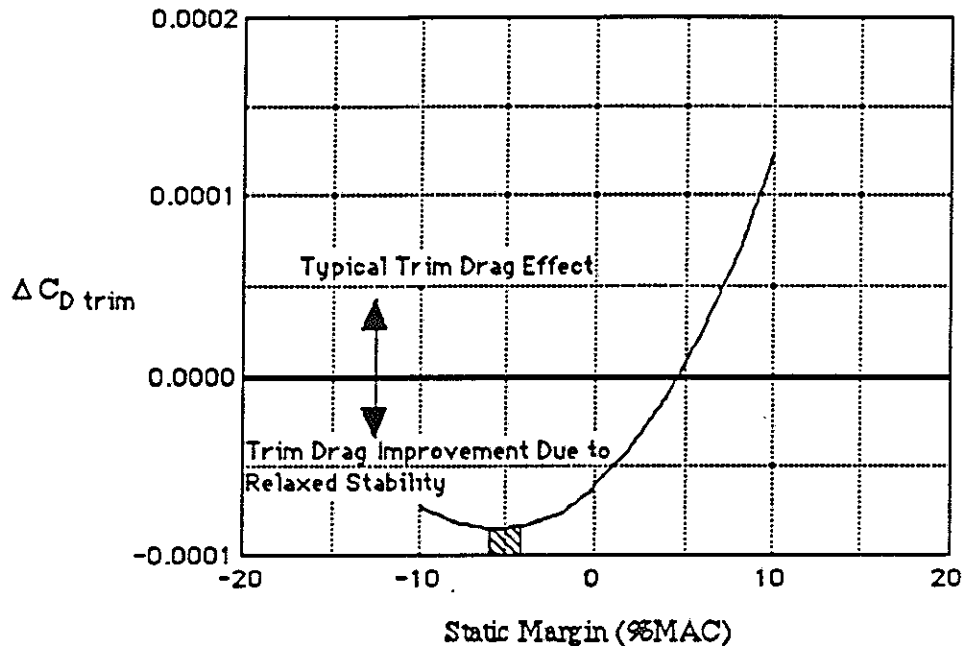


Figure 8-2: Trim drag increment

The mission operating envelope is represented by the shaded segment on the plot. As shown, the trim drag is at or near the minimum throughout the operational envelope for the chosen wing placement.

8.3 Control Surface Concept Selection and Sizing

The Griffen uses an all movable horizontal stabilizer which deflects symmetrically to provide pitching moment and asymmetrically to provide auxiliary rolling moment. Outboard ailerons are used for primary roll control. The ailerons split to act as speed brakes. A dual rudder system provides yawing moments and is used in conjunction with asymmetric speed brake and differential tail deployment to provide pure side force.

The horizontal stabilizer was sized to meet the takeoff requirement of the RFP without the use of 2-D Thrust Vectoring. The 2000 ft takeoff capability translates into a 2 second rotation time constraint. A closed form solution of the moment equation about the main landing gear wheel contact point was used to determine the rotation time at 80% of the takeoff speed. The tail was sized to 80 square feet of total exposed area to rotate the aircraft in 1.8 seconds with a deflection of 20 degrees without the use of Thrust Vectoring at Sea Level conditions.

Level 1 Ground Attack roll performance requirements as dictated by the MIL-F-8785C specifications²² governed the sizing of the ailerons. The need for large flaps to provide high lift at takeoff restricts the aileron size so that auxiliary roll control must be provided through asymmetric tail deflections. The closed form solution of a simplified 1-DOF moment equation about the roll axis, as presented in Reference 23, was used to determine the time-to-bank. The ailerons were sized to 8.25 sq ft total area. The resulting GA 180 degree time-to-bank was computed to be 2.69 seconds using four degrees of aileron and 8 degrees of asymmetric tail deflection, compared to the requirement to perform the maneuver in under three seconds.

The dual rudder/vertical tail assembly was designed to trim the Griffen in a 30 kt crosswind with one engine out at takeoff with 17 degrees of rudder deflection. A static moment equation about the yaw axis was used considering a moments due to the rudder, asymmetric afterburning thrust, and an asymmetric flat face drag on the engine-out inlet face. The vertical tails were sized to 49 sq ft each, with the rudders comprising 25% of this area. The associated tail volume coefficient is 0.117.

Side force generation is used to enhance precision ground attack while the Griffen is performing terrorist counteraction and foreign internal defense roles. Side force generation is produced using a 5.96:1 control ratio between the speed brake and rudder deflection to counteract adverse yaw moment and a 1.67:1 control ratio between rudder and asymmetric tail deflection to counteract adverse roll moment. This control ratio is computed to give zero side force in the Ground Attack and Approach flight conditions. Side force generation is engaged by pressing a button on the throttle. Once this option is engaged, pilot rudder pedal inputs result in the employment of the control ratios.

A sensor package is placed at the tip of a 72 inch nose boom to reduce the effect of actuator lag. The signal from a gust detected by a sensor on the boom can be acted on approximately 0.045 seconds faster than a signal from cg placed sensors.

8.4 Open Loop Dynamic Characteristics

The longitudinal and lateral/directional stability and control derivatives were computed and tabulated in Appendix A along with various other pertinent parameters describing each flight condition. The *open loop* response characteristics of the Griffen were computed using the SSAAP program and are shown in Table 8-1 for each flight condition along with the appropriate MIL specification. Because the Griffen is a statically unstable aircraft ($SM=-5\%$), the open loop short period poles consist of one nonoscillatory stable root and one nonoscillatory unstable root and are not shown in Table 8-1. The phugoid damping meets the requirements for all flight conditions. The open loop roll mode time constant is too high at high altitudes. The dutch roll mode does not meet requirements at all flight conditions except for the dash segment.

Parameters & MIL-SPECS:	AP	RD	GA	CR
Phugoid: ζ_p ($\zeta_p > 0.04$)	0.17	0.19	0.07	0.05
Short Period MIL-Spec: ($.35 < \zeta_{sp} < 1.3$) ($\omega_{sp} \min$) ($\omega_{sp} \max$)	(1.0) (3.2)	(3.16) (11.33)	(1.19) (4.25)	(1.68) (6.02)
Dutch Roll ζ_{dr} ($\zeta_{dr} \min$) ω_{dr} ($\omega_{dr} \min$)	-0.105 (0.08) 1.29 (1.0)	0.087 (0.08) 3.90 (1.0)	0.066 (0.40) 2.65 (1.0)	0.014 (0.08) 1.91 (1.0)
Roll Mode T_r ($T_r \max$)	0.888 (1.0)	0.479 (1.4)	0.813 (1.0)	2.25 (1.4)
Spiral Mode: T_{2s} ($T_{2s} \min$)	-178.1 (2.0)	-29.37 (20.0)	-18.3 (12)	-36.7 (20.0)

Table 8-1: Open loop response characteristics and associated specifications

8.5 Open Loop Ride Quality Characteristics

One of the most stringent requirements imposed on the Griffen is the 500 kt dash on the deck. The low level buffeting associated with this flight phase may cause significant pilot discomfort reducing the ability of the pilot to carry out the mission work load. Reference 23 suggests that if the cockpit g-level per unit gust input (A) is greater than 0.005 then an active gust relief system should be investigated. Typical values of the A parameter are computed through the dash segments of the mission:

Dash to target: $A = 0.011$ g per fps

Dash to Base : $A = 0.013$ g per fps

8.6 Stability Augmentation and Active Ride Quality Control

On the basis of the open loop response of the Griffen, a stability augmentation system is proposed to force the Griffen response characteristics to meet the MIL specifications in the AP,GA, and CR flight conditions. Longitudinal stability augmentation is provided through tail deflections. Lateral/Directional stability augmentation is provided through aileron and rudder deflections.

An Active Ride Quality Control System (ARQCS) is proposed for use in the dash segments in order to minimize cockpit g-levels while keeping the response characteristics within MIL specs. For the purpose of analysis, a Longitudinal control law consisting of commanded tail inputs is designed to perform this task.

A linear state variable feedback control law, $u = [K](x_c - x)$, was designed for each flight condition to tailor the closed loop response characteristics of the Griffen as shown in Figure 8-3.

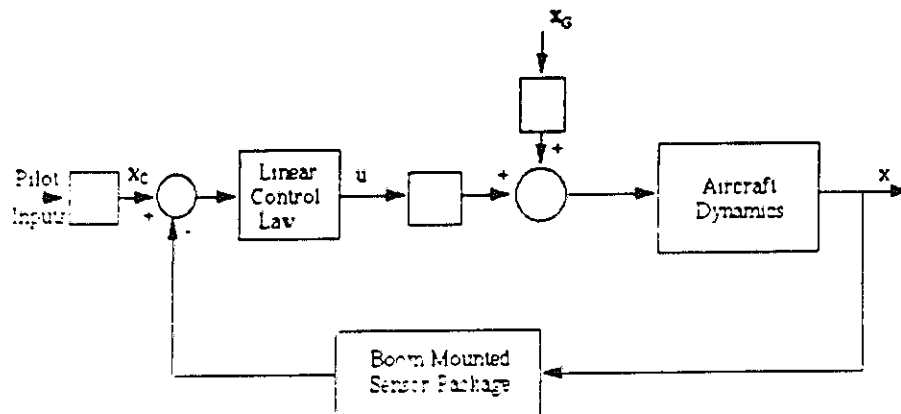


Figure 8-3: Schematic of the Griffen stability augmentation/ARQCS

A longitudinal stability augmentation system is required in order to force the short period characteristics to meet the MIL specifications for damping and natural frequency. The Bass-Gura method of pole placement was employed in the choice of gains for this control law as outlined in Reference 24. The resulting response characteristics and required closed loop gains are shown in Table 8-2.

Parameters & MIL-SPECS:	AP	GA	CR
Phugoid: ζ_p ($\zeta_p > 0.04$)	0.07	0.10	0.07
Short Period MIL-Spec: ($.35 < \zeta_{sp} < 1.3$)	0.7	0.7	0.7
ω_{sp} ($\omega_{sp \text{ min}}$) ($\omega_{sp \text{ max}}$)	2.0 (1.0) (3.2)	2.72 (1.19) (4.25)	3.86 (1.68) (6.02)
Gain Schedule			
K_u	0.0031	0.00033	-0.00081
K_w	-0.0101	-0.00151	-0.00403
K_1	-1.3670	-0.2970	-1.0850
K_θ	-0.093	-0.0046	-0.13033

Table 8-2: Closed loop longitudinal response characteristics and gain schedule

A yaw rate damper control system is required for the GA, AP, and CR flight conditions in order for the Griffen to meet the dutch roll specifications. A roll rate damper control system is required to meet the roll specifications in the CR flight condition. Table 8-3 shows the proposed gain schedule and resulting lateral/directional closed loop response characteristics.

Parameters & MIL-SPECS:	AP	GA	CR
Dutch Roll ζ_{dr} ($\zeta_{dr \text{ min}}$)	0.160 (0.08)	0.482 (0.40)	0.093 (0.08)
ω_{dr} ($\omega_{dr \text{ min}}$)	1.16 (1.0)	2.53 (1.0)	2.36 (1.0)
Roll Mode T_r ($T_r \text{ max}$)	0.740 (1.0)	0.740 (1.0)	1.13 (1.4)
Spiral Mode: T_{2s} ($T_{2s \text{ min}}$)	-14.0 (12.0)	-17.2 (12.0)	-43.2 (20.0)
Gain Schedule			
$K_{r \delta}$	-1.8	-0.8	-1.32
$K_{r \delta a}$	-1.8	-0.8	-1.32
$K_{r \delta a}$	0.0	0.0	-0.30

Table 8-3: Lateral/directional closed loop response characteristics and gain schedule

The design problem underlying the ARQCS is to place the system poles to meet MIL specifications while at the same time minimizing the cockpit g-level response of the aircraft to low-level turbulence. An expression for normal cockpit accelerations can be derived from aircraft kinematics taking advantage of the linearized equations of motion:

$$a_N = \{c_1\}^T \{x\} + \{c_2\}^T \{u\}$$

A quadratic performance index is derived from the square of the normal acceleration:

$$a_N^2 = x^T [Q] x + 2x^T [S^T] u + u^T [R] u$$

A linear control law was found to minimize this performance index by solving the Matrix Riccati Equations for a Linear-Quadratic-Regulator (L-Q-R) as outlined by Reference 24. The results of this analysis are shown in Table 8-4. The Griffen short period response characteristics under this control

Parameters & MIL-SPECS:	L-Q-R	ARQCS
Phugoid: ζ_p ($\zeta_p > 0.04$)	0.1844	0.90
Short Period MIL-Spec: ($.35 < \zeta_{sp} < 1.3$)	17.55	1.28
ω_{sp} ($\omega_{sp} \text{ min}$) ($\omega_{sp} \text{ max}$)	1.904 (3.16) (11.33)	3.2 (3.16) (11.33)
Gain Schedule		
K_u	0.00055	0.00025
K_w	0.00843	-0.00034
K_q	-5.3106	-0.33079
K_θ	-0.00049	-0.02213

Table 8-4: Longitudinal closed loop response characteristics during RD flight condition

law fall outside of MIL specs, however, the ARQCS is designed to place the system poles against the critical constraints as interpreted from the results of the L-Q-R analysis.

Figure 8-4 shows the longitudinal steady state cockpit g-level response of the Griffen (unaugmented, under the L-Q-R control law, and under ARQCS control law) to a unit sinusoidal vertical gust input. These curves were computed using the SSAAP program, and the sinusoidal gust frequencies were converted into gust lengths at a dash speed of 500 kts. A marked improvement can be seen between the unaugmented Griffen and that of the Griffen augmented by the ARQCS in the frequency range of interest corresponding to gust lengths between 2500 ft and 25 ft. However, if the upper short period damping constraint and the lower short period frequency constraint are relaxed, we can expect further improvements in ride quality as indicated by the lower curve on the figure.

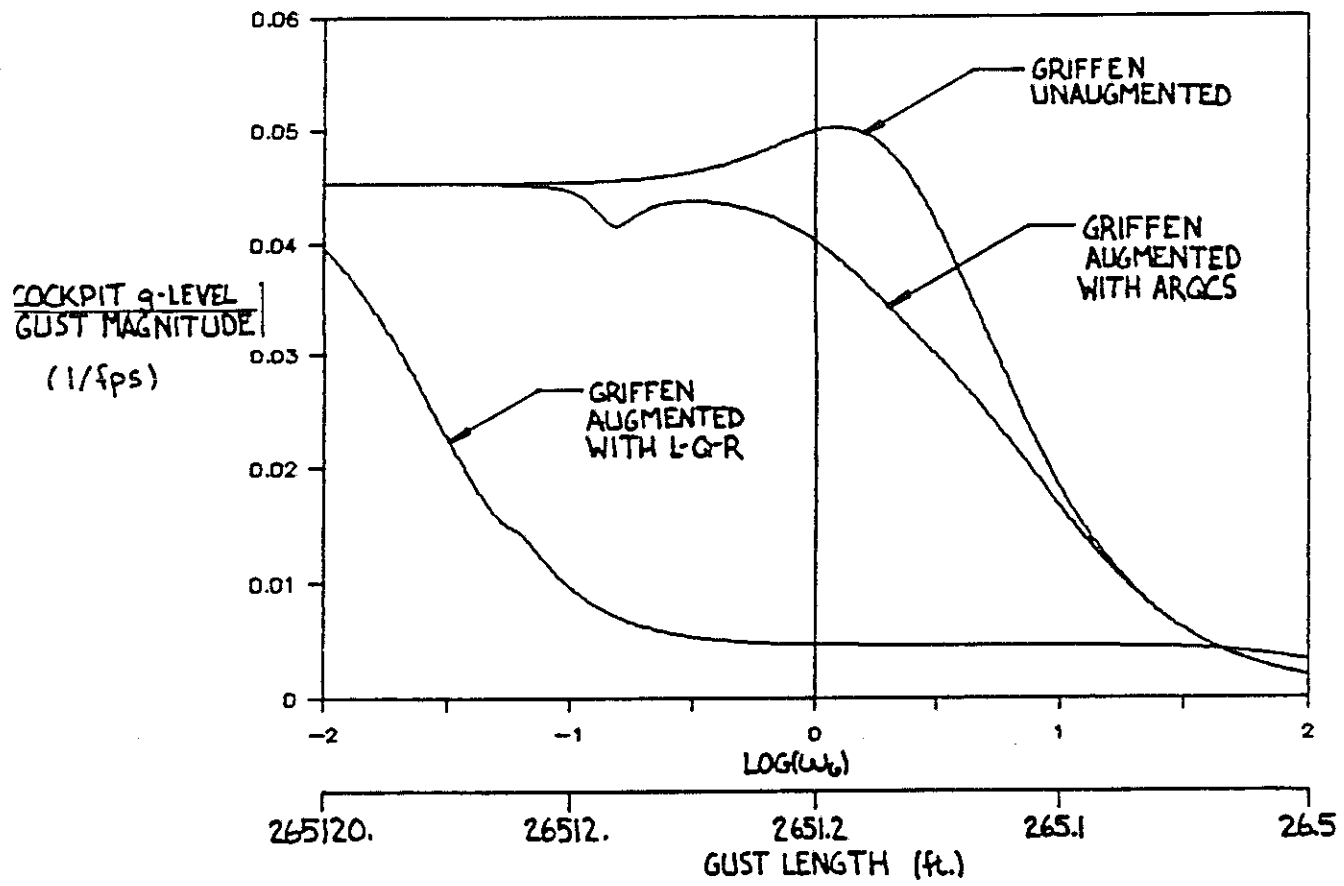


Figure 8-4: Cockpit g-level vs gust length

9. Performance

9.1 Methods

ACSYNT⁵, a mission analysis and sizing program developed by NASA-Ames, served as the primary analysis tool for computing point performance and mission data while methods presented in Raymer⁴ and Houghton and Carruthers²⁵ served as a supplement.

9.2 Mission Performance

The low-level mission outlined in Table 9-1 served as the basis for designing the aircraft relative to the other two mission profiles. The combat speed of Mach 0.8 at sea level was obtained by setting the maximum speed in military power and accounting for the q limit of 1000 psf. The fuel weight given in Table 9-1 includes 572 lbs of trapped and unusable fuel.

After the Griffen's design was finalized, both the high-low attack mission and the ferry mission were analyzed. Specific information on both of these profiles is provided in Table 9-2. The ferry mission utilizes six 300 gallon tanks, two tanks on the wing pylons and four tanks in dual tandem underneath the fuselage, to provide a maximum of 11,700 lbs of additional fuel.

The change in altitude for the high-low mission is needed to optimize fuel performance after the combat phases. The maximum rate of climb speed of 508 knots was computed for small angles under takeoff conditions and military power.

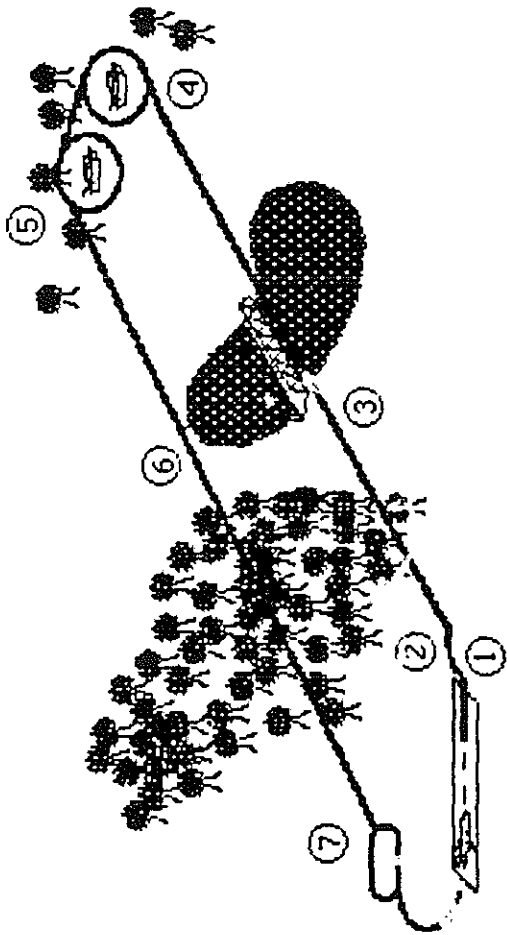
9.3 Point Performance

The primary performance specifications outlined in the RFP¹ and mentioned in Chapter 2 for the competing aircraft are summarized along with the Griffen's data in Table 9-3. The acceleration and both turning conditions are to be met with no bombs and 50% internal fuel. The reattack condition is 50% of the bomb load and 50% internal fuel.

As can be seen in Table 9-3, Griffen exceeds all given performance requirements carrying self-defense stores and half fuel. The addition of afterburning engines facilitates a : of the point requirements, especially the acceleration in 20 seconds. The high instantaneous and sustained turning g -levels derive from the $A/BT/W$ (1.39) as well as a W/S (94.2 psf) for the conditions specified above.

Low Level Mission

TOGW48,145 lbs
 T/W at takeoff (A/B).....0.857
 W/S at takeoff137.6 lb/ft
 Takeoff/Landing
 Distance893 / 1662 ft
 AltitudeSea Level
 Payload15,800 lbs



Phase	Mach No.	L/D	SFC lb/hr.lb	Time min	Fuel lbs	Distance nm
1.) Warm up/Takeoff	0 - 0.4	-	-	5.0	435	-
2.) Accelerate	0.4 - 0.76	-	2.34	0.30	502	2.0
3.) Cruise out	0.76	3.83	0.80	29.80	3534	248
4.) Combat	0.80	-	2.34	0.50	818	-
5.) Combat	0.80	-	2.34	0.50	818	-
6.) Cruise back	0.76	3.43	0.85	29.80	2478	250
7.) Loiter	0.33	7.74	0.77	20.00	960	-
				85.9	10,118	500

Table 9-1: Design mission summary

<u>High - Low Mission</u>	
Max rate of climb	508 knots
Fall-out loiter time	19.0 min
Best attack cruise - altitude/speed	15,000 ft Mach 0.7
Best return cruise - altitude/speed	22,500 ft Mach 0.6
<u>Ferry</u>	
Maximum loiter after 1500 nm	74 min
Maximum range with 20 min loiter	1914 nm
Maximum range with no loiter	1997 nm
Best cruise - altitude/speed	30034 ft Mach 0.81

Table 9-2: Secondary mission summary

Performance Requirement	Conditions		RFP Specification		Griffen Data
	W/S (psf)	T/W			
Accelerate Mach 0.3 to 0.5	94.2	1.39	<20	(sec)	8.3
Sustained g's	94.2	1.39	≥4.5	(g)	7.5
Instantaneous g's	94.2	1.39	≥6.0	(g)	7.5
Reattack time	107	1.22	<25	(sec)	24.2
Takeoff distance	137.6	.857	<2000	(ft)	893
Landing distance	110	1.07	<2000	(ft)	1662

Table 9-3: Requirement summary

The reattack time of 25 seconds spelled out in the RFP¹ proved to be the most challenging requirement for the Griffen to meet. The carpet plot (Figure 3-4) reveals that the sizing of the Griffen revolved around the reattack constraint as all but one constraint line fell below the sizing grid. The constraint of $W/S = 135$ psf was selected to provide passive buffet suppression. Upscaling of the

referee engines to an ESF of 1.25 (A/B T/W at takeoff of .9525) as well as the addition of 2-D vector nozzles to align the exhaust flow with the free stream allows Griffen a reattack time of 24.2 seconds at a load factor of 7.27. The addition of the 2-D nozzles saved 1006 lbs. over the weight required to obtain the desired reattack time solely by upscaling the engines with the added benefit of improved field performance.

Griffen's field performance under several conditions is presented in Figure 9-1. All data given in Figure 9-1 was calculated considering a 11% thrust bleed on both landing and takeoff for the blown flap system. Landing distances are based on a weight equal to .8*TOGW and a split aileron system that produces 754 counts of drag when fully deployed. The takeoff distance of 2000 ft. from a hard dry strip mandated by the RFP¹ can be met without thrust vectoring with a rotation time of 1.8 seconds, but the alternate field conditions require the use of the 2-D nozzles. Landing in under 2000 ft. in any condition is only feasible with the activation of the the thrust-reversers built in to the engines. The combination of thrust-reversers and split ailerons allows landing distances meeting specifications.

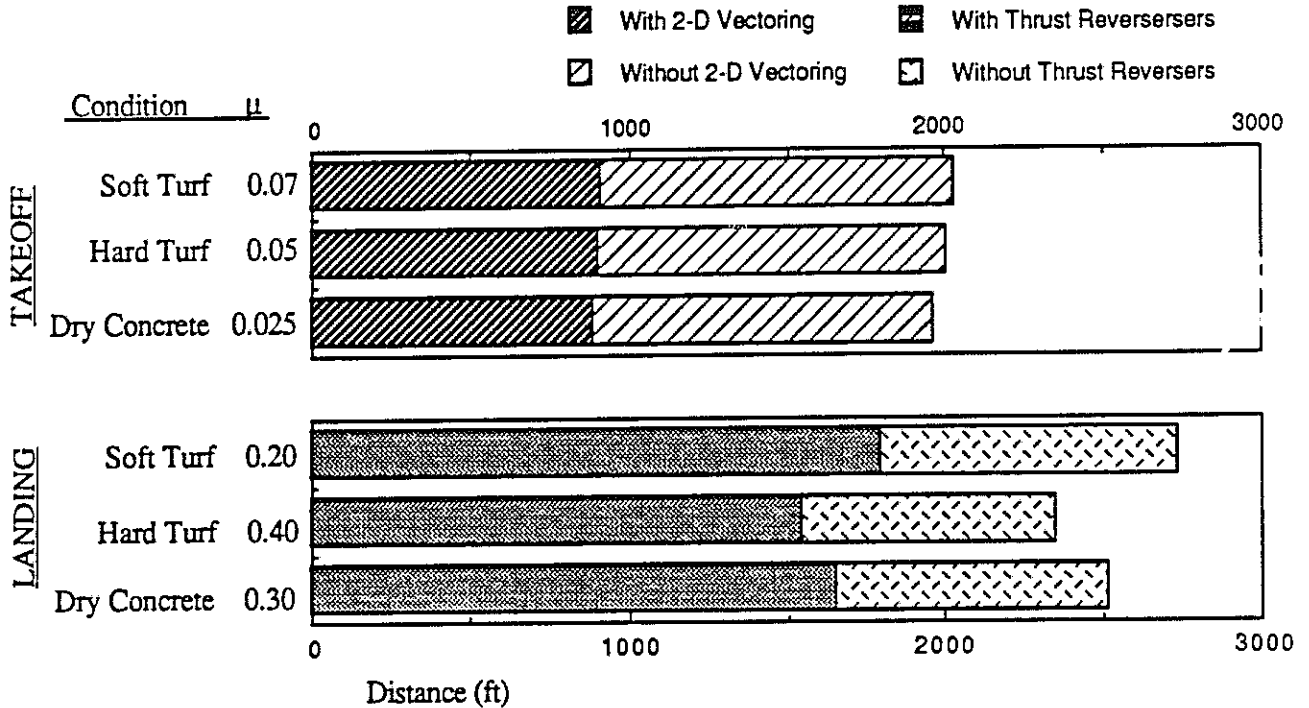


Figure 9-1: Field performance

9.4 Flight Conditions and Sensitivities

The capability of the Griffen to operate at a particular flight condition is summarized in the operational envelope (figure 9-2). The excess energy (P_e) curves were calculated with no bombs, half of the internal fuel, and n equal one. The upper limit on the flight range given in figure 9-2 for the Griffen is the engine ceiling (40,000 ft.) which is well below the typical 50,000 ft. bail-out condition imposed for pilots without full environment suits.

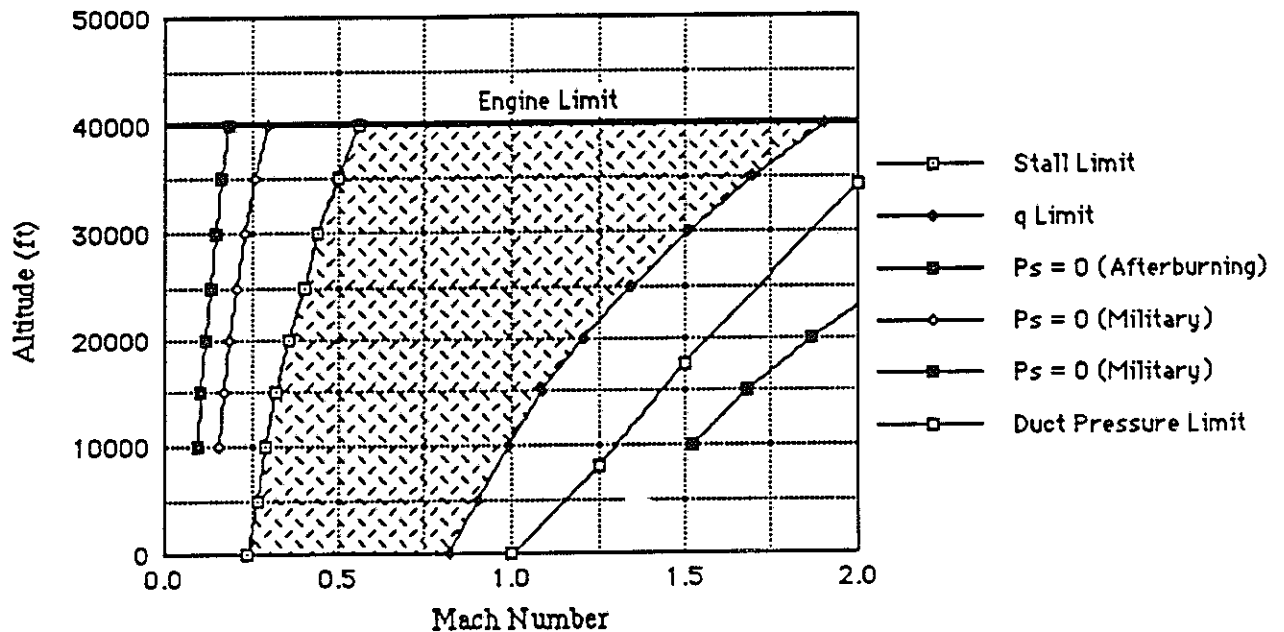


Figure 9-2: Operating Envelope

Changes resulting from any modifications to the basic aircraft can be anticipated by analyzing the sensitivities given in Figure 9-3. The basic growth factor of 1.97 lb. of TOGW per 1 lb. of fixed weight allows Griffen to be easily modified and additional capabilities included with little weight penalty.

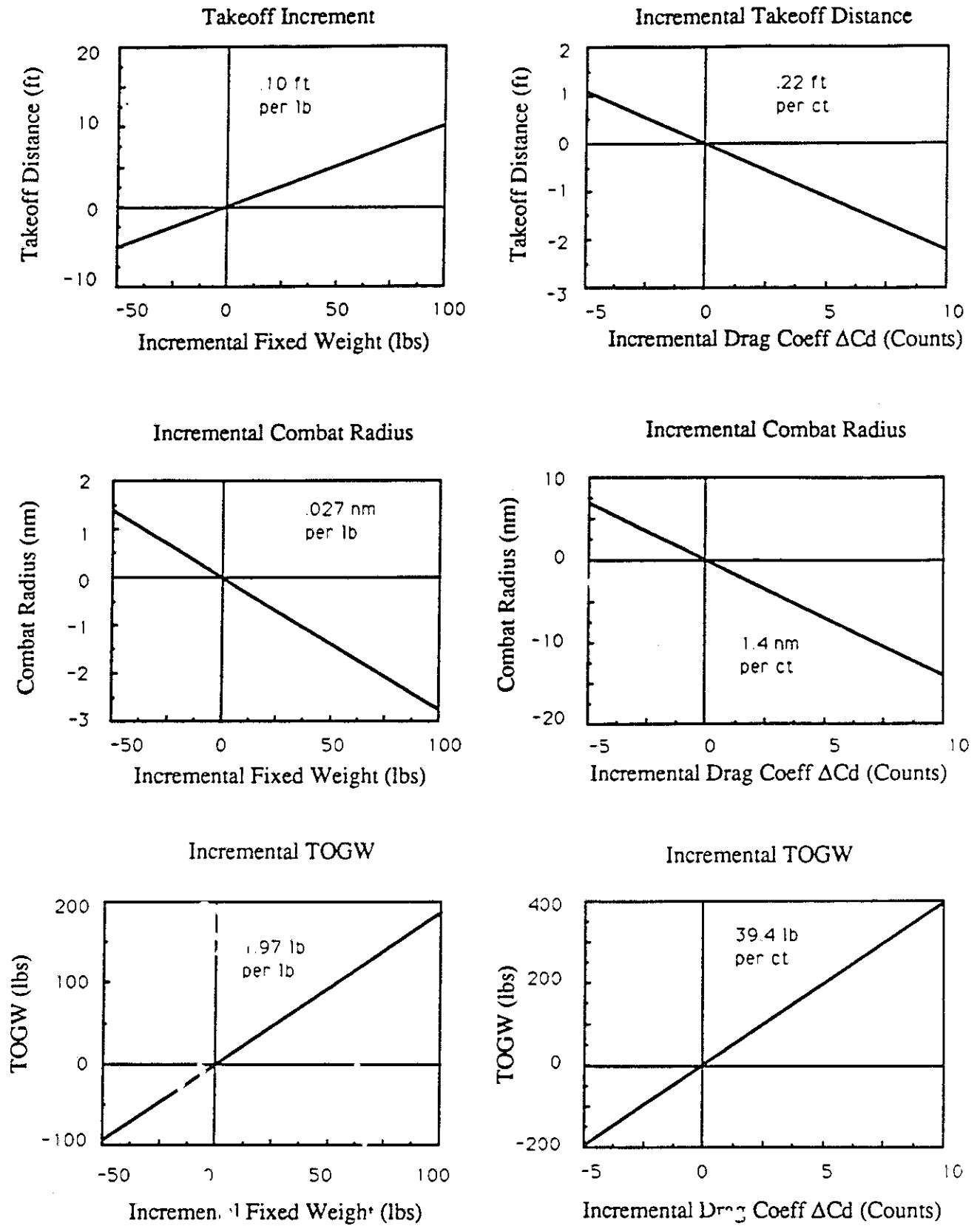


Figure 9-3: Sensitivities

10. Systems and Avionics

10.1 Hydraulics

There are two independent 4000 psi hydraulic systems powered by two separate independently driven pumps, each mounted on the AMAD. Each system is supplied by a bootstrap type reservoir and provides duplicated power to the primary flight control systems including the tailerons, rudders, flaps, slats, ailerons, and speed brakes. Duties for the secondary systems, canopy, landing gears, wheel brakes, nose wheel steering, and thrust reversers, are divided between the two. Both pumps are mechanically cross-connected through accessory gearboxes so in the event of a single engine failure, the remaining operational engine would drive both systems. There are three individual sets of piping and line runs spaced throughout the aircraft for redundancy. If one of the lines is damaged, the plane would not be disabled. The 4000 psi system was chosen because of its weight and space savings over lesser pressure systems. Also, this system is widely used among other aircraft so existing components can be used, reducing costs. The hydraulic fluid itself is non-flammable so it will not start or exacerbate an onboard fire. Both the leading edge flaps and ailerons are moved by geared hinge rotary actuators. These actuators consist of a series of gears contained within a tube. This system is activated by a hydraulic actuator mounted in the fuselage. By using this system, there are no unnecessary bulges in the wing which would take away from the performance of the airplane. All the other control surfaces have single hydraulic actuators mounted in the fuselage (Figure 10-1).

- 1 Nose gear hydraulic actuator
- 2 Canopy hydraulic actuator
- 3 Leading edge flap hydraulic actuator
- 4 Trailing edge flap hydraulic actuator
- 5 Aileron/airbrake hydraulic actuator
- 6 Hydraulic reservoir
- 7 Elevator hydraulic actuator
- 8 Rudder hydraulic actuator
- 9 Port hydraulic line (starboard line not shown)
- 10 Thrust vectoring system hydraulic actuator
- 11 Starboard hydraulic service to port actuators
- 12 Port hydraulic service to starboard actuators
- 13 L.E. Flap geared hinge rotary actuator
- 14 Aileron geared hinge rotary actuator

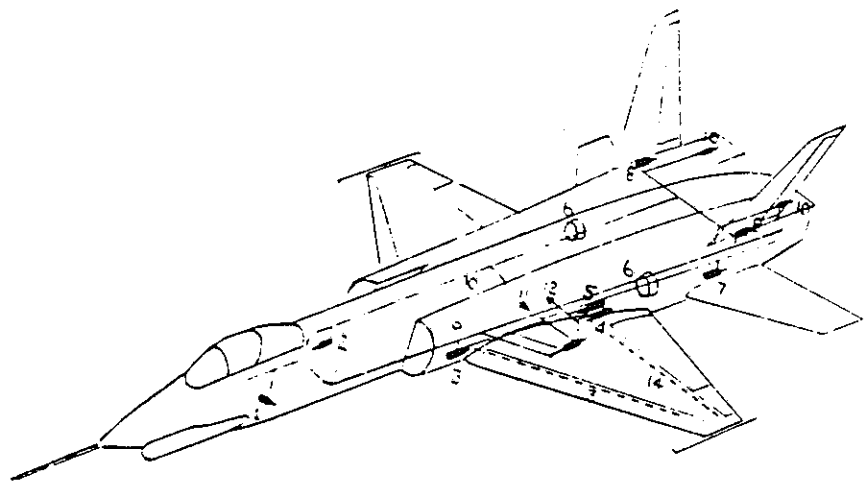


Figure 10-1: Hydraulic system layout

10.2 Electrical

The electrical system consists of two 50 kVa 115/200V AC engine driven generators, one on each AMAD. Each generator is mechanically cross-linked so in the event of an engine failure, the remaining engine can drive both generators. If one of the generators were to fail, the remaining one is capable of supplying the required amount of electricity.

10.3 Back-up

If a dual engine failure were to occur, a ram air turbine (RAT) deploys. This powers an electrical generator which in turn powers the hydraulic pumps. The RAT is capable of supplying the needed power to maintain the essential systems required to return to base. Sealed Ni-Cad batteries, located between the engines near the AMAD, provide transient power until the RAT comes online.

10.4 Environmental Control System (ECS)

A regenerative environmental control system similar to that on the General Dynamics F-16 is used. This system uses engine bleed air for cockpit pressurization, cooling of the crew station and avionics bays, and pressurization of the pilot's g-suit. An onboard oxygen generation system like that of the McDonnell-Douglas Harrier is used to supply fresh air to the pilot. A by-product of this system is nitrogen which will be used to purge the fuel tanks and gun compartment²⁶.

10.5 Windscreen and Canopy

The windscreen is made of glass and acrylic laminate capable of withstanding a 1kg bird strike at 528 knots and bulletproof against small arms fire. The canopy is made of stretched acrylic. An embedded miniature detonating cord is provided to break the canopy during seat ejection if the aircraft has insufficient airspeed for canopy clearance with respect to the seat ejection envelope. The windscreen and canopy are covered by an electrically conductive heating film for anti-icing and demisting²⁶.

10.6 Flight Controls

A quadruple redundant fly-by-wire flight control system with an air data computer is utilized.

The primary reason for the selection of this system is its proven capability. By using off-the-shelf components, cost is reduced²⁷.

10.7 Fuel System

Three fuselage mounted bladder tanks hold the fuel required to fulfill the mission. The volume of these tanks are 89.06 ft³, 88.81 ft³, and 34.40 ft³. Bladder tanks were chosen so if a tank is punctured by enemy fire, it seals itself preventing leaks and possible explosion. The three tanks are interconnected to allow for fuel transfer between them. The second tanks has lines connecting it to the engine. The bottom of this tank is armored and is designated the "go home" tank since it will be used for the return trip home after the mission is completed (Figure 10-2). All three tanks are removed from the top of the aircraft. The Griffen has in-flight refueling capability with the receptical located on the nose of the aircraft just ahead of the cockpit. This positioning meets Air Force requirements and allows the pilot to view the alignment of the airplane while approaching the boom. It also allows for emergency ejection during refueling.

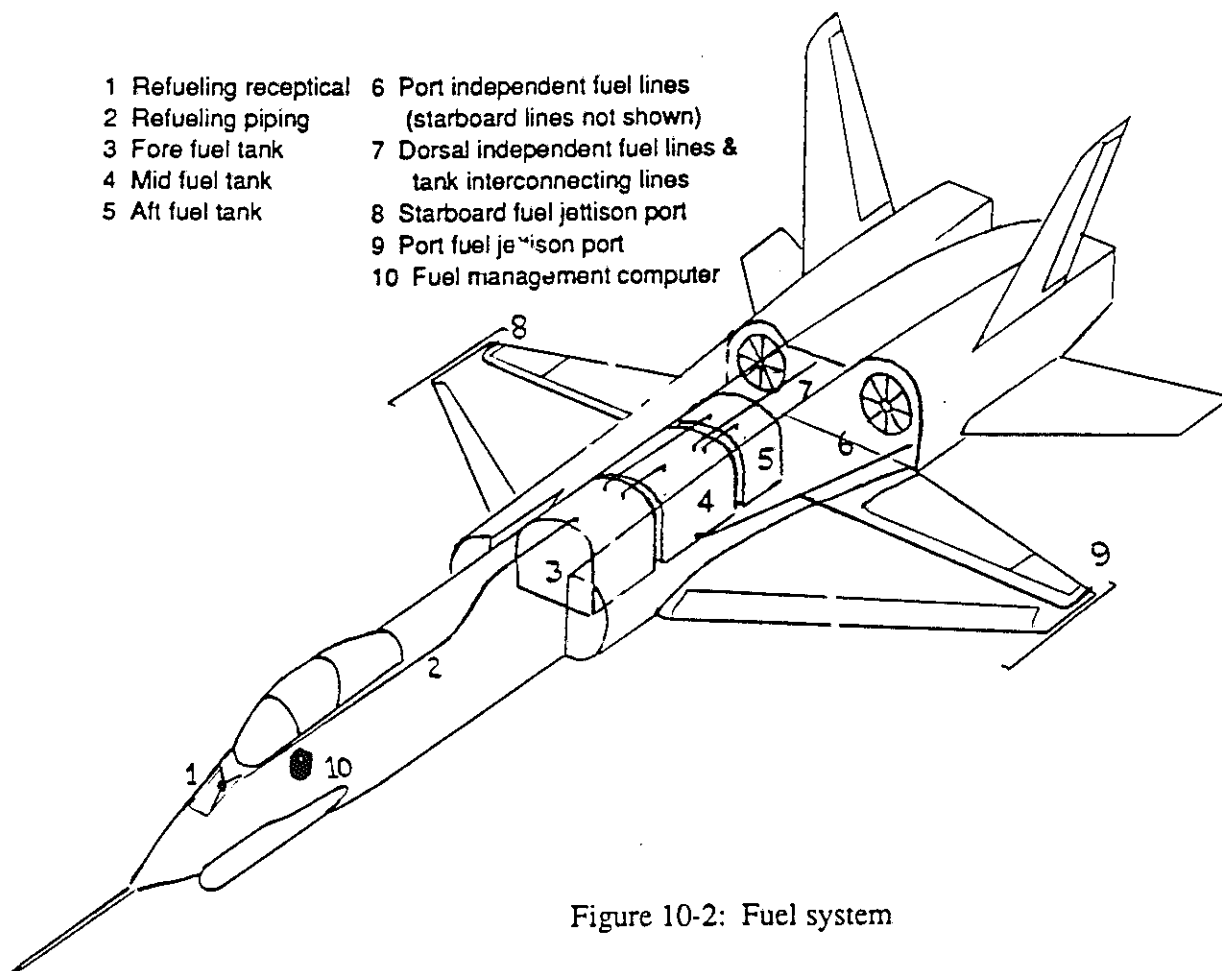


Figure 10-2: Fuel system

10.8 Landing Gear

All three landing gear will be those used on the McDonnell-Douglas F-15 Eagle with minor modifications. These gear were chosen because they fit the size requirements and retract in the same fashion as needed on the Griffen (Figure 10-3). All three struts retract forward so in the event of hydraulic system failure, gravity can be used to deploy the gear with dynamic pressure lockdown. The nose wheel strut is slightly offset to the right to avoid the gun barrel. The main landing gears rotate 90 degrees and are stowed in the root apex of the wing. The main gear strut is stowed beneath the wing box along with the strut pivot and retracting actuator. All of these are housed with a fairing having a single door enclose both the wheel and landing gear strut. Since the Griffen will use off-the-shelf landing gear, design costs will be non-existent. Also, testing will not be required since the gear are already in use.

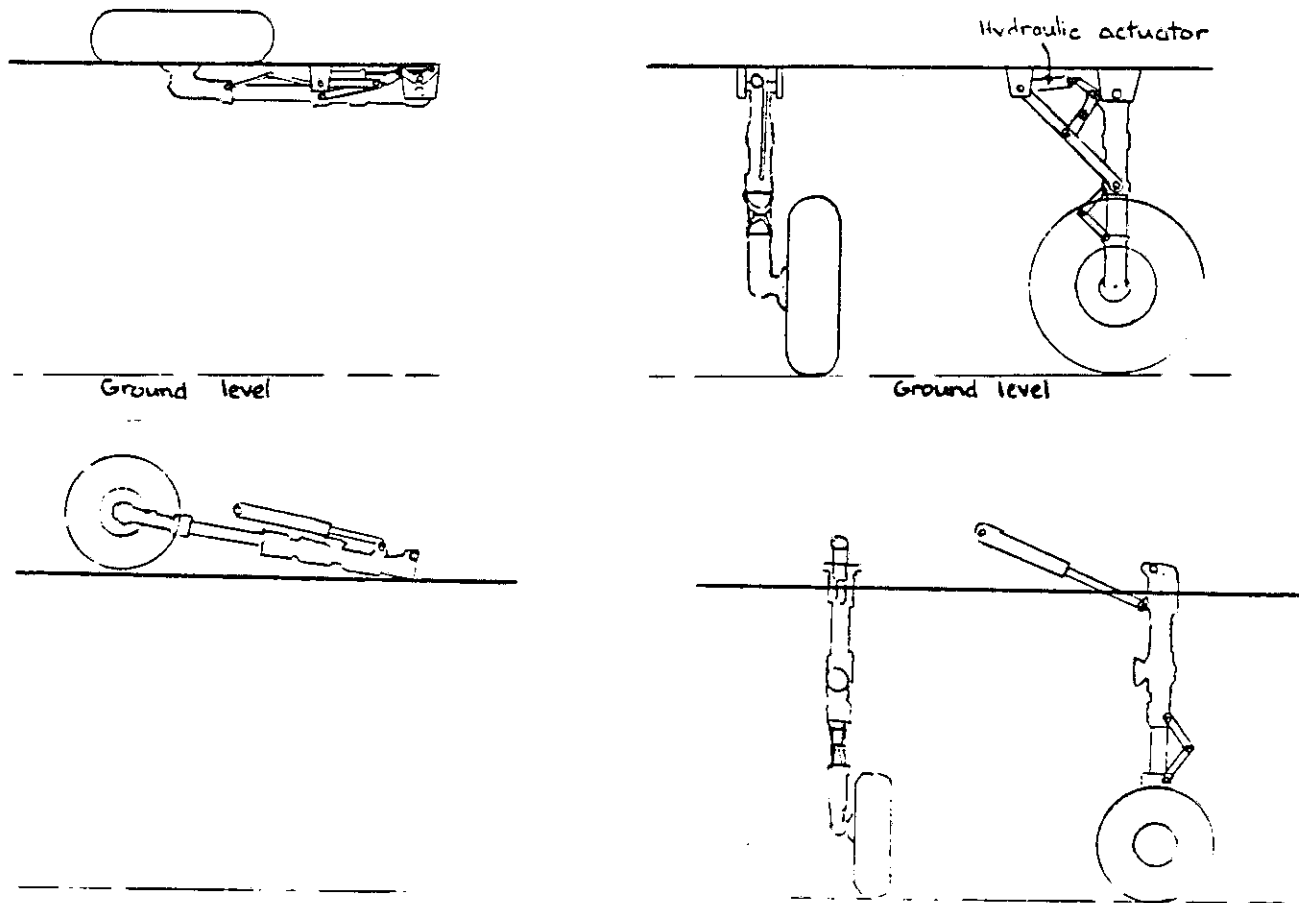


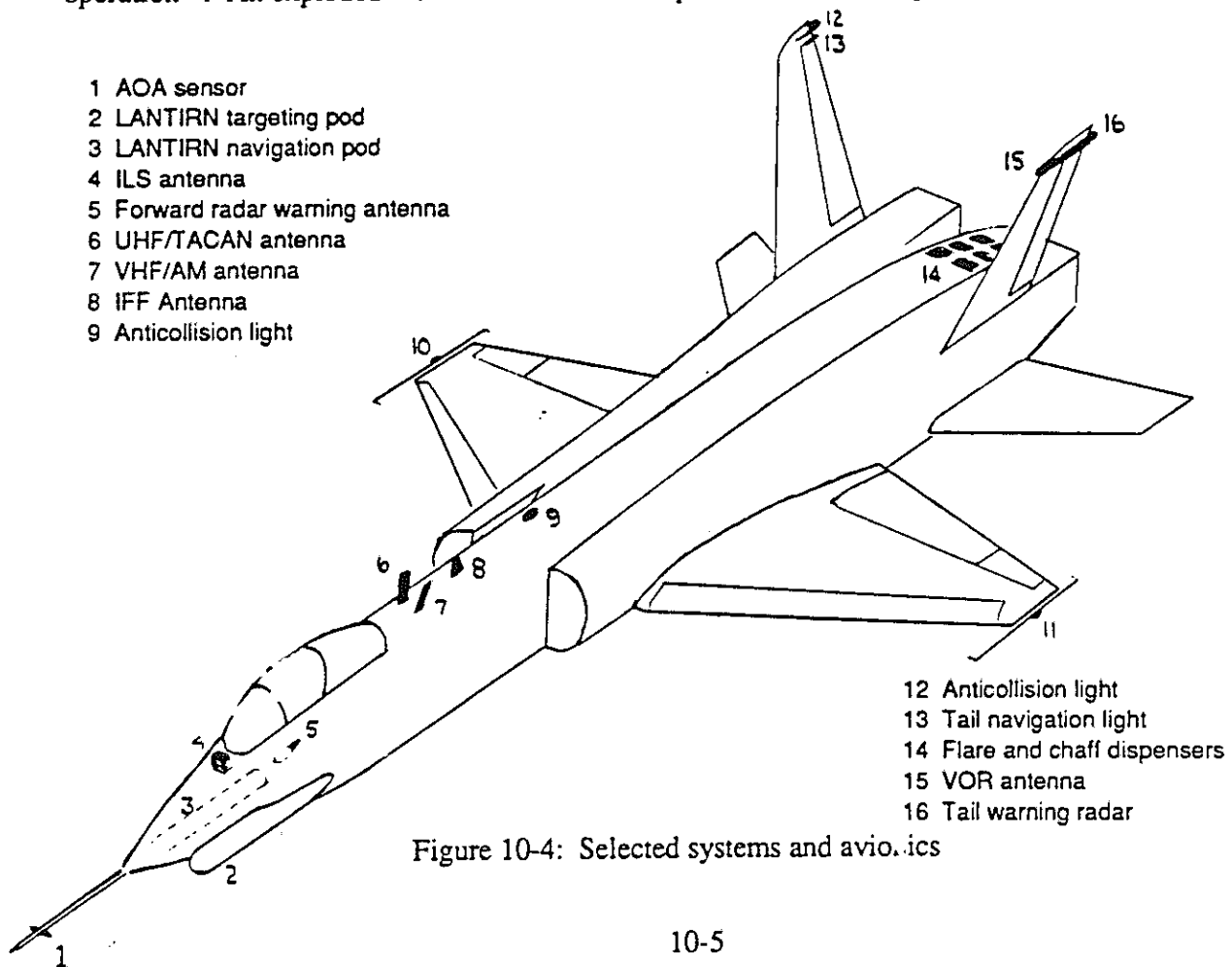
Figure 10-3: Landing gear

10.9 Miscellaneous Systems

There are two independent hydraulic motors to drive the gun barrel. Either system by itself is capable of half-rate firing. A jet fuel starter is used for self-starting capability, eliminating the need for ground equipment. There is also an onboard halon fire extinguishing system to put out any in-flight fires.

10.10 LANTIRN

Martin Marietta's Low-Altitude Navigation and Targeting Infrared System for Night (LANTIRN) system is used for terrain following and target acquisition. The system is mounted in the nose of the aircraft with the navigation pod on the starboard side and the targeting pod on the port side of the nose centerline (Figure 10-4). This provides some protection from ground fire and allows the sensors the best field of view. The LANTIRN uses terrain following to allow the Griffen to fly itself at treetop level. The targeting pod uses infrared sensors to locate targets which are then displayed within the cockpit. This system is capable of day or night as well as under-the-weather operation²⁷. An exploded view of the LANTIRN pods is shown in Figure 10-5.



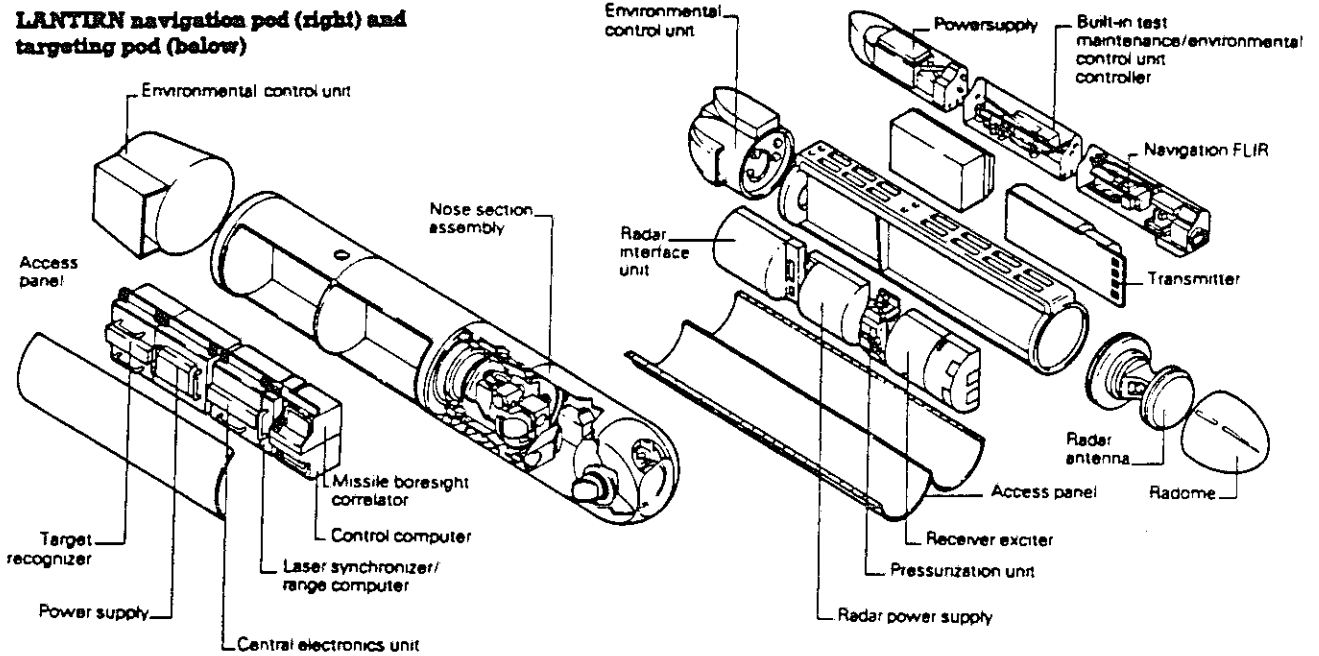


Figure 10-5: LANTIRN navigation and targeting pods²⁹

10.11 Radar

A synthetic aperture radar is NOT used on this aircraft for several reasons. A radar incurs a weight and cost penalty and the primary mission does not infer its need. To utilize the radar, the Griffen would have to "pop-up" from its terrain following altitude so the radar can paint a picture of the geography ahead. By doing this, the plane becomes more vulnerable to surface-to-air missiles and by activating the radar, the enemy can receive its transmission, alerting them to the planes presence and location. The radar would, however, be useful over the battlefield to search for targets of opportunity but the LANTIRN system is almost as capable and the pilot could also use intelligence collected by different sources to locate alternative targets. Finally, the use of a radar would add more complexity to the pilot's activities.

10.12 Inertial Navigation System (INS)

The Griffen uses INS in conjunction with the LANTIRN navigation pod's terrain following mode to navigate over the mission distance. This system also be use a moving map display to direct the airplane into close proximity of the battlefield. At that time, the LANTIRN system takes over sole responsibility for flying the airplane to the target.

10.13 Electronic Counter Measures (ECM)

The Griffen's main form of ECM is the Tracor ALE-40 flare/chaff dispenser mounted on the bottom of the fuselage between the engines. This system carries 240 flare and 240 chaff canisters (Figure 10-4). Additionally, the Griffen is equipped with passive ECM.

10.14 Radar Warning Receivers

The Griffen has both forward and rearward radar warning receivers (Figure 10-4). These sensors alert the pilot to incoming missiles or enemy aircraft.

10.15 Identify Friend or Foe (IFF)

The Griffen has both an IFF transponder and interrogator installed (Figure 10-4). This system allows friendly aircraft to identify themselves to others.

10.16 TACAN Capability

A TACAN system is not installed on the aircraft, however, provisions are made for future installation. The TACAN system was found to be unnecessary since the airplane flies at such low altitude, the signal from the TACAN system would be blocked by the terrain and the horizon.

10.16 Miscellaneous Avionics

The Griffen uses an Instrument Landing System (ILS) for under-the-weather landings, a UHF/VHF/Secure Voice communication system, a fire control system, and a gun camera to take battlefield photographs for later analysis¹⁵.

11. Crew Station

11.1 Cockpit

The main console of the cockpit uses four multi-function displays (MFD) and a wide-angle holographic head-up display (HUD) (Figure 11-1). The multi-function displays are cathode ray tube (CRT) screens with buttons around the perimeter of the screen. CRTs were chosen because of their better visibility in direct sunlight. CRT screens are also less costly than other alternatives.

The top screen is the vertical situation display (VSD) which gives the pilot his altitude, airspeed, pitch angle, and roll angle for example. This screen essentially duplicates the HUD. When the LANTIRN system is in use, this screen becomes the display for the forward-looking infrared sensor.

The bottom screen is the moving map display. Digitized map information, relevant to the current mission, is stored on an exchangeable optical laser disk read by the flight computer. In coordination with the INS, this disk provides an accurate real-time moving map of the terrain below.

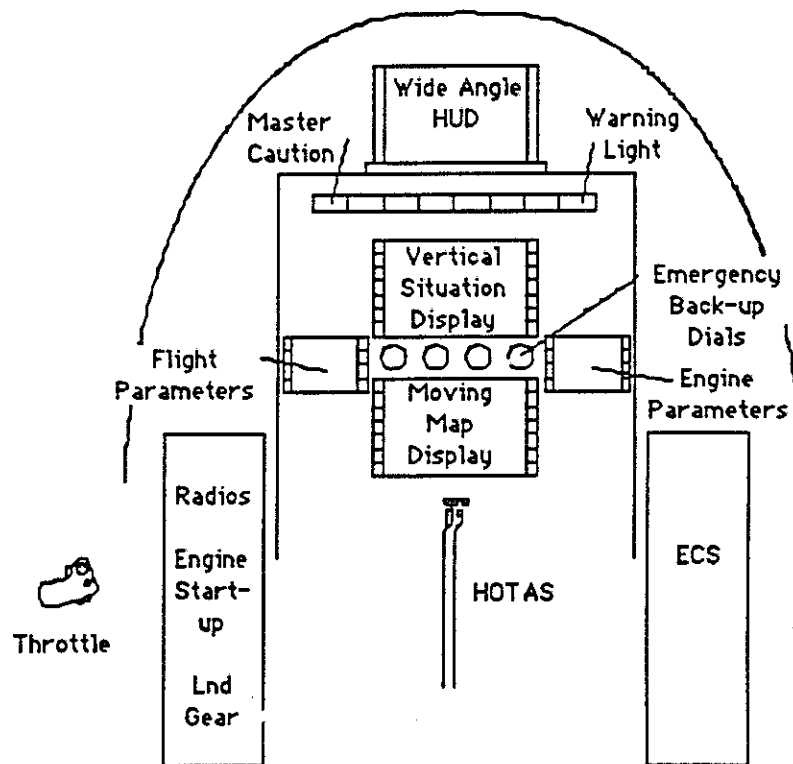


Figure 11-1: Cockpit layout

The left MFD displays flight parameters and the right MFD displays engine parameters. At any time, the pilot can alter what is displayed on the MFDs. For example, once over the battlefield, the pilot may wish to move the VSD to the left and activate the stores display.

Between the upper and lower MFDs are the four emergency back-up dials. These dials are standard analog instruments consisting of an attitude indicator, airspeed indicator, altitude indicator, and vertical speed indicator. Above the VSD are a row of warning lights with the master caution light at the left end.

The panel on the left side of the pilot contains controls for the throttle, radios, engine start-up, landing gear operation, fuel management, IFF, and exterior lights. The right panel contains controls for the environmental control system, navigation, compass control, interior lights, and instrument landing system.

The wide-angle holographic HUD was selected because it will not block out the view of the real world behind it and is less susceptible to direct sunlight distortion²⁷.

11.2 Control Stick

The Griffen utilizes the hands-on throttle and stick (HOTAS) system with a center stick. The throttle is located on the left control panel. The center stick has full movement forward and aft but only the upper portion moves left and right. This allows the pilot's legs to be positioned closer together since no space is required for side-to-side motion of the stick. The center stick handle has controls for trim, weapon release, autopilot nose gear steering, gun trigger, and camera activation. The throttle has controls for the microphone, IFF interrogator, target designation, ECM dispenser, weapon selection, and speed brakes²⁹.

11.3 Ejection Seat

The Griffen uses the McDonnell-Douglas ACES II zero-zero rocket ejection seat (Figure 11-2). This seat is the best currently available for military aircraft allowing for ejection while on the ground sitting still. A miniature detonating cord system is used to break the canopy before the seat ejects²⁹.

**McDonnell Douglas ACES II
ejection seat**

- | | |
|-----------------------------------|--|
| A Environmental sensor ports | H Ejection control safety lever |
| B Recovery parachute container | I Radio beacon switch |
| C FLCS data recorder | J Survival kit (under seat pan) |
| D Recovery parachute risers | K Ejection handle |
| E Emergency oxygen bottle | L Restraint emergency release handle |
| F Emergency oxygen pressure gauge | M Lap belt and survival kit attachment |
| G Inertia reel knob | N Emergency oxygen fitting |

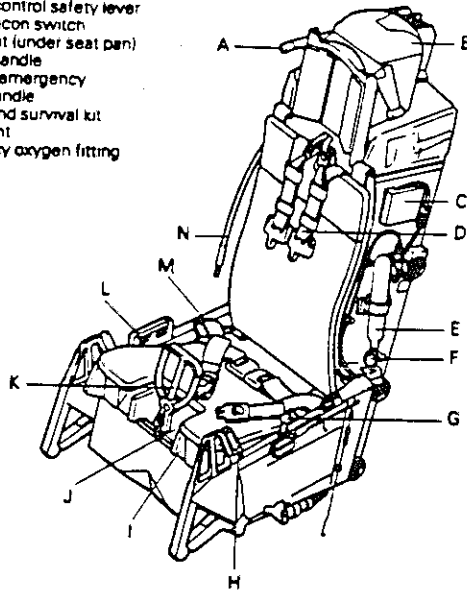


Figure 11-2: McDonnell-Douglas ACES II zero-zero rocket ejection seat²⁹

12. Structural Design and Material Selection

12.1 V-n Diagram

The operating flight envelope of the Griffen, shown in Figure 12-1, represents the aircraft's limit load factor as a function of airspeed. Calculations to obtain the stall boundaries and the gust diagram were performed using the design criteria of $n_{\max} = 7.5$ and $n_{\min} = -3.0$ along with basic equations from Aircraft Structures³⁰. By observing the V-n diagram it is seen that the gust diagram shown in dashed lines does not influence the maneuver diagram. This is typical of most fighter aircraft. It is also relevant to note that the dive speed of 543 knots (calculated from the maximum dynamic pressure of 1000 psf as given in the RFP) is lower than would be expected for a final design. The dive speed for most military aircraft is at least 30% greater than the cruise speed, which would give this aircraft a dive speed of 650 knots³⁰.

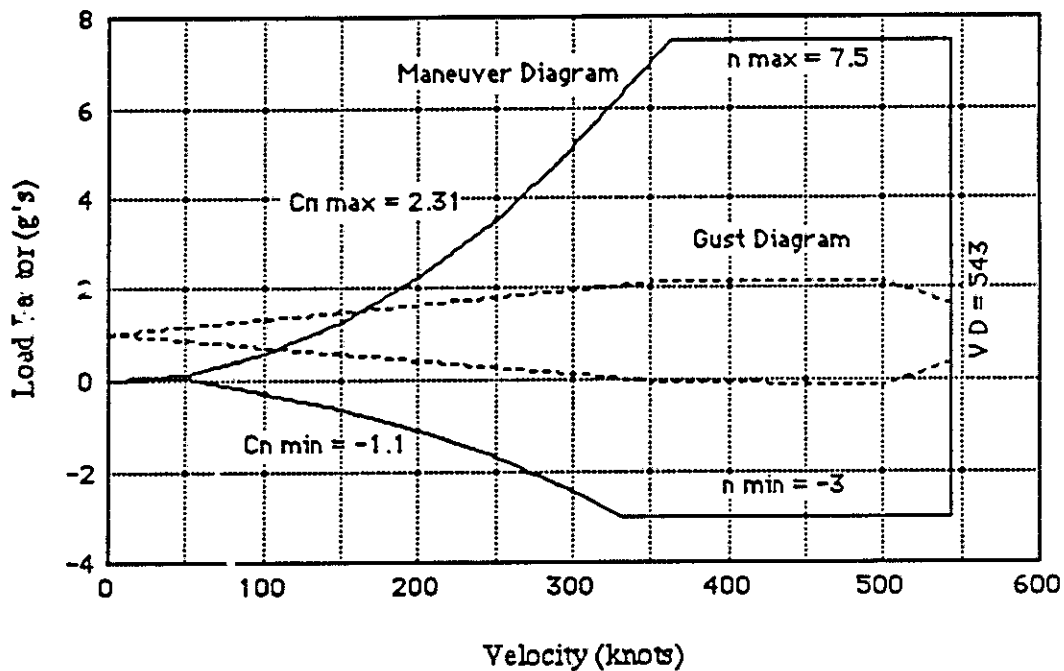


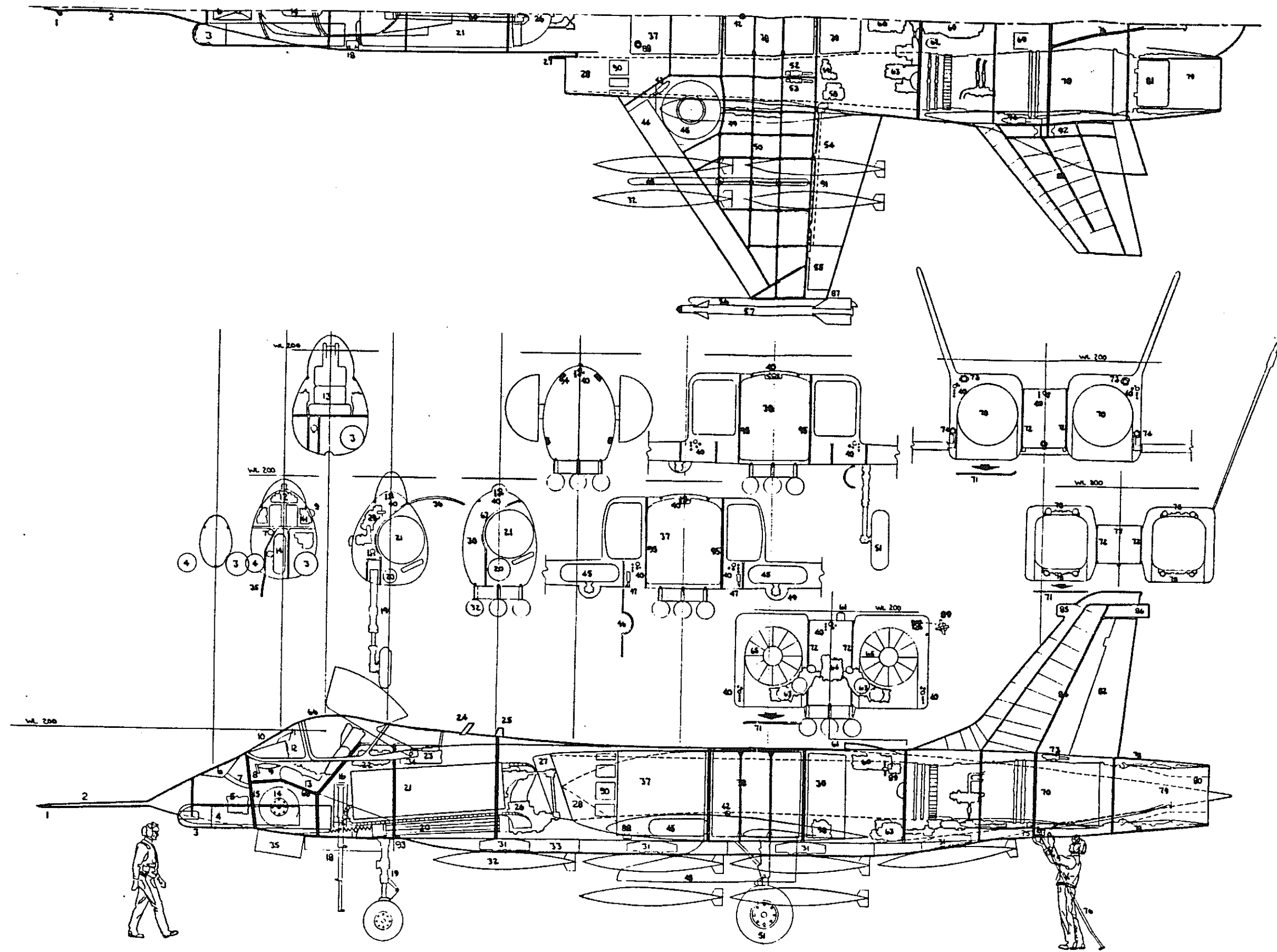
Figure 12-1: V-n diagram of the Griffen

12.2 Structural Arrangement

The structural arrangement for the primary members in the fuselage, wing, and empennage structures are shown in Figure 12-2. The semi-monocoque fuselage structure is covered with a skin supported mainly by stiffening members, frames, bulkheads positioned at or near the vertical, keels, stringers, and longerons running longitudinally. The wing and the tail surfaces are composed mainly of spars and ribs. The wing spars are perpendicular to the longitudinal axis of the airplane and the ribs are parallel to the free stream direction. The substructure for the tail surfaces is composed of spars that run at constant chord percentages and ribs that remain essentially perpendicular to the trailing edge spar.

The longerons, which carry the major longitudinal fuselage loads, run fore and aft and are attached to the skin between the vertically oriented bulkheads. Proper alignment of the longerons avoids any kinks which cause unnecessary kick load stresses. Also seen in Figure 12-2 are the major bulkheads, which act to distribute applied loads into the fuselage skin. The number of major bulkheads are minimized by having each one carry as many concentrated loads as possible. The major bulkheads are listed below giving their Fuselage Station (F.S.) and function:

- Boom and avionics support at F.S. 156
- Forward pressure bulkhead, LANTIRN, Avionics, and Canopy support at F.S. 195
- Ejection rail and LANTIRN support at F.S. 235
- Rear pressure bulkhead/firewall to provide Gun, Landing gear, and Ammunition drum support at F.S. 285
- Firewall, Gun and Ammunition drum support at F.S. 350
- Wing support at F.S. 485, 505, 525, & 546.
Gear support at F.S. 525
- Firewall, Engine and AMAD support at F.S. 615
- Engine and Vertical tail support at F.S. 662
- Engine, Vertical tail, & Horizontal tail support at F.S. 697
- Engine, Nozzle, and Nozzle actuator support at F.S. 750



Fuselage Stations

100 200 300 400 500 600 700 800

Figure 12-2: Structural configuration

The fuselage uses two keels, located outboard of the fuel tanks and engine installations, to carry the bending loads and to support the tail hook and bomb pallet.

Four jack points, located at F.S. 285 and F.S. 697 on both sides of the aircraft, are used during the production process, engine, gun and ammunition drum removal, along with repair and check of the landing gear during the service life of the aircraft.

The low mounted wing of the Griffen is a two piece structure using four spars attached to center section bulkheads. The two piece wing structure is chosen to reduce the downtime of the Griffen in the event of battle damage. The removable outer panels of the wing are attached to the center section bulkheads through shear fittings located 75 in. from the center line. Weapon pylons on each wing are located on hard points 115 in. from the aircraft centerline.

The design of the empennage structure is similar to the wing with the main structural support coming from spars and ribs. The all-flying horizontal tail, which is similar to that on the Tornado, uses three spars with the leading edge spar being 17% of the chord, the intermediate spar being 45% of the chord, and the trailing edge spar being 74% of the chord. The loads from the horizontal tail are transmitted directly to the bulkhead at F.S. 697 through a pivot fitting. The vertical tails use a two spar construction with the leading edge spar being 17% of the chord, and the trailing edge spar being 51% of the chord. The loads from the vertical tails are transmitted into the fuselage structure by having the two spars terminate on aft bulkheads at F.S. 662 and F.S. 697.

12.3 Material Selection

The materials proposed for this aircraft consist mainly of aluminum alloys, composite materials, and titanium. These materials are chosen based on the operating envelope shown in Figure 9-2 along with the following selection criteria:

- Strength-to-weight ratio
- Material costs
- Fatigue properties
- Corrosion resistance
- Crack growth behavior
- Survivability
- Advanced structural concepts & New manufacturing techniques

The primary reason for the use of composite materials, such as graphite/epoxy and Kevlar, is

to provide structural simplification, reduce part count and save on the overall structural weight, and eliminate costly design features. There are several concerns that must be dealt with when using composites. One problem is galvanic corrosion, since graphite is cathodic in nature and aluminum anodic. One of the best joiners for the two materials is titanium, which is used in rivet and bolt form in the Griffen. Another concern with composites is its elevated costs when compared to Al alloys. The higher initial cost associated with most composite materials can be recovered by reducing the part count on various structures and through lowering the life cycle cost of the aircraft due to lower fuel consumption, fewer maintenance hours required because of the reduction in structural corrosion, and increased fatigue properties³¹.

The materials for the Griffen are shown Figure 12-3 and 12-4. The reasoning behind the selection for each of the aircraft components is listed below.

Wing and Empennage - The wing is formed from a combination of aluminum-lithium, graphite/epoxy, and a small portion of Ti-6Al-4V. The main requirement of the upper wing spar box surface is for resistance to compression, and this part of the wing is constructed from graphite/epoxy because of its superior compressive strength along with its lighter weight compared to the Al alloys. The laminate pattern (defined with respect to the spanwise direction) will probably be similar to that on the F/A-18 with ≈50% of ±45° plies, ≈45% of 0° plies, and ≈5% of 90° plies. The ±45° plies carry the shear loads, the 0° plies carry the longitudinal loads, and the 90° plies are for transverse loading. The buckling strength and damage tolerance capability of the upper wing surface is improved by locating a pair of ±45° plies at the extreme of the laminate³². The lower wing spar box surface is mainly in tension during the flight and because of its high vulnerability to ground fire is formed from aluminum-lithium (Alithalite 2090). Al-Li is chosen because of its superior fatigue characteristics and potential weight savings of up to 10% with respect to Al 2024. It was not advantageous to use graphite epoxy on this section of the wing because of its excessive tensile strength reduction in the event of a ground strike³². On the lower wing surface, fatigue performance is a primary design criterion, and in the case of damage tolerant design philosophies, crack growth behavior is relevant. Fatigue behavioral tests were conducted on the lower wing

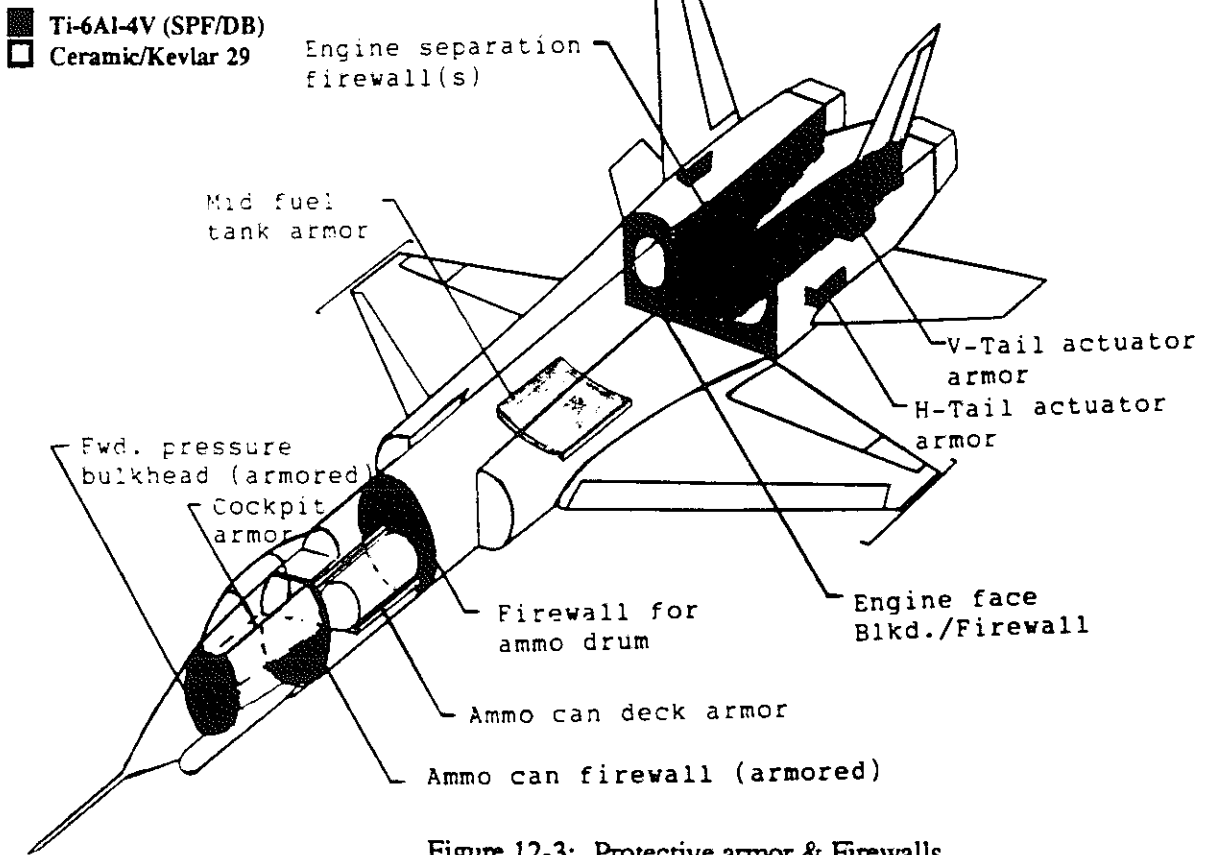


Figure 12-3: Protective armor & Firewalls

Materials Not Shown	
Graphite/Epoxy	[Ribs, Hidden access panels]
Ti-6Al-4V (SPF/DB)	[Spars, Engine access doors]
Al-Li 2090	[Lower spar box surface]
Steel 300M	[Landing gear & Wing fittings]
Steel 4030	[Control Surface pivots]

- Graphite/Epoxy
- Al-Li 2090
- Al 2024
- Ti-6Al-4V (SPF/DB)
- Steel 4030
- Rene 41

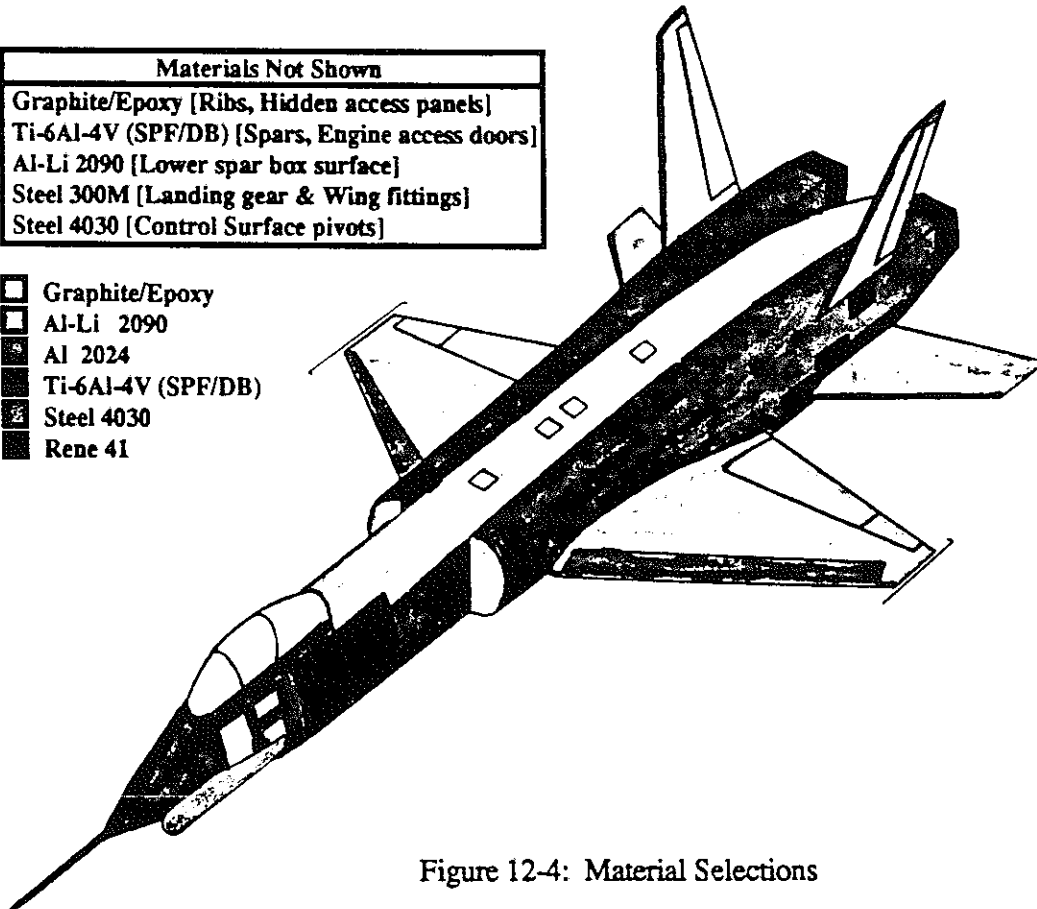


Figure 12-4: Material Selections

the spectrum crack growth life of 2090-T8 exceeds by more than a factor of 5 the performance of other alloys including 2024-T351, which is widely considered to be the alloy most resistant to fatigue crack growth³³.

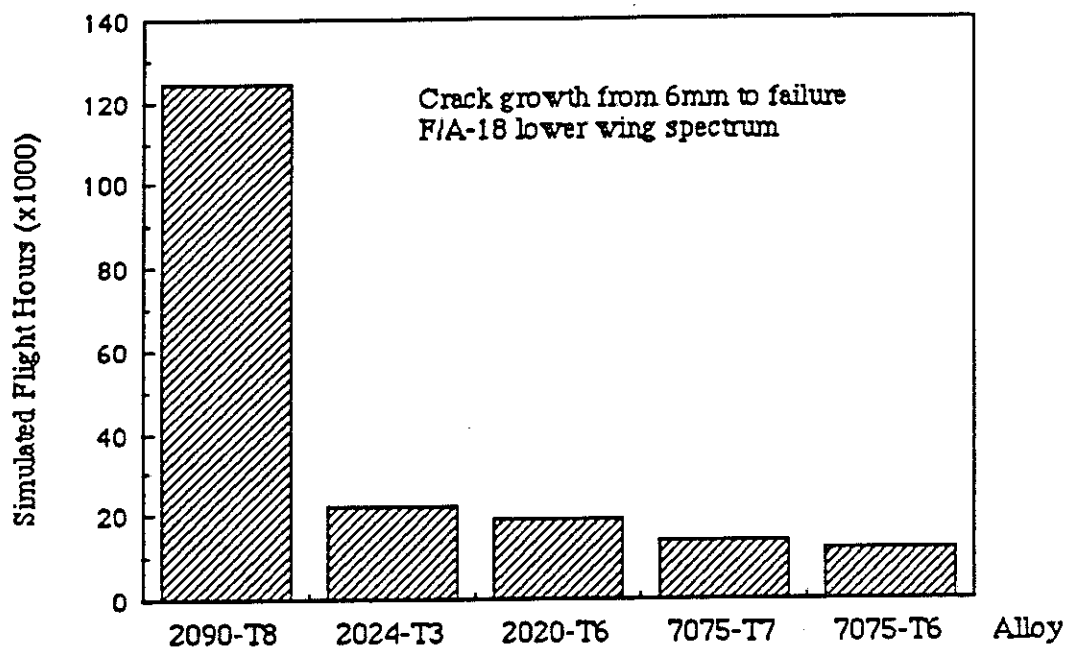


Figure 12-5: Fatigue crack growth

The ailerons and the trailing edge flaps of the wing are constructed from graphite/epoxy. These surfaces are expected to experience a larger amount of chordwise bending and thus a greater portion of 90° plies will be contained in the skins. The leading edge slats on the wing are made from Al-Li. A composite structure is not used on the leading edge flaps because of delamination problems with respect to sharp impacts and the inability to detect them. The remaining portion of the leading edge of the wing along with the leading edges of the empennage structures uses Ti-6Al-4V to preclude inflight and foreign object damage.

The substructure of the wing consists of titanium spars and graphite/epoxy ribs. The four spars, as well as all other titanium members, are formed from the SuperPlastic Forming/Diffusion Bonding (SPF/DB) process. This process takes advantage of titanium's high temperature characteristics and allows it to be bonded to itself without the use of rivots and fasteners. This more

efficient structural configuration has potential weight savings of 30-40% and cost reductions of up to 50%³⁴. It is currently being used extensively on the F-15E Dual Role Fighter³⁵.

The vertical and horizontal tails are both constructed with all composite skins and a substructure that consists of SPF/DB Ti-6Al-4V spars and graphite/epoxy ribs. The skin for the horizontal tail must provide adequate torsional strength and stiffness, and thus a higher percentage of 45° plies are required, even up to 80%³². The construction of the vertical tail is similar to that of the wing.

Fuselage - There are several factors when considering the fuselage that favor metallic materials over composites. In a typical fuselage with a complex loading distribution (pressurization, bending, torsion) and multiple cutouts, the possibility of orienting the fibers in the direction of the principal loads no longer exists. The process of filament winding exists, but this was seen as too costly³¹. Crashworthy considerations were also taken into account, and from recent studies it was shown that aluminum alloys can sustain more than 24 times the deformation and possess up to 65 times the energy absorption capability of graphite/epoxy³⁶. Therefore, the majority fuselage of the Griffen is constructed primarily from Al 2024. Graphite/epoxy is used on the top center section of the fuselage, on non-structural access panels, on the speed brakes, and on the engine intake duct skinning due to the primary hoop tension loads.

Firewalls and protective armor - The bulk of SPF/DB Ti-6Al-4V is used to provide shielding and protection for the engine, the ammunition drum, and the cockpit. The protective armor around the cockpit, underneath the mid fuel tank, and around the ammunition drum is constructed from Kevlar 29 with an outer lining of ceramic material to defeat armor-piercing projectiles. The reason behind the selection of these materials is presented in the Survivability and Vulnerability section.

Other Material Considerations - Steel alloys are used on the landing gear and their attachments, the angle of attack sensor boom, the control surface pivots, and for the wing shear fittings. Steel alloy 300M is used on the landing gear and the wing fittings due to the high loads that both will experience. The boom and the control surface pivots are constructed from steel 4130.

Rene 41 nickel alloy will be used for the nozzles due to its good heat resistance and weldability.

Lightning Protection - Aircraft regulations usually require that some sort of lightning-strike protection be provided on all nonmetallic surfaces. The technique to be used on the Griffen is to bond thin (0.004 in.) aluminum-foil strips 2 inches wide on 4 inch centers to the wing, vertical tail, and horizontal tail. These strips are grounded to the titanium frame member, which, in turn, grounds the surface to the rest of the airframe ³¹.

Repair Procedures - Repair of composite materials will consist of two levels. One level will repair minor structural damage, and is accomplished through resin injection. More serious damages will require patch repairs. Holes up to 100mm in diameter are repaired either using bonding graphite/epoxy patches or bolted titanium patches ³².

Al-Li surfaces will be repaired in a similar manner to conventional Al alloy structures, using Al-Li material when available.

12.4 Weight Savings

The following section presents the weight savings obtained through the use of various advanced materials. Calculations are performed, using a McDonnell Douglas report ³⁵, to make a quick material comparison and calculate the resulting weight reductions. An example of this procedure is presented in Appendix C. The basic procedure is listed below followed by Table 12-1, which presents the weight savings for the various components.

- 1) Establish failure mode percentages for the component in question (Tension, buckling, compression, shear ...)
- 2) Choose alternate material
- 3) Calculate the strength-to-weight ratios for each failure mode [ex. $K_{TN} = (\rho_1/\rho_0)*(FTU_0/FTU_1)$]
- 4) Compute the weight adjustment factor (K)
 $K = \sum [(\%failure\ mode)*(strength-to-weight\ ratio)]$
- 5) Calculate the weight of the adjusted structure

$$WT_{adj} = K * WT_{base} * \%Appl. * CF + WT_{base} * (1 - \%Appl.)$$

[CF is a construction factor (1.1 for graphite/epoxy)]

Component	% Weight savings
Wing	20.0
V-tail	31.7
H-tail	31.3
Fuselage	8.2

Table 12-1: Weight savings

It should be noted that the weight savings calculated are for a direct material substitution. If the components are designed and manufactured from the alternative materials with respect to the unique properties and forming characteristics, even greater weight savings can be expected.

13. Management and Manufacturing

13.1 Management

The corporate structure for the Griffen project is shown in Figure 13-1. The Griffen program is lead by a civilian executive who has a direct line to a military liaison. This assures an open line of communication between the military and the corporation. The civilian representative responds to a board of directors which oversees progress in all programs related to the aircraft manufacturer.

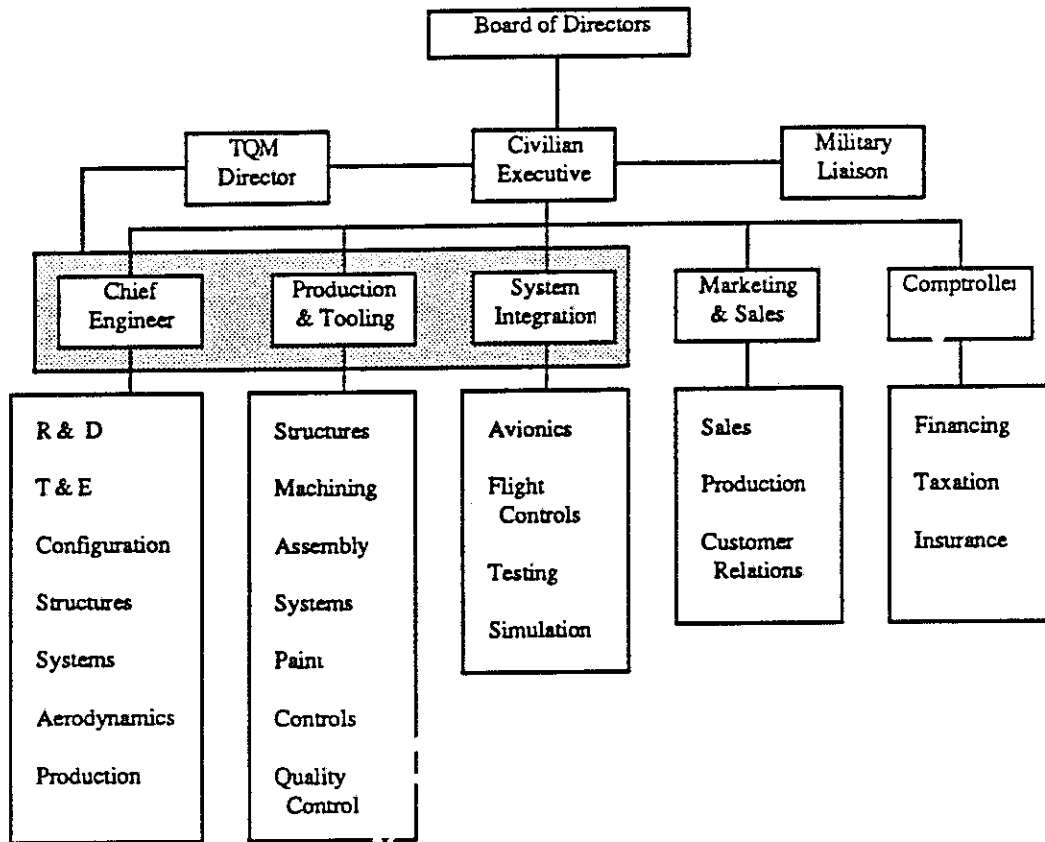
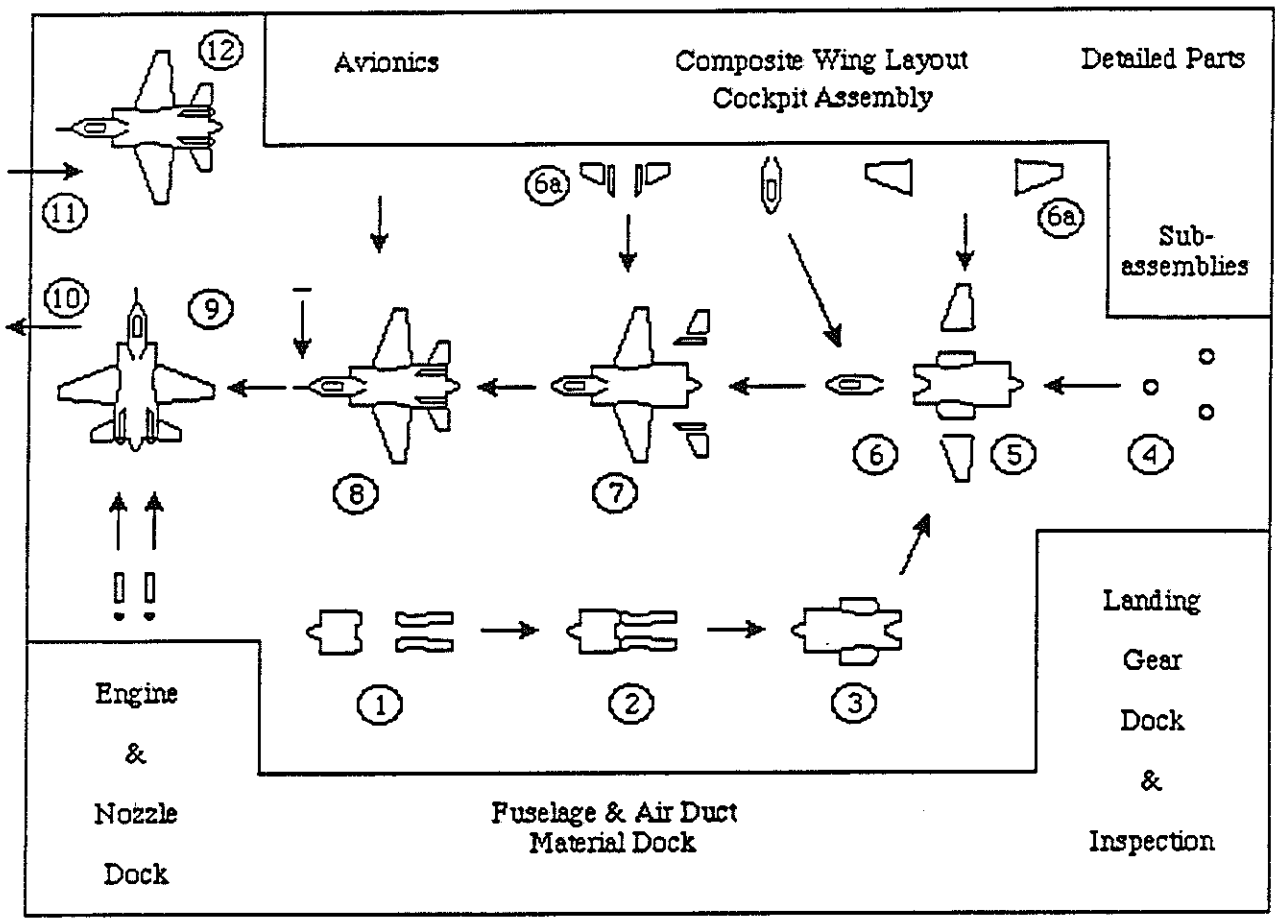


Figure 13-1: Corporate Structure^{37.2}

Quality of work is enhanced by a Total Quality Management (TQM) system. In this system, the TQM director oversees that all managers are aware of any design decisions and changes done to any part of the Griffen program. Further, before any change is finalized, all managers have the opportunity for further input and suggestion to the improvement. This system avoids errors and complications arising from disciplines which are not in the expertise of the designer.



- | | |
|--------------------------------------|--|
| 1.) Aft Fuselage Assembly | 7.) Tail Installation |
| 2.) Air Duct Installation | 8.) Avionics Installation |
| 3.) Mid Fuselage Assembly | 9.) Engine/Nozzle Installation |
| 4.) Landing Gear Installation | 10.) Corrosion Protection/
Painting/Decal Fitting |
| 5.) Wing Installation | 11.) ECM/Avionic System Check |
| 6.) Forward Fuselage/Canopy Assembly | 12.) Final Inspection |
| 6a.) Wing/Control Surface Assembly | |

Figure 13.2 Proposed Manufacturing Facility

13.2 Manufacturing

The manufacturing plant for the Griffen is designed for maximum efficiency in the production of the aircraft. The proposed plant, Figure 13-2, uses approximately 87,500 ft² of floor space to handle 10 aircraft on the production line. Aircraft production begins with a fuselage aft section, air ducts, and mid section. As soon as the wing and forward section are installed, the landing gear is added to facilitate the movement of the aircraft from station to station. The landing gear is purchased from a subcontractor and inspected prior to installation in step 4. The engines and avionics are added last in the production sequence. After all the systems are added to the aircraft, the plane is moved to an existing paint shop where the aircraft is thoroughly cleaned, protected against corrosion, and painted to the needs of the customer. Decals are applied last. The separate painting facility has two major advantages: 1.) it can be used for other aircraft types currently under production by the company, and 2.) toxic paint fumes can be easily ventilated. After painting, the aircraft is moved to the manufacturer's facility for an ECM and avionic system check. The aircraft then returns to the original plant for final inspection.

Production of the 500 aircraft fleet will take approximately 58 months. Production rate will increase linearly from 0 to 10 aircraft per month (see Figures 13-3 and 13-4) to accommodate any design changes or manufacturing problems that may have arisen from the production of the test aircraft. Full scale production will be reached in the ninth month. Production rate will decrease steadily in the 53rd month to allow for the labor force to gradually be transferred to other projects.

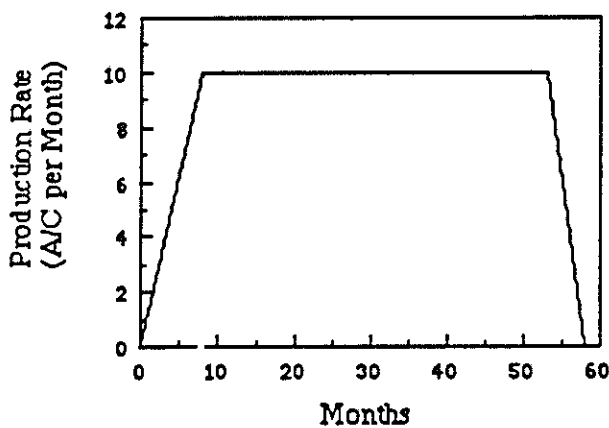


Figure 13.3 Proposed Production Rate

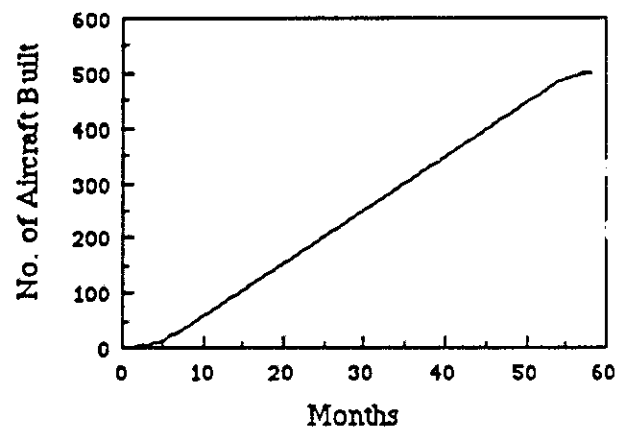


Figure 13.4 Proposed Aircraft Schedule

14. Cost Estimation

Recent purchases of military aircraft have met considerable resistance in both the American public and Congress. The Griffen is particularly attractive to both of these groups since it furnishes the military with a state-of-the-art CAS fighter at a competitive cost. Table 14-1 shows the cost per aircraft of selected military aircraft.

A-10	\$19,100,000
F-14	\$25,000,000
F-15	\$20,500,000
F-16	\$20,000,000
F-18	\$28,000,000
Griffen	\$21,828,721

Table 14-1: Comparative price list³⁸

The cost estimation technique was based on equations from Roskam³⁸. Special considerations in the cost analysis include composite materials, ease of manufacturing and testing, and Computer Aided Design (CAD) capability. Historical data was based on an average of F-4 Phantom and A-10 Thunderbolt data. The analysis was performed for 500 production standard aircraft, 5 static test aircraft, and 5 flight test aircraft. Avionics cost is estimated to be 40% of the total cost of the aircraft.

The Griffen is available for the military at a cost of 21.8 million per aircraft based on 1990 dollars. A cost breakdown is presented in Table 14-2.

Research, Development, Test, and Evaluation	
Airframe Engineering & Design Cost.....	\$159,884,576
Development Support & Testing Cost	\$55,202,418
Flight Test Airplane Cost	\$436,315,578
Flight Test Operation Cost	\$42,328,605
Test & Simulation Facilities	\$0
RDT&E Profit	\$86,716,397
Cost to Finance	\$86,716,397
Total RDT&E	\$867,163,971
Acquisition:	
Manufacturing Cost	\$8,693,138,115
Manufacturing Profit	\$869,313,811
Total	\$9,562,451,926
Total Cost for 500 Production Aircraft.....	
	\$10,914,360,500
Total Cost per Aircraft	\$21,828,721

Table 14-2: Aircraft cost breakdown

Operation cost for the Griffen is based on 650 sorties per year and assumes 51 aircraft assigned to the reserves, 107 lost in accidents and 406 aircraft in active service. Total operation cost is 69 billion 1990 dollars to be paid over the 30 year life of the aircraft. Operation breakdown is presented in Table 14-3.

Program Fuel, Oil, & Lubrication Cost	\$9,209,275,467
Program Cost of Direct Personnel	\$6,298,934,928
Program Cost of Indirect Personnel	\$14,272,845,031
Cost of Consumable Material	\$642,640,561
Program Cost of Spares	\$4,507,214,220
Program Cost of Miscellaneous Items	\$2,629,208,295
Total	\$37,560,118,503

Table 14-3: Operation cost breakdown

Total life cycle cost for the aircraft is made up of Research, Development, Test and Evaluation, Acquisition, Operations, and Disposal. Disposal cost is difficult to predict and is assumed to be 1% of the total life cycle cost. Life cycle cost for the Griffen is 48.5 billion.

15. Future Considerations

The Griffen can be equipped rapidly with different weapons loads using the palletized fuselage bomb system to perform various attack missions outside of the CAS role. Three of these possible mission scenarios are runway denial, anti-armor, and naval attack. A two-seat trainer version is also possible with a reduction in the ammunition drum size.

In the runway denial configuration the standard four pallets each hold three Mk-20 Rock Eye Mod-2 486 lbs cluster bombs or similar cluster bomb units. The Rock Eye bombs are only three inches longer than the Mk-82's they replace and will fit four end-to-end on the fuselage. The bombs are very effective against grounded aircraft and fuel supplies during a first pass of the airfield. Eight Durandal Runway Buster 440 lbs bombs can be carried on the wing hardpoints used by the Mk-82's and are especially effective in damaging runways. Both AIM-9L Sidewinders and cannon ammunition can be carried as well, with a 748 lb lower TOGW.

An effective anti-armor system can be assembled combining six Maverick missiles for use against heavy armor and 12 Rock Eye cluster bombs, effective against light armor. The Rock Eyes are carried on the fuselage in the same manner as for the runway denial role, while the AGM-65 E Maverick 634 lbs air-to-ground missiles are placed three to a wing on a three-launch rail "tree" mounted on the pylons. TOGW for this mission with the standard AIM-9L missiles and ammunition for the GAU-8 cannon is 464 lbs less than for the primary mission.

A naval attack mission launched from land bases against hostile fleets mirrors the CAS role. The Griffen would follow a sea level dash under ship born radar to fleet interception, launch weapons against multiple targets, and return at sea level. Four 1,142 lb Harpoon anti-ship missiles are carried in side-by-side, tandem configurations on twin 153 inch fuselage pallets. Another 4 Harpoons are carried underwing, two to a pylon. The GAU-8 cannon also provides an effective weapon against smaller ships or critical command posts on larger ships. The Sidewinders are retained for self defense. The TOGW for this arrangement is 964 lbs less than for the primary mission.

A two seat trainer version can be readily adapted from the present Griffen design. The standard ammunition canister is replaced by a half-size ammunition drum and the second seat is

added in the area behind and slightly above the front seat, above the cannon barrels and ahead of the foreshortened ammunition drum. The ECS system is relocated rearward to above and to the side of the ammo can. A single, upward-extension canopy is utilized for both crew member ingress/egress. Larger dorsal fin area may be provided to the two vertical tails to maintain lateral characteristics in relation to the increased frontal side area due to the larger canopy. This design provides the rearward seat pilot a good forward view while keeping the aircraft dynamics as similar to the single seat versions are possible. The fuel system is unaltered providing similar range and endurance with its single seat counter part.

16. Conclusion

The Griffen, which has been analyzed using the proven routines of ACSYNT, VLM, DATCOM, SSAAP, and the sizing method of Raymer, more than exceeds the requirements specified in the AIAA/GD RFP by incorporating the following advanced features:

- Thrust vectoring
- Fly-by-wire technology
- Active gust alleviation system
- Side force generation
- Low drag, palletized conformal bomb carriage
- Lightweight armor protection
- State-of-the-art materials and construction techniques

Flexibility was designed into the Griffen so that the aircraft can be adapted to the full range of attack and interdiction roles. Through the integration of alternate navigation and attack systems and expanded weapon loads, the Griffen will be able to maintain state-of-the-art close air support to meet future threats well into the next century.

Appendix A: Flight Conditions Used for Computation of Dynamic Response Characteristics

Sref = 350. sq ft c_{raz} = 12.83 ft b_{raz} = 30.6

Parameter	AP	RD	GA	CR
Mach	0.20	0.76	0.50	0.80
Altitude (ft)	0.00	0.00	0.00	20000.
Weight (lb)	28728.	32878.	40000.	45000.
SM (%MAC)	-5.0	-5.6	-4.8	-5.0
Ixx (sl-ft ²)	14546.	14723.	20157.	26945.
Iyy (sl-ft ²)	168898.	171838.	183646.	197153.
Izz (sl-ft ²)	176889.	180076.	195378.	212309.
Ixz (sl-ft ²)	8531.	4825.	4723.	9283.
<u>Longitudinal:</u>				
C _L	1.105	0.10 ⁰	0.313	0.512
C _{Lα}	3.966	3.919	3.954	3.932
C _{Dα}	1.21	0.118	0.341	0.555
C _{mα}	0.116	0.193	0.122	0.172
C _{Lαdot}	0.699	0.611	0.676	0.634
C _{mαdot}	-1.18	-1.03	-1.14	-1.07
C _{Lq}	2.33	2.04	2.25	2.11
C _{mq}	-3.94	-3.43	-3.80	-3.57
C _{Lr}	0.033	0.047	0.032	0.138
C _{Dr}	0.0069	0.00094	0.0019	0.0126
C _{mr}	0.00096	0.0023	0.00099	0.0060
C _{Lp}	0.550	0.483	0.533	0.502
C _{mp}	-0.948	-0.838	-0.917	-0.868
C _{Lδa}	0.0967	0.0849	0.0938	0.0882
C _{mδa}	0.0056	0.0049	0.0054	0.0051

Appendix A: (cont'd)

	AP	RD	GA	CR
Lateral/ Directional:				
C _{ya}	-0.696	-0.611	-0.674	-0.639
C _{ra}	-0.187	-0.160	-0.180	-0.170
C _{na}	0.374	0.318	0.359	0.333
C _{rp}	-0.214	-0.182	-0.205	-0.191
C _{np}	0.0712	0.0623	0.0689	0.0646
C _{rx}	0.201	0.176	0.194	0.182
C _{nz}	-0.643	-0.560	-0.620	-0.581
C _{raa}	0.022	0.019	0.021	0.020
C _{naa}	0.015	0.017	0.019	0.018
C _{yar}	0.127	0.127	0.127	0.127
C _{nar}	-0.161	-0.160	-0.161	-0.161
C _{rar}	0.050	0.050	0.050	0.050
C _{rat}	0.031	0.028	0.030	0.029
C _{naab}	0.028	0.025	0.027	0.026

Appendix B: Description of SSAAP Program Features

SSAAP: State Space Analysis of an Airplane FORTRAN program

1. Interactive user data input for:
 - a) Airplane stability and control derivatives
 - b) Flight conditions
 - c) Actuator constants
 - d) Output matrix
 - e) Gain matrix
 - f) Observer matrix
2. Storage and retrieval of user input data
3. Problem types:
 - a) Longitudinal / Lateral-Directional
 - b) With or Without Actuator Dynamics
4. Control Effector Options:
 - a) Elevator
 - b) Rudder
 - c) Symmetric and Assymetric Aileron
 - d) Throttle
5. Analysis
 - a) Computes eigenvalues/vectors for uncoupled, linearized, quasisteady
 - i) Open loop system
 - ii) Closed loop system
 - b) Computes resolvent matrix using Fedeeva algorithm
 - c) Computes transfer functions between:
 - i) Ouput/control input
 - ii) Output/initial condition
 - iii) Output/disturbance input
 - iv) Cockpit g-level/gust input
 - d) Creates root-locus and frequency response files for transfer functions
 - e) Determines aircraft controllability
 - f) Generates L-Q-R performance index for the minimization of cockpit g-level

Appendix C

Weight Reduction Calculations:

To demonstrate the weight reduction process, the adjusted structural weight of the wing torque box is calculated using the procedure given in section 12.4. The baseline A1 2024 structure weighs 1252 lbs. The weight of the subcomponents of the wing torque box is found by using the average values from Figure C-1, which is compiled from historical data. The components weight and failure modes are given in Table C-1.

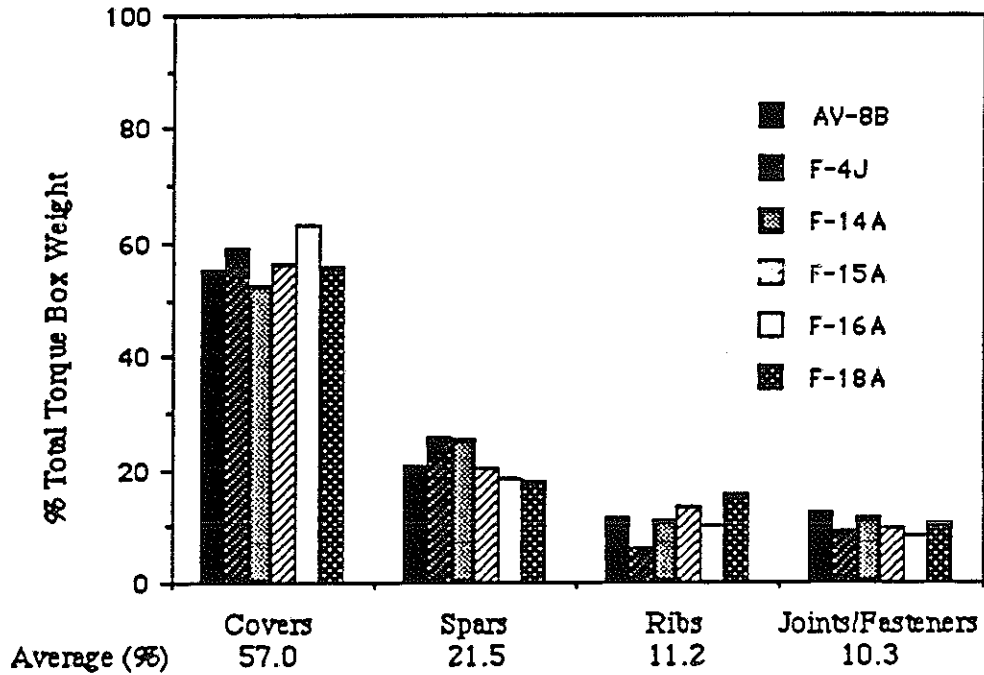


Figure C-1: Wing torque box weight distribution

Wing Component	Weight	Failure Modes						
		TN	CM	BU	CR	SH	FS	TS
Covers	$(57\%)(1252) = 713.6 \text{ lbs}$	30	30	20	0	0	10	10
Spars	$(21.5\%)(1252) = 269.2 \text{ lbs}$	25	25	10	5	25	5	5
Ribs	$(11.2\%)(1252) = 140.2 \text{ lbs}$	25	25	10	5	25	5	5
Joint/Fasteners	$(10.3\%)(1252) = 129.0 \text{ lbs}$	-	-	-	-	-	-	-

Table C-1: Wing components failure modes

Once the new and baseline material properties are established, they can be converted to strength-to-weight ratios, which are defined in Table C-2. Using these strength-to-weight ratios, the weight adjustment factors can be found using the equation 1.

Criterion	Equation	Graphite/ Epoxy	Al-Li
Tension K(TN)	$\left(\frac{\rho_1}{\rho_0}\right) \left(\frac{FTU_0}{FTU_1}\right)$	0.654	0.773
Compression K(CM)	$\left(\frac{\rho_1}{\rho_0}\right) \left(\frac{FCY_0}{FCY_1}\right)$	0.800	0.611
Buckling K(BU)	$\left(\frac{\rho_1}{\rho_0}\right) \left(\frac{E_0}{E_1}\right)^{.333}$	0.550	0.940
Crippling K(CR)	$\left(\frac{\rho_1}{\rho_0}\right) \left(\frac{E_0}{E_1}\right)^{.225} \left(\frac{FCY_0}{FCY_1}\right)^{.325}$	0.621	0.817
Shear K(SH)	$\left(\frac{\rho_1}{\rho_0}\right) \left(\frac{FSU_0}{FSU_1}\right)$	0.692	—
Flextural Stiffness K(FS)	$\left(\frac{\rho_1}{\rho_0}\right) \left(\frac{E_0}{E_1}\right)$	0.530	0.901
Torsional Stiffness K(TS)	$\left(\frac{\rho_1}{\rho_0}\right) \left(\frac{G_0}{G_1}\right)$	0.700	0.876

0 = Original 1 = New (Al 2024 baseline material)

Table C-2: Strength to weight ratios

$$K = \sum [(\% \text{ Failure Mode}) * (\text{Strength-to-Weight ratio})] \quad (\text{eq. 1})$$

Covers: (Weight adjustment factor(s))

$$K\left(\frac{GR}{EP}\right)_{\text{upper}} = \sum [(.30)(.654) + \dots + (.10)(.700)] = 0.6692$$

$$K(\text{Al-Li})_{\text{lower}} = \sum [(.30)(.773) + \dots + (.10)(.876)] = 0.7807$$

Ribs: (Weight adjustment factor)

$$K\left(\frac{GR}{EP}\right) = \sum [(.25)(.654) + \dots + (.05)(.700)] = 0.6840$$

Now that the weight adjustment factors have been calculated the weight of the adjusted structure can be found using the equation 2. The results are shown in Table C-3.

$$WT_{adj} = K * WT_{base} * \% Appl. * CF + WT_{base} * (1 - \% Appl.) \quad (eq. 2)$$

Covers (50% GR/EP, 50% Al-Li)			Ribs (100% GR/EP)		
Weight	Equation	Total lbs	Weight	Equation	Total lbs
Alternate Material Graphite/Epoxy	$k * WT_{base} * \% APPL$ (.669)(713.6)(.5)	238.8	Alternate Material Graphite/Epoxy	$k * WT_{base} * \% APPL$ (.6840)(140.2)(1)	95.9
Al-Li	(.781)(713.6)(.5)	278.6			
	Total	517.4			
Construction Factor	$WT_{Adj} * CF$ (517.4)(.1)	51.7	Construction Factor	$WT_{Adj} * CF$ (95.9)(.1)	9.6
Baseline Material	$WT (1 - \% APPL)$ (713.6)(0)	0	Baseline Material	$WT (1 - \% APPL)$ (140.2)(0)	0
Adjusted Structure		569.1lbs	Adjusted Structure		105.5 lbs

Table C-3: Adjusted weight calculation

The expected weight savings obtained by using the SPF/DB technique is approximately 30%³⁴.

Thus,

$$\text{Spar adjusted structural weight} = (269.2)(0.70) = \underline{188.4 \text{ lbs}}$$

$$\text{Total Torque Box weight} = 569.1 + 188.4 + 105.5 = \underline{920 \text{ lbs}}$$

A similar procedure is used to calculate the weight savings on the control surfaces, the vertical and horizontal tails, and the upper portion of the fuselage.

References

- 1.) AIAA / General Dynamics Corporation Team Aircraft Design Competition, 1990-91.
- 2.) Kirschbaum & Mason, Class notes from "Aircraft Design, 1990-91.
- 3.) Smith, Daniel L., "Flight Test Demonstrated Performance Improvements with a Conformal Weapons Carriage", presented at Aircraft/Stores Compatibility Symposium, JTCG/ALNNO Sept 18-20, 1973, Sacramento California.
- 4.) Raymer, Daniel P., *Aircraft Design: A Conceptual Approach*, AIAA Education Series, Washington D.C., 1989.
- 5.) "ACSYNT Analysis Bible," NASA-Ames Research Center and VPI&SU.
- 6.) Harris, Charles D., "NASA Supercritical Airfoils," NASA TP 2969, April 1990.
- 7.) Moran, Jack, *An Introduction to Theoretical and Computational Aerodynamics*, John Wiley & Sons, New York, 1984.
- 8.) Abbot, Ira and von Doenhoff, Albert E., *Theory of Wing Sections*, Dover Publications, Inc., 1959.
- 9.) Jameson, A., "Acceleration of Transonic Potential Flow Calculations on Arbitrary Meshes by the Multiple Grid Method," AIAA Paper No. 1458, July, 1979.
- 10.) Lamar, J.E., and Herbert, H.E., ""Production Version of the Extended NASA-Langley Vortex Lattice FORTRAN Computer Code," Volume 1, User's Guide, NASA TM 83303, April 1982.
- 11.) Lachmann, G.V., *Boundary Layer and Flow Control: Its Principles and Applications*, Volume 1, Pergamon Press, New York, 1961.
- 12.) Carr, John E., "An Aerodynamic Comparison of Blown and Mechanical High Lift Airfoils," Proceedings of the Circulation Control Workshop, NASA CP 2432, 1986.
- 13.) FRICTION, W.H. Mason, AEROTOOLS, VPI&SU.
- 14.) Bore, C.L., "Airframe/Store Compatibility," Special Course on the fundamentals of Fighter Aircraft Design, AGARD-R-740, February 1985.
- 15.) Haines, A.B., "External Stores Interference," AGARD-R-712.
- 16.) Ives, David, LIDRAG from "An Automated Procedure for Computing the Three Dimensional Transonic Flow Over Wing Body Combinations, Including Viscous Effects," AFFDL-TR-77-122, February 1978.
- 17.) Oates, Gordon C., *Aircraft Propulsion Systems Technology and Design*, AIAA Education Series, Washington D.C., 1989.
- 18.) Roskam, J., *Airplane Design, Part VI*, Aviation Engineering Corporation, 1989.
- 19.) Burse, R., "Flight Test Results of the F-15 SMTD Thrust Vectoring/Thrust Reversing Exhaust Nozzle," AIAA/SAE/ASME/ASEE 26th Joint Propulsion Conference, Orlando Florida, July 16-18, 1990.

- 20.) Herbst, Dr. W.B., "Thrust Vectoring - Why and How?", 8th International Symposium on Airbreathing Engines, Cincinnati, Ohio, June 14-19, 1987.
- 21.) Etkin, B., *Dynamics of Flight: Stability and Control*, John Wiley & Sons, New York, 1982.
- 22.) MIL-F-8785C, "Military Specification: Flying Qualities of Piloted Airplanes," 1980.
- 23.) Roskam, J., *Airplane Design, Part VII*, Aviation Engineering Corporation, 1989.
- 24.) Friedland, B., *Control System Design: An Introduction to State Space Methods*, 1986.
- 25.) Houghton, E.L., Carruthers, N.B., *Aerodynamics for Engineering Students*, Third ed., Edward Arnold Baltimore, Md., 1982.
- 26.) *Jane's All the World's Aircraft, 1987-88*, Jane's Publishing Company Limited, London, England, 1988.
- 27.) *Jane's Avionics*, Jane's Publishing Company Limited, London, England, 1988.
- 28.) Interview with Paul Kemmerling, former Air Force Pilot, current Human Factors Professor Blacksburg, Virginia, January 1991.
- 29.) Sweetman, Bill, et al., *The Great Book of Modern War Planes*, Salamander Books, Portland House, 1987.
- 30.) Peery, David, J., *Aircraft Structures*, McGraw-Hill Book Co., Inc., New York, 1950.
- 31.) Forsch, Hans, H., "Advanced Materials and Processes in Aircraft Structures," Grumman Aerospace Corporation.
- 32.) Hoskin, B.C., & Baker, A.A., *Composite Materials for Aircraft Structures*, AIAA Education Series, Washington D.C., 1986.
- 33.) Baker, C., Gregson, P.J., Harris, S.J., Peel, C.J., "Aluminum-Lithium Alloys", Institute of Metals, 1986.
- 34.) Donaldson, J., Jr., "Titanium and Titanium Alloys," The Hartford Graduate Center, 1982.
- 35.) Zaidel, Steven, J., "Impact of Advanced Materials/Structural Concepts, on Future Weight Estimation," McDonnell Aircraft Company, May, 1982.
- 36.) Chun Michael, Niu, Yung, *Airframe Structural Design*, Lockheed Aeronautical Systems Company, Burbank, California, 1988.
- 37.) Shumate, Steven, F., et al., "Preliminary Design Study of A Low-Cost Supersonic STOVL Fighter," The University of Kansas, 8 June, 1990.
- 38.) Roskam, J., *Airplane Design, Part VIII*, Aviation Engineering Corporation, 1989.